UNIVERSITY OF LIVERPOOL

Upgrading Plan for Conventional Distribution Networks Considering Virtual Microgrid Systems

Thesis submitted in accordance with the requirements of the

University of Liverpool

for the degree of Doctor in Philosophy

by

Xiaotong XU

Department of Electrical Engineering and Electronics

School of Electrical Engineering and Electronics and Computer Science

University of Liverpool

Feb. 2019

Abstract

It is widely agreed that the integration of distributed generators (DGs) to power systems is an inevitable trend, which can help to solve many issues in conventional power systems, such as environmental pollution and load demand increasing. According to the study of European Liaison on Electricity grid Committed Towards long-term Research Activities (ELECTRA), in the future, the control center of power systems might transfer from transmission networks to distribution networks since most of DGs will be integrated to distribution networks. However, the infrastructure of conventional distribution networks (CDNs) has not enough capabilities to face challenges from DG integration. Therefore, it is necessary to make a long-term planning to construct smart distribution networks (SDNs).

Although many planning strategies are already proposed for constructing SDNs, most of them are passive methods which are based on traditional control and operating mechanisms. In this thesis, an active planning framework for upgrading CDNs to SDNs is introduced by considering both current infrastructure of CDNs and future requirements of SDNs. Since conventional centralised control methods have limited capabilities to deal with huge amount of information and manage flexible structure of SDNs, virtual microgrids (VMs) are designed as basic units to realise decentralised control in this framework. Based on the idea of cyber-physical-socioeconomic system (CPSS), the structure and interaction of cyber system layer, physical system layer as well as socioeconomic system layer are considered in this framework to improve the performance of electrical networks.

Since physical system layer is the most fundamental and important part in the active planning framework, and it affects the function of the other two layers, a two-phase strategy to construct the physical system layer is proposed. In the two-phase strategy, phase 1 is to partition CDNs and determine VM boundaries, and phase 2 is to determine DG allocation based on the partitioning results obtained in phase 1.

In phase 1, a partitioning method considering structural characteristics of electrical networks rather than operating states is proposed. Considering specific characteristics of electrical networks, electrical coupling strength (ECS) is defined to describe electrical connection among buses. Based on the modularity in complex network theories, electrical modularity is defined to judge the performance of partitioning results. The effectiveness of this method is tested in three popular distribution networks. The partitioning method can detect VM boundaries and partitioning results are in accord with structural characteristics of distribution networks.

Based on the partitioning results obtained in phase 1, phase 2 is to optimise DG allocation in electrical networks. A bi-level optimisation method is proposed, including an outer optimisation and an inner optimisation. The outer optimisation focus on long-term planning goals to realise autonomy of VMs while the inner optimisation focus on improving the ability of active energy management. Both genetic algorithm and probabilistic optimal power flow are applied to determine the type, size, location and number of DGs. The feasibility of this method is verified by applying it to PG&E 69-bus distribution network.

The operation of SDNs with VMs is a very important topic since the integration of DGs will lead to bidirectional power flow and fault current variation in networks. Considering the similarity between microgrids and VMs, a hybrid control and protection scheme for microgrids is introduced, and its effectiveness is tested through Power Systems Computer Aided Design (PSCAD) simulation. Although more research is needed because SDNs are more complicated than microgrids, the hybrid scheme has great potential to be applied to VMs.

Key Words: Distributed generators (DGs), electrical coupling strength (ECS), electrical modularity, genetic algorithm (GA), probabilistic optimal power flow (POPF), virtual microgrids (VMs).

Acknowledgements

Firstly, I would like to thank my supervisors, Dr. Shaofeng LU and Dr. Fei XUE, who gave me much guidance and support my Ph.D. study. They always encouraged me to become a researcher with critical thinking and problem solving skills, and they were very generous to share some experience with me to help me solve problems in both research and my life. Besides, I would like to thank my Liverpool supervisor, Dr. Lin JIANG, who gave me many meaningful ideas for my research. I would also thank Dr. Huiqing WEN, who provided many suggestions to get me familiar with the research at the beginning of my study.

Furthermore, I would send my thanks to Dr. Yang DU, Prof. Joseph YAN, Prof. Kaizhu HUANG, and Dr. Wen LIU, who gave me many suggestions and support me both in academic and in my Ph.D. life. Additional thanks would be sent to Mr. Hengyang LUO, Mr. Bing HAN, Mr. Xiaoliang WANG, Mr. Haochuang JIANG, Mr. Shufei ZHANG, Ms. Jingchen WANG and other friends. They provided useful advice and helped me to solve many technical issues.

The grateful gratitude would be sent to my family members, they always encouraged me to have a positive attitude to overcome challenges in the research and my life. I would like to thank my mother especially, who gave me much escort and support during my studies.

Contents

List of Figures

List of Tables

Chapter 1
Introduction

Since the late 1860s, humans have entered the age of electricity. Electricity plays an important role in the industry and our daily life. A number of activities, such as lighting, textiles, communications, broadcasting and so on, should rely on stable electrical power supply.

In conventional power grids, electricity is generated by power plants, through substations, transmission networks and distribution networks, finally, it is delivered to customers. Currently, most of power grids in the world operate in this way. However, conventional power grids are facing many challenges, including [1], [2]:

- In most countries, electricity is generated from traditional thermal power plants which use fossil fuels as main fuels, but fossil fuels are running out and this kind of energy sources also cause many environmental issues;
- Since most of infrastructure in power systems has served for many years, it is prone to fail, which affects normal operation of power systems;
- With the development of social economy, load demands will continue increasing, but it is difficult for conventional power grids to meet increasing load demands due to limited expansion space; and
- For some large countries, such as China, very long-distance transmission is needed to deliver electricity to cities. It decreases transmission efficiency and increases costs and power losses.

All these issues affect the stability and efficiency of power supply. It is widely agreed that the integration of distributed generators (DGs) to power systems is an inevitable trend, which helps to solve the issues in conventional power grids and improve the performance of power systems. The benefits of DG integration can be summarised as [3]:

- Decrease environmental pollution by deploying renewable energy resources;

- Reduce power losses and improve power supply efficiency as DGs can be closely installed to loads;
- Provide reliable electricity to customers to meet the increasing load requirements;
- Reduce generation costs of traditional fossil fuels;
- Relieve the electricity pressure in peak demand periods; and
- Encourage consumers to participate in energy trading markets.

In the future, more and more DGs will be deployed to distribution networks. The integration of DGs can bring many benefits, but it also affects the normal operation of conventional distribution networks (CDNs). For CDNs, its main function is to distribute electricity from substations to customers, and there is almost no generator in CDNs. The power flow in a CDN is always in the single direction (which flows from substations to loads), but the connection of DGs leads to bidirectional power flow in networks. In addition, voltage and fault current variation, and stochastic nature of renewable DGs also cause some problems if DGs are directly connected to CDNs. To overcome these problems, constructing smart distribution networks (SDNs) becomes a popular topic, and it can be seen as a possible form of future distribution networks.

1.1 Smart Distribution Networks (SDNs)

Until now, there is no universally accepted definition of SDNs. According to the discussion in [4] and [5], SDNs should contain following characteristics:

- Enable the deployment of renewable energies;
- Allow the connection of new electricity users and meet their electricity consuming characteristics, such as plug and play service of electric vehicles.
- Encourage the emergency of innovative energy efficiency solutions and the development of smart cities or neighborhoods.
- Improve the quality of electricity supply;
- Control the cost of routine; and
- Interconnected in structure and complexity in operation.

In addition to SDNs, many studies propose to develop active distribution networks (ADNs), which are also called active distribution systems, to adapt to the changes of future power systems. A global definition of ADN is [6]: 'ADNs are distribution networks that have systems in place to control a combination of distributed energy resources (generators, loads and storage). Distribution system operators (DSOs) have the possibility of managing electricity flows using a flexible network topology. Distributed energy resources take some degree of responsibility for system support, which will depend on a suitable regulatory environment and connection agreement.' According to the definition of ADN, the ability of active energy management is pointed out as an important characteristic. ADNs are advanced visions of SDNs.

Many new concepts, which can be applied to different scenarios, have been proposed as the backbone for SDNs, such as smart homes, smart cities, virtual power plants and microgrids [4].

Smart homes focus on the technologies in customer sides, including sensor networks, home area networks, smart information boxes, home display units, in-house AC/DC distribution with smart plugs, advanced converters and inverters, and diverse loads [4]. Communication security of smart homes is an important topic, detailed issues and possible solutions are reviewed in [7].

A smart city is a new concept and it has the ability to manage the assets and resources of an urban area by using a variety of data collection sensors, therefore, the communication and city infrastructure can be directly interacted to operate more efficiently. There are five energy-related activities in smart cities, including generation, storage, infrastructure, facilities and transport. A general energy system design model is introduced to develop a smart city in [8].

A virtual power plant is a system containing a variety of DGs and loads in a large geography, and it can also be seen as a system with a number of interconnected small systems. A virtual power plant is controlled by a central operator, and it is a grid-tied system. A virtual power operates with the connection to the main grid. Smart meters,

demand response and real time pricing are very important for the market trading of virtual power plants [9].

A microgrid is another popular concept. According to the U.S. Department of Energy, a microgrid is defined as "a group of interconnected loads and distributed energy resources within clearly defined electrical boundaries that acts as a single controllable entity with respect to the grid. A microgrid can connect and disconnect from the grid to enable it to operate in both grid-connected or island mode. [10]." A microgrid is a much smaller system compared to the main power system, but it has similar functions as power systems. A microgrid has a vital characteristic which refers to the operation in islanding mode, which is not allowed in CDN planning because of voltage stability and synchronization issues. It is stated in [11] that constructing microgrids is an essential step in the electricity development pathway.

However, microgrids have limited energy handling capability [12], [13], and it is impossible to completely reconstruct new microgrids in existing distribution networks. Therefore, virtual microgrids (VMs) have drawn much attention these days, and it is based on partitioning a CDN into a group of areas which will be constructed to microgrids eventually [13], [14]. The definition and characteristics of VMs are explained in Chapter 2.

1.2 Distribution Network Planning

To develop a SDN, suitable planning is very important. Conventional distribution network planning aims to determine the location, capacity, and time of investment by minimising costs to meet the load growth and ensure the safe operation of systems [15]. It always based on the principle of 'fit and forget', which aims to find optimal solutions considering the worst-case scenario, but the probability of occurrence for the worst-case scenario is very low. What is more, it is a deterministic method based on given load forecast, but the uncertainty and variability of some kinds of DGs, such as solar power generators and wind turbine generators, are not considered [16]. Therefore, conventional distribution network planning is no longer suitable for SDNs with high

penetration of DGs. It is necessary to develop appropriate methodologies for SDN planning.

Many planning strategies for constructing SDNs have already been proposed. In [17], a multi-level model was introduced to deal with the high penetration of DGs and storage devices. Operation issues and planning issues were combined by minimising cost, maximising reliability and the penetration of DGs with renewable resources. Koutsoukis, Georgilakis, and Hatziargyriou in [15] put forward a multistage coordinated planning for developing SDNs. The location, capacity and installation time of new distribution lines, substations, capacitor banks and voltage regulators were determined with the aim to minimise investment costs, and different active network management schemes were also considered during the planning. In this work, the allocation of DGs were assumed to be given. Martins and Borges [18] introduced an expansion planning of active distribution system. Topology changes, DG integration, rewiring and new load points were determined by applying two different methodologies. The first methodology analysed each individual scenario while the second methodology analysed all scenarios simultaneously. It was found that the second methodology could achieve better solutions in terms of costs and reliability while the first methodology could offer various solutions for planners. X. Shen, *et al*. in [19] presented a co-optimization model by considering both investment decisions and operation strategies to determine optimal reconfiguration of SDNs and the output of DGs.

Although many methods are proposed for SDN planning, most of them are based on traditional control and operating mechanisms. These methods are called passive planning, their ‘Passive’ features can be summarised as:

(1) It is based on conventional centralized control of power systems.

(2) Its objective function cannot reflect the ability of active energy management of future networks.

(3) It is difficult to deal with constraints of active energy management capabilities caused by the structure of CDNs.

To make a more comprehensive planning for constructing SDNs, a long-term guidance is needed considering the future vision of distribution networks. This thesis proposes a new concept of 'Active planning' for SDNs. 'Active' features should be considered in both its energy management and also its planning. Especially, the planning from CDNs to SDNs should reflect following 'Active' characteristics:

(1) It has a guidance from a long-term development perspective which is based on decentralized control by swarm intelligence.

(2) It is oriented to maximisation of ability in future active energy management;

(3) It actively adapts to the existing characteristics of CDNs, including network structure and infrastructure.

Conventional power systems are already formed, and they have served for so many years. To develop SDNs, a reasonable and economic way is to upgrade CDNs to SDNs. Therefore, in this thesis, a three-layer framework to upgrade CDNs to SDNs is put forward, and it is designed based on the principles of active planning. In this framework, both regional operation and overall management are considered, and VMs are constructed as basic units to realise the goal of decentralization control and swarm intelligence. Related planning issues, such as network topology, resource allocation, communication and power transaction mode, are carefully considered and designed.

1.3 Chapter Breakdown

The remainder of this thesis is organized as follows:

Chapter 2 discusses control methods of conventional power systems and future power systems. Based on future decentralised control methods, a three-layer framework for upgrading CDNs to SDNs, which is based on VMs, is proposed. To construct the fundamental layer (physical system layer) of this framework, a two-phase strategy is introduced.

Chapter 3 explains basic theories and tools which can be used to solve technical issues in the two-phase strategy, including some important concepts of complex network theories and a general review of optimisation methodologies.

Chapter 4 discusses the methodology which is applied to determine the structure of VMs. To determine VM boundaries, a partitioning method based on structural information is introduced, and the electrical coupling strength (ECS) is defined to describe electrical connection while electrical modularity is used to judge partitioning results.

Chapter 5 introduces a bi-level optimisation method for DG allocation with the consideration of both autonomy of VMs and active energy management of networks. Based on the partitioning results in Chapter 4, the type, location, capacity and number of DGs are optimised based on probabilistic optimal power flow (POPF) calculation and genetic algorithm (GA).

Chapter 6 focuses on operating issues of SDNs consisting of VMs. Possible issues of VM systems are discussed. Considering the similar characteristics between microgrids and VMs, a hybrid control and protection scheme for microgrids are studied and the feasibility of applying this scheme to VM systems is analysed.

Finally, Chapter 7 summarises the main contributions of the thesis and provides recommendations for the future work.

Chapter 2
The Development of the Active Planning for Constructing SDNs

For a distribution network, control methods are very important as they determine operating ways and also affect the performance of power systems. As discussed in Section 1.2, a significant difference between conventional distribution network planning and active planning for SDN is the change of control methods in networks. In this chapter, the characteristics of conventional centralised control and future decentralised control are discussed, and the advantages of future decentralised control are summarised. Based on future decentralised control methods, an active planning framework for developing SDNs is proposed.

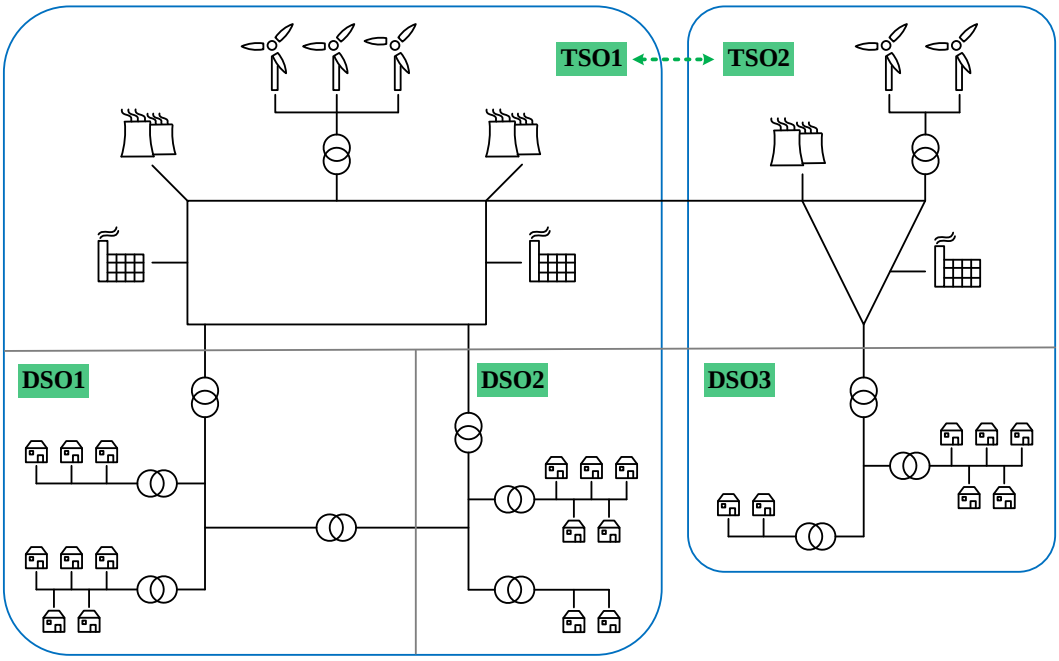

Fig. 2.1 A power system based on conventional centralised control.

2.1 Conventional Centralised Control Systems

A conventional centralised control system is shown in Fig. 2.1. It is a hierarchical control system. As shown in Fig. 2.1, the electrical power is supplied by large power plants, and loads are located in distribution networks. The power system is mainly controlled by transmission system operators (TSOs), who are responsible for maintaining the power balance between generation and loads. Information is shared among different TSOs. A TSO distributes the electrical power from power plants to distribution networks which belong to its control areas. Distribution networks are controlled by corresponding DSOs. A DSO is responsible for dispatching the power from transmission networks to loads, and it also monitors and controls the state of its own distribution network. There is no communication between DSOs. The reliability and stability of centralised control systems have been proven through practical applications for so many years.

2.2 Future Decentralised Control Systems

According to the study carried out by Electricity grid Committed Towards long-term Research Activities (ELECTRA), an important development trend of future power systems is that power generation units will transfer from central transmission system connected units to distributed distribution system connected units [20]. TSOs will not be as important as before, and they will control fewer number of conventional generators comparing to numerous number of DGs [21]. If future power systems are still in conventional centralised control, various problems will arise. For example, the randomness and intermittent characteristics of DGs will increase the information monitoring and process burden of TSOs. What is more, if a central processor fails, it will affect the operation of the entire network. Therefore, conventional centralised control is not suitable for future power systems anymore. In [22], a four-visions developing topology from current centralised control systems to future decentralised

control systems was proposed. It stated that future power systems would transfer from centralised systems with DGs to fully decentralised systems.

2.2.1 Web-of-Cells (WoCs)

To develop future decentralised power systems, one possible way is to partition a power system to several units, for example constructing Web-of-Cells (WoCs) system. It is a new idea which was recently proposed by ELECTRA Integrated Research Programme (IRP) in [20]. A WoCs system is shown in Fig. 2.2. In this system, the partitioned units are called control cells. Control cells are defined as

"A group of interconnected loads, distributed energy resources and storage units within well-defined grid boundaries corresponding to a physical portion of the grid and corresponding to a confined geographical area."

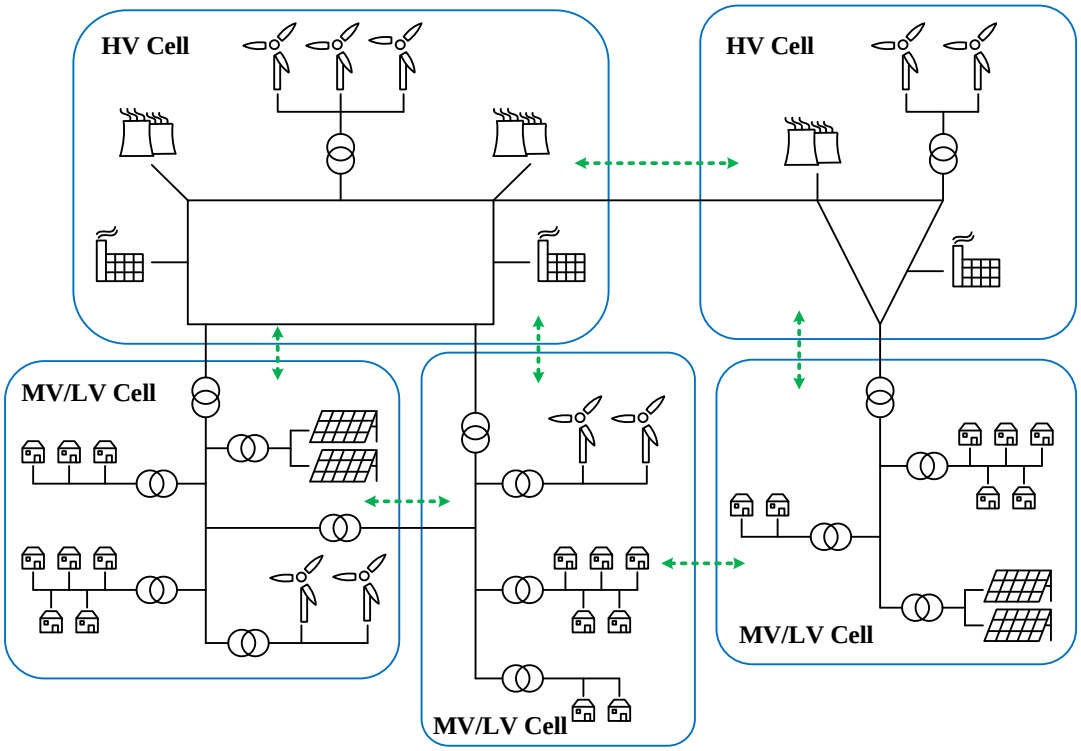

Fig. 2.2 A power system based on decentralised control with control cells.

According to this definition, the characteristics of a control cell can be summarised as

(1) It has the basic function of power systems, including DGs and load.

(2) It has storage units to provide ancillary services.

(3) It is a single entity with well-defined boundaries.

(4) It is one part of a grid.

In addition to boundary limitation, all control cells should be autonomous systems. Each cell has its own controller which is called a control cell operator (CCO). For each control cell, a CCO has the responsibility to know the real-time state of the cell and balance the power between generation and loads within its own cell. CCOs can communicate with each other. To keep the power balancing, power can be dispatched not only in each cell but also in other cells [23], which means power can be exchanged with other cells via boundaries. Accordingly, a control cell can operate either in islanding mode or with the connection to other control cells.

Developing a decentralised control system like WoCs can not only adapt to the future vision of power systems but also bring many benefits, including:

(1) It has lower burden of information processing as CCOs do not need to monitor the global state of power systems like TSOs;

(2) It is flexible and efficient due to various operating modes. The utilization efficiency of reserve capacity is also improved;

(3) It can deal with faults efficiently and ensure the security of systems. Since each partitioned unit has its own operator, unbalance problems or faults can be solved locally within specific areas, and the impact of fault on the other areas is reduced; and

(4) It is compatible with TSO and DSO, so it is a good way to realise the smooth transaction from centralised control system based on existing facilities to future decentralised control system based on partitioned units.

2.2.2 Virtual Microgrids (VMs)

In some countries, such as China, the distribution of energy resources and load demands is unbalanced. A large amount of energy is located in the southwest regions,

while the load center is located in the central and eastern regions. It is much more expensive to transmit energy than electricity to load center due to long distance between energy resources and load center. In this case, ultra-high voltage transmission is necessary. It is not an economic way to completely construct WoCs in the whole power system.

Since most of DGs are integrated to distribution networks, similar to the idea of WoCs systems, many studies propose to partition a distribution network to several small units in distribution networks, and different items are used to represent these partitioned units, such as island systems [24], networked microgrids [25], multi-microgrids [26], and virtual microgrids (VMs) [27]. Among these four words, three of them contain the word of 'microgrid', which indicates that there should be some links between microgrids and partitioned units in distribution networks. Although there is no widely accepted definition about this kind of networks, their characteristics can be summarised according to existing studies. These partitioned units have similar characteristics with microgrids, such as high penetration of DGs, various operating modes [10], [28], and they also have the ability of self-adequacy, self-sufficient and self-healing [25], [27], [29]–[31]. For each partitioned unit, it should be self-adequate, which refers to power generation and consumption should keep balanced within each unit [25], [29]. For the whole distribution network, self-sufficient refers to minimise the power flow between partitioned units, and the imbalance between generation and loads [30]. Self-healing is the capability of autonomous restoration after faults or disturbances [27], [29], [31]. These units also have some special features which are different from microgrids, such as these units are virtual systems, which refers to they all belong to parts of the main network rather than completely islanding systems. Additionally, they are developed from existing CDNs. In this thesis, 'virtual microgrids' is used to represent this kind of distribution networks with partitioned units.

Based on the discussion above-mentioned, VMs can be defined as: "Virtual microgrids are virtually autonomous systems based on the structure of CDNs, they have similar control strategies and operating modes as microgrids and can adapt to

future requirements of SDNs". VMs should have the following three characteristics, including:

1) They are developed from CDNs;

2) They have characteristics of microgrids; and

3) They have flexible structure based on virtual boundaries.

Constructing VMs in distribution networks can not only meet the integration requirements of DGs but also in accord with the decentralised control vision of future power systems.

2.3 Active Planning for Upgrading CDNs to SDNs

2.3.1 Cyber-physical Systems and Cyber-physical-socioeconomic Systems

Based on traditional network analysis methods, the network structure (physical part), data processing and communication (cyber part) are always studied separately [32]. The interaction between physical parts and cyber parts is not considered or considered in a simple approach. If the design of physical parts and cyber parts cannot adapt to the characteristics of each other very well, it will lead to some issues in real applications. Hence, constructing cyber-physical system (CPS) becomes a hot topic recently and it aims to integrate embedded computing technologies (cyber part) into physical systems [33]. The framework of a CPS is shown in Fig. 2.3. Cyber systems are responsible for monitoring the state of physical systems. They collect and analyse useful information from physical systems. Physical systems receive commands from cyber systems to control the behaviors of physical systems. CPS technologies can be used to deal with complex problems in modern industry fields [33]. In the last decade, CPSs are considered in the planning of SDNs. Some SDNs are seen as typical CPS systems [34], [35]. The interaction of physical parts and cyber parts in the planning of SDNs can make SDNs more efficient in operation and more responsive to customers [33].

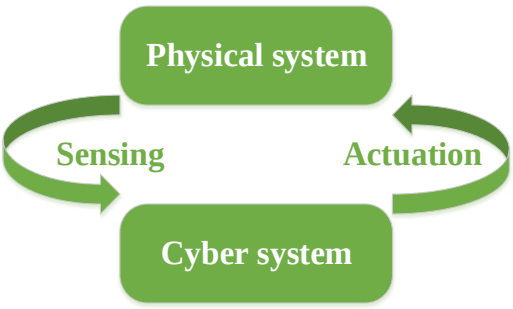

Fig. 2.3 The framework of CPS.

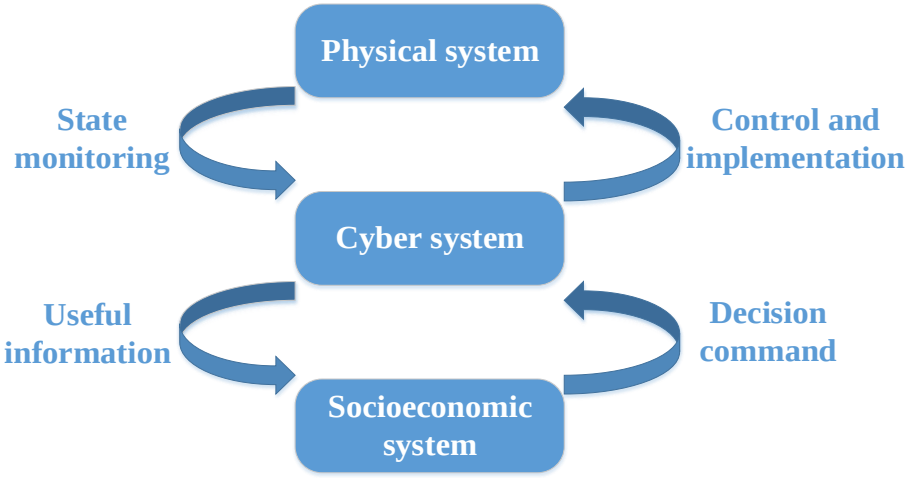

Fig. 2.4 The framework of CPSS.

Actually, energy transformation and consumption are driven by the requirements of social production and life. Hence, in a CPS, the command sent by cyber systems to physical systems is actually decided by socioeconomic behaviors. Therefore, in [36], an extended version of CPS is proposed, which is called cyber-physical-socioeconomic system (CPSS). The framework of a CPSS is shown in Fig. 2.4. In addition to the physical systems and cyber systems, the interaction of socioeconomic systems with the other two systems are also considered. In this framework, socioeconomic systems send decision commands to physical systems via cyber systems by analysing the information from cyber systems. Cyber systems play vital roles as they provide information support in the operational interaction between physical systems and socioeconomic systems. A CPSS is a more comprehensive

version which can reflect the interaction relationship among different aspects in a system.

2.3.2 Three-layer Active Distribution Network Planning

Based on the idea of CPSS, a three-layer framework for upgrading CDNs to SDNs is proposed, and it is presented in Fig. 2.5. In this framework, VMs are basic units to realise the decentralised control of SDNs.

The bottom layer is the physical system. In this layer, a CDN is divided into several units, and different partitioning results can be obtained based on specific goals. The allocation of new resources and devices, such as DGs, energy storage devices, is optimised to form VMs. To achieve operating mode transformation, and realise fast and accurate power exchange between VMs, intelligent devices are required on boundaries between VMs. Nowadays, the development of electronic devices can provide many choices, and soft open point (SOP) is one of the most popular devices. Although it is very expensive to apply SOP into distribution networks nowadays, the combination of SOP with traditional switches is a good choice. Moreover, based on VM systems, the integration of other resources can contribute to developing energy internet through the interconnection of these local networks.

The top layer is the socioeconomic system, and it is responsible for power transaction. It receives the information from cyber systems and sends the transaction decision from VM operators to cyber systems and also affect the behavior of physical systems. Since numerous DGs and other devices will be integrated to SDNs, it makes the power transaction become complicated. Considering the decentralised structure of VMs, each VM should have its own operator (which is named as a VM operator) who takes similar responsibilities as a EV aggregator [37]. A VM operator is responsible for making final transaction decisions and control the power distribution in its own VM. Power exchange happens not only among VMs which belong to specific distribution networks, but also between distribution networks and other parts of the

system (the main grid). Therefore, in this layer, the transaction between VMs and the main grid is also considered.

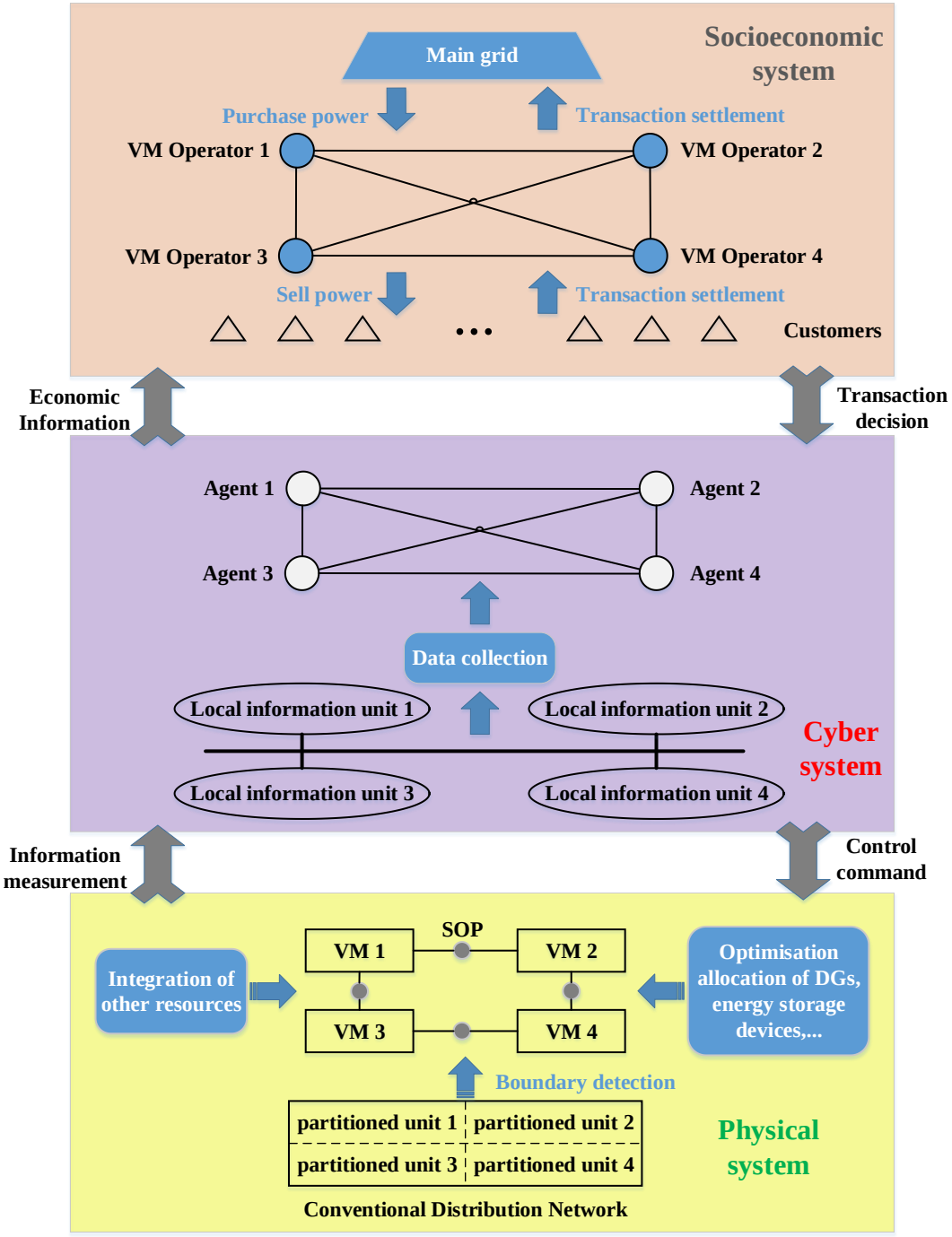

Fig. 2.5 An active planning framework based on VMs.

The core layer of this framework is the cyber system, which links the other two layers together, and its ability of information collection and data analysis affects the behaviors and performance of the whole network. Measurement layout and local information utilization are important issues in this layer. Measurement layout should be in accord with physical structure and resource configuration of networks to improve the efficiency and effectiveness of information utilization. Therefore, in this layer, a multi-agent system is developed. Local information units are used to collect information from corresponding VMs in physical systems, and the collected information is analysed and shared among different agents. After analysing the collected information, information is sent to socioeconomic systems. Cyber systems provide some suggestions to VM operators for deciding transaction ways. The transaction decision made by socioeconomic systems is sent to cyber systems, and it is transformed to corresponding commands to control the behaviors in physical systems.

This framework can well accord with the features of the active planning (which are discussed in Section 1.2). Firstly, it is based on a decentralised control system which consists of VMs. Secondly, optimising the ability of self-adequate and autonomous in VMs can ensure the flexibility and efficiency of active energy management. Thirdly, it is developed based on upgrading an existing CDN, so the existing infrastructure of CDNs can be utilised as much as possible, which can actively adapt to the structure of CDNs. What is more, the interaction of different parts (physical, cyber and socioeconomic systems) in a distribution network is considered in the planning stage, which can improve the performance of the whole system.

2.3.3 Two-phase Strategy for Constructing Physical System

According to the discussion in Section 2.3.2, the physical system layer should be the most fundamental part in this framework as it affects the structure and functions of the other two layers. A comprehensive planning is required to determine VM structure and resource allocation of DGs in the physical system layer. In most of existing studies,

VM structure and resource allocation of DGs are considered as separated issues. However, both of them affect the performance of networks. Combining the consideration of these two issues together, a two-phase strategy to construct the physical system is proposed. Phase 1 is the partitioning step, which refers to identifying boundaries of VMs considering structural characteristics. Based on the structure of interconnected VMs obtained in phase 1, phase 2 is the resource allocation step, which refers to optimising the resource allocation of DGs for each VM considering both conventional generators and DGs with renewable resources.

In Chapter 4 and Chapter 5, related methodologies for the implementation of this strategy are discussed. To ensure normal operation and improve the performance of VM systems, control and protection issues are discussed in Chapter 6.

2.4 Summary

In this section, conventional centralised control systems are introduced. Obviously, large-scale installation of DGs into power grids is an inevitable development trend. With DG penetration level increases, traditional centralised control systems are not suitable for power systems. Developing a decentralised control system with partitioned units is a possible solution. In a decentralised control system, each partitioned unit has its own operator to monitor operating states and control its own unit, and it can also coordinate with other units. Constructing WoCs systems and VMs are examples of decentralised control systems. By constructing this kind of systems, power systems can be more flexible, efficient and stable.

In the last decade, CPS is considered in SDN planning. CPSS is a more comprehensive version of CPS. The consideration of the interaction among physical, cyber and socioeconomic systems in the CPSS can improve the operational efficiency and effectiveness of a distribution network. Therefore, based on the idea of CPSS, a three-layer active planning framework is proposed to upgrade CDNs to SDNs. The structure and function of the active planning is explained, including the physical system layer, cyber system layer and socioeconomic system layer. In this framework,

VMs are basic units to adapt to the future decentralised control systems, and this framework is in accord with the characteristics of the active planning.

Since the physical system is the most fundamental step in the active planning framework. A two-phase strategy is proposed to construct the physical system. The first phase is to determine VM boundaries and the second phase is to optimise the resource allocation of DGs based on VM structure. The methodologies about this strategy are discussed in Chapter 4 and Chapter 5.

Chapter 3
Technical Backgrounds for Developing SDNs

To meet development requirements of future power systems, diverse kinds of methods are proposed to solve technical issues for constructing SDNs. To determine the decentralised structure of SDNs, many partitioning methods are proposed [38]–[41]. With the development of complex network theories, several studies propose to solve electrical network issues based on complex network theories due to the similarity between electrical networks and other complex networks [42], [43]. Since characteristics of communities in complex networks are similar to features of VMs in distribution networks, community detection methods are good choices to determine VM boundaries in distribution networks. In this chapter, to find an appropriate method to partition VMs (which is the goal of phase 1 in the two-phase strategy proposed in Section 2.3.3), a brief review of related technologies in complex network theories is given. In addition, to select an optimisation method to determine optimal DG allocation in phase 2 of the two-phase strategy, basic principles, merits and defects of different optimisation methods are discussed.

3.1 A Review of Complex Network Theories

Complex network theory is a young and popular research topic, which is used to analyse many real networks, including computer networks, technological networks, brain networks and social networks. In complex network theories, different networks can be represented by simplified graphs, which consist of a series of nodes (vertices) B with a set of edges (links) L. Fig. 3.1 shows several important components in a network. There are three kinds of edges in complex networks. An edge usually refers to only one edge between two nodes (such as the edge between node 1 and node 2). A multiedge means there is more than one edge between two nodes (such as the edges between node 2 and node 3). A self-edge is the edge whose two ends are connected to

the same node (such as the edge in node 4). Since electrical networks are always considered as simple networks (which means there is only one edge between any two nodes if these two nodes have connection), in this thesis, research is carried out based on simple networks. The research of networks with multiedges and self-edges is not considered.

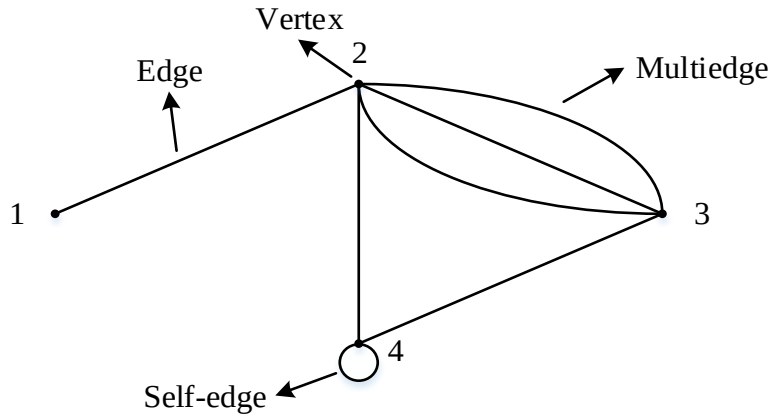

Fig. 3.1 A diagram of different components in complex networks.

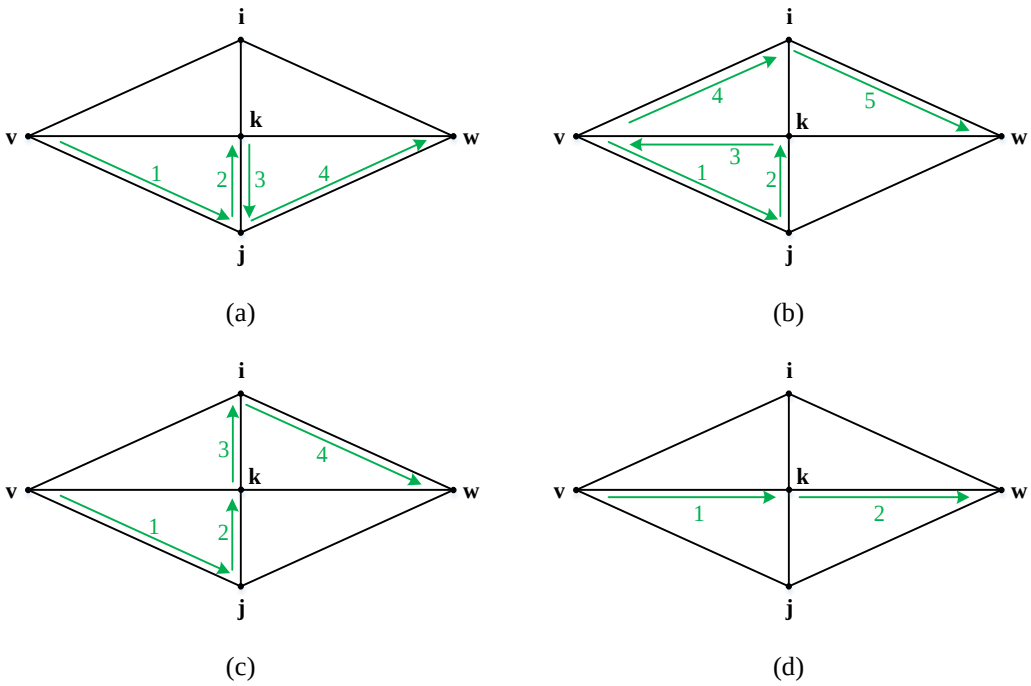

Fig. 3.2 Description of the route from node v to node w using different concepts. (a) A walk; (b) A trail; (c) A path; (d) A geodesic path.

In complex networks, several concepts are defined to describe the route between nodes in a graph. A *walk* from node v to node w is a series of edges and nodes which start at node v and end at node w. A *trail* is a walk in which no edge is visited more than once. A *path* is a walk in which no node is repeated. A *geodesic path (shortest path)* is a walk which has the minimum number of edges between node v and w [44]. The difference of these four definitions can be found from Fig. 3.2. For each subfigure, the way in the figure is not the only choice from node v to node w.

Unweighted networks and weighted networks are two kinds of complex networks which are commonly analyzed. For unweighted networks, the connection between any two nodes is either present or not. A social network can be an example of unweighted network when there are two kinds of connection between people, which refers to knowing each other or not knowing each other. A $N \times N$ *adjacent matrix* A can be used to describe the connection in an unweighted network. Imagine v and w are two nodes in a network, the element a_{vw} in matrix A can be written as

$$a_{vw} = \begin{cases} 1 & \text{there is an edge between vertex v and w} \\ 0 & \text{otherwise} \end{cases} \tag{3.1}$$

For a social network, node v and node w can be seen as any two people in this network. If they know each other, $a_{vw} = 1$, otherwise, $a_{vw} = 0$.

To distinguish nodes and measure the connection of unweighted networks. The *degree* of any node v k_v is defined as the number of edges connecting to it.

$$k_v = \sum_{w=1}^{N_B} A_{vw} \tag{3.2}$$

where N_B is the total number of nodes. A_{vw} is the elements in the adjacent matrix which is defined in Equation (3.1).

For weighted networks, strength of ties among nodes is considered. Taking the social network as an example, considering deeper relationship among individuals,

social ties are different, which means some people have stronger or weaker relationship than others even if these people all know each other. In this case, if edges are used to represent the relationship among people, different numbers can be assigned to represent the weight of edges. A larger number shows a stronger relationship while a smaller number means a weaker relationship. A $N \times N$ matrix B can be used to describe a weighted network, and the element b_{vw} in this matrix is expressed as [45]

$$b_{vw} = \text{connection weigth between vertex v and w} \tag{3.3}$$

Similarly, for weighted networks, the degree of a node v s_v is equal to total weight of the edges connecting to this node.

$$s_v = \sum_{w=1}^{N_B} b_{vw} \tag{3.4}$$

where b_{vw} is the elements in matrix B as defined in Equation (3.3).

Aforementioned concepts are some general methods based on topological information or simple weight distribution, which can be applied to analyse most of complex networks. However, these concepts may not be appropriate for electrical engineers to analyse electrical networks since electrical networks have specific characteristics. Firstly, electrical networks should be regarded as weighted networks rather than unweighted networks since the power flowing on transmission lines is different. Secondly, according to the principle of power transmission, which refers to transmitting the maximum power with the least losses, a line can transmit more power if the capacity of this line is bigger, while a line has less losses if the distance of this line is smaller. Hence, capacity and distance are two factors which affect the ability and efficiency of power transmission. These two factors (capacity and distance) should be considered as weight factors to describe characteristics of electrical networks.

3.1.1 Concepts Related to Distance and Capacity

For most of complex networks, *small world* is an important characteristic, and it means that these networks have small average distance. An example is famous 'six degrees of separation', which indicates that a person can be connected to any person in the world by six, or fewer, social connections [46].

In complex networks, the *length* of a walk between node v and node w is defined as the number of edges between these two nodes. *Geodesic distance* is always used to describe the distance between any two nodes in complex networks, and it is the length of geodesic paths. Based on geodesic distance, *betweenness centrality*, which is also called *betweenness* for short, is defined to distinguish which nodes or edges are more important than others. Betweenness of a node v *X(v)* and an edge l *X(l)* are

$$X(v) = \sum_{i}^{N} \sum_{j}^{N} \frac{\tau_{ij}^{v}}{\tau_{ij}}, \quad i \neq j \neq v \in B \tag{3.5}$$

$$X(l) = \sum_{i}^{N} \sum_{j}^{N} \frac{\tau_{ij}^{l}}{\tau_{ij}}, \quad i \neq j \in B,\ l \in L \tag{3.6}$$

where τ_{ij}^{v} is the number of geodesic paths passing through node v between node *i* and node *j*. τ_{ij}^{l} is the number of geodesic paths passing through edge *l* between node *i* and node *j*. τ_{ij} is the total number of geodesic paths between node *i* and node *j*.

However, average distance or geodesic distance is not suitable to be applied to measure distance in electrical networks, since the power flowing from one node v to another node w in electrical networks does not follow specific paths, such as genetic paths. Equivalent impedance which reflects electrical characteristics is a good way to describe the distance in electrical networks [47].

In addition to distance, another important factor is capacity, which can be seen as weight of edges. To describe characteristics of weighted networks, several factors should be considered:

(1) The total weight of edges, which reflects connection strength;

(2) The number of edges connecting to nodes; and

(3) The weight distribution among edges.

The definitions of degree in Equation (3.2) and Equation (3.4) only reflect the first and second factors respectively, but neither of them can reflect the last factor.

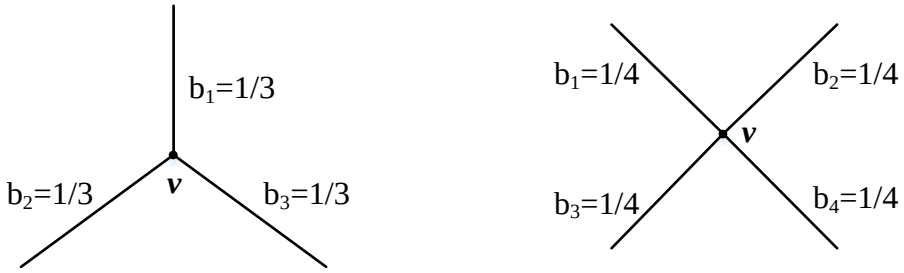

(a) (b)

Fig. 3.3 A network with the same total weight but different connection.

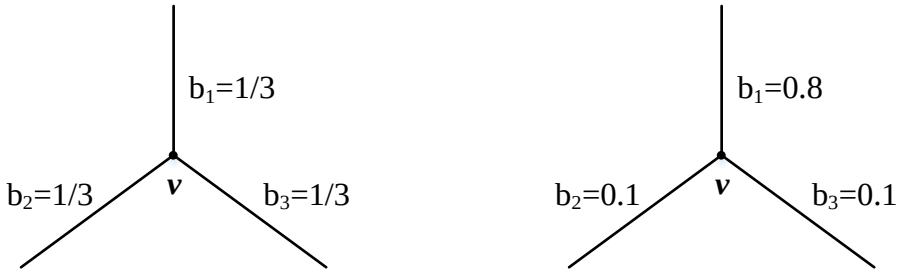

(a) (b)

Fig. 3.4 A network with the same connection but different weight distribution.

Taking simple networks in Fig. 3.3 and Fig. 3.4 as examples, in Fig. 3.3, $k_{v(a)} = 3$, $k_{v(b)} = 4$, and $s_{v(a)} = s_{v(b)} = 1$. The results using Equation (3.2) are different while the results using Equation (3.4) are same. In Fig. 3.4, $k_{v(a)} = k_{v(b)} = 3$, and $s_{v(a)} = s_{v(b)} = 1$. In this case, the results using Equation (3.2) and Equation (3.4) are same. However, it can be found that the weight distribution of (a) and (b) in Fig. 3.4 has a big difference. In (a), the weight of three edges are equal, but in (b), b_1 has a larger weight than the other two edges. To describe the degree in weighed networks with the consideration of

all three factors together, a degree based on entropy was proposed in [47]. Firstly, the weight of an edge t_{vw} is normalised as

$$t_{vw} = s_{vw} \Big/ \sum_{w=1}^{N_B} s_{vw} \tag{3.7}$$

Considering all the edges connecting to node v, $\sum_{w=1}^{N_B} t_{vw} = 1$. The *entropic degree* of node v g_v is defined as

$$g_v = (1 - \sum_{w=1}^{N_B} t_{vw} \ln t_{vw}) \sum_{w=1}^{N_B} s_{vw} \tag{3.8}$$

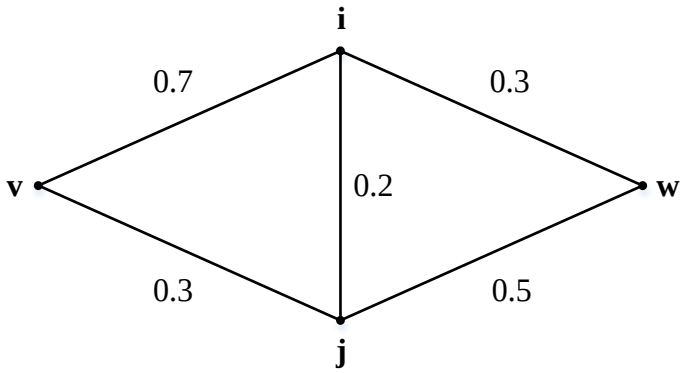

Fig. 3.5 A simple network with different power distributions.

Entropic degree is a good way to describe weighted networks by taking capacity as weight. For electrical power systems, each transmission line has a maximum transmission limit, which is designed by engineers to ensure the stability and security operation of power networks, so maximum transmission limit is an important item to define the capacity of power transmission. However, capacity cannot be determined only by transmission limit, power distribution should also be considered as it determines which line first reaches the transmission limit. Taking the network in Fig.

3.5 as an example, if a generator is installed at bus v and a load is located at bus w, the number on different lines shows the power distribution of the network when a unit of power is injected to bus v and withdraws from bus w. Imagining transmission limit of all lines is equal to 1, it can be easily calculated that the line $l_{v\text{-}i}$ (which connects node v and node i) reaches its limit first when more power is injected. Therefore, the real power transmission capacity C_g^d from generator bus g to load bus d is actually determined by this line ($l_{v\text{-}i}$) [48]. The real power transmission capacity between load bus d and generator bus g C_g^d is defined as

$$C_g^d = \min_{l \in L} \left(\frac{p_l^{\max}}{\left| f_l^{gd} \right|} \right) \tag{3.9}$$

where p_l^{max} is the transmission limit of line l. f_l^{gd} is the power change on line l when a unit of power is injected to bus g and withdraws from bus d.

Based on power transmission capacity C_g^d, betweenness of node v $I(v)$ in power networks can be defined as [48]

$$I(\mathrm{v}) = \frac{1}{2} \sum_{g \in G} \sum_{d \in D} C_g^d \sum_{l \in L^v} \left| f_l^{gd} \right|, \qquad \mathrm{v} \neq \mathrm{g} \neq \mathrm{d} \in \mathrm{B} \tag{3.10}$$

where $\sum_{l \in L^v} \left| f_l^{gd} \right|$ is the total power on all lines connecting to bus v when a unit of power is injected to bus g and withdraws from bus d. $I(v)$ is the total power passing through bus v considering all pairs of power transmission routes from generator buses to load buses with the power injection of C_g^d.

Line betweenness of power networks can be expressed as

$$I(l) = \max\left[I^p(l), \left| I^n(l) \right| \right], \qquad l \in L \tag{3.11}$$

$$I^p(l) = \sum_{g \in G} \sum_{d \in D} C_g^d f_l^{gd}, \qquad \text{if } f_l^{gd} > 0 \tag{3.12}$$

$$I^n(l) = \sum_{g \in G} \sum_{d \in D} C_g^d f_l^{gd}, \quad \text{if } f_l^{gd} < 0 \tag{3.13}$$

where $I^p(l)$ is the positive betweenness of line l while $I^m(l)$ is the negative betweenness of line l. Similarly, line betweenness is the maximum total power on line l considering all possible transmission routes from generator buses to load buses with the power injection of C_g^d.

Net-ability H(Y) is a concept which is used to measure the ability of power networks in the normal operation, and it is expressed as [49]

$$H(\mathrm{Y}) = \frac{1}{N_G N_D} \sum_{g \in G} \sum_{d \in D} \frac{C_g^d}{Z_g^d} \tag{3.14}$$

where N_G and N_D are total number of generator buses and load buses respectively. Z_g^d is the equivalent impedance between bus g and bus d.

Based on the definition in Equation (3.14), both distance (equivalent impedance) and capacity (power transmission capacity) are considered. The inverse relationship between power transmission capacity and equivalent impedance can well reflect the ability of power transmission by considering all routes between generator buses and load buses, and it is in accord with the power transmission principle mentioned in Section 3.1. Based on this idea, electrical coupling strength (ECS) is defined in Chapter 4 to measure electrical connection of electrical networks.

3.1.2 Community Detection

In complex network theories, another important concept is called *community.* A community is the group in which some nodes have higher connections among them than other nodes [50]. Fig. 3.6 shows an example of a network with four communities. In Fig. 3.6, the nodes within each oval belong to the same community, and it can be found that there are more physical connections among the nodes in the same community than the other nodes in this network. Communities can be classified as

disjoint communities and overlapping communities according to different characteristics of communities. For disjoint communities, each node only belongs to one community, while for overlapping communities, each node can be the components of several communities.

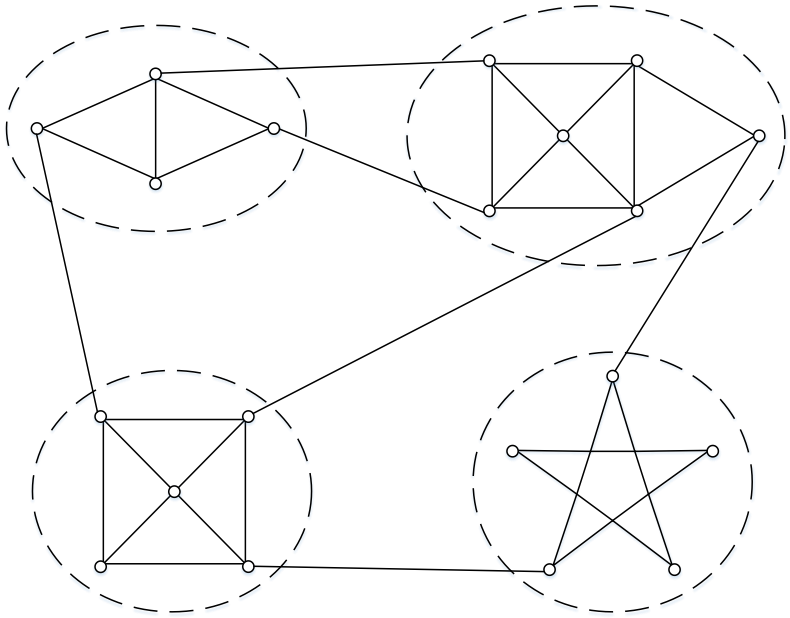

Fig. 3.6 A network with four communities.

According to the two-phase strategy proposed in Section 2.3.3, CDNs are partitioned to many VMs in phase 1. Since VMs are self-sufficient and autonomous systems, the electrical connection inside these VMs should be higher than the rest of the network, which is similar to characteristics of communities in complex networks. Therefore, community detection methods in complex networks have great potential to be applied to solve partitioning problems in CDNs. In this thesis, communities in electrical networks are considered as disjoint communities for efficient management, which is a common assumption in many studies [42], [43]

To find communities in a network, various methods are proposed, but currently, there is no general algorithms that are effective to detect community structure of all networks since networks have different characteristics, but algorithms have their own limitations. For detecting disjoint communities, *partitional clustering* is effective by

minimising or maximising loss functions. K-means clustering is a representative algorithm of partitional clustering based on minimising the squared loss function of intra-cluster distance [51]. However, K-means clustering cannot detect the optimal community number of a network since the community number k must be given for initialization. What is more, it is difficult to get a unique solution because k center points are generated randomly.

Since the number of communities is always unknown, a series of *hierarchical clustering methods* are proposed. Based on different partitioning mechanisms, hierarchical clustering methods can be classified as *agglomerative algorithms* and *divisive algorithms*. Agglomerative algorithms are bottom-up. At first, each node acts as a community. Then the closest node with higher similarity score is merged iteratively until all nodes form a unique community. On the contrary, divisive algorithms are top-down. It begins with the assumption that all nodes belong to a unique community. Then the edge with low similarity is removed iteratively until each node forms a single community. Accordingly, partitioning process of hierarchical clustering mainly depends on the value of similarity, and there are many ways to measure the similarity. For an n-dimensional Euclidean space, measuring the distance between nodes is a common way to define similarity. Given two nodes V (v_1,v_2,…v_n) and W (w_1,w_2,…w_n), several definitions of distance-based similarity are listed in Table 3.1 [52]. In addition, based on random walk in graphs, commute-time [53], escape probability [54] and resistance distance [55] can also be used to measure similarities for particular graphs. The advantage of hierarchical clustering is that community number is not required to be set in advance. However, there are several limitations. Although a series of results with different community numbers can be obtained, there is no judgment criteria to discriminate which result is better. In many cases, partitioning results are unreasonable as the nodes with only one neighbor are partitioned to different communities. Moreover, several nodes may be missed in the partitioning procedure even they are important in a community [52].

Partitional clustering and hierarchical clustering are always considered as traditional algorithms for community detection. Nowadays, *modularity-based algorithms* have drawn much attention due to their advantages. These algorithms rely on '*modularity*', which is defined by Newman, as an important index to judge the performance of partitioning results. Modularity Q is defined as [45], [56]

$$Q = \frac{1}{2m}\sum_{vw}\left[A_{vw} - \frac{k_v k_w}{2m}\right]\delta\left(C_v, C_w\right) \tag{3.15}$$

where A_{vw} is the adjacent matrix as defined in Equation (3.1). k_v (k_w) is the degree of node v (w), and it is the number of edges connecting to node v (w). $m = \frac{1}{2}\sum_{vw} A_{vw}$ is the total number of edges in a network. $\delta(a,b)$ is the Kronecker delta, and C_v (C_w) represents the community to which node v (w) belongs. If node v and node w are in the same community, $\delta(\mathrm{C}_v, \mathrm{C}_w) = 1$. Otherwise, $\delta(\mathrm{C}_v, \mathrm{C}_w) = 0$.

Table 3.1 Several definitions of distance-based similarity

Type	Expression
Euclidean distance	$d_{vw}^{E} = \sum_{k=1}^{n}\sqrt{\left(v_k - w_k\right)^2}$
Manhattan distance	$d_{vw}^{M} = \sum_{k=1}^{n}\left\|v_k - w_k\right\|$
Chebychev distance	$d_{vw}^{C} = \max_{k\in[1,\mathrm{n}]}\left\|v_k - w_k\right\|$
Cosine similarity	$d_{vw}^{\rho} = \arccos\frac{\mathbf{v}\cdot\mathbf{w}}{\sqrt{\sum_{k=1}^{n} v_k^2}\sqrt{\sum_{k=1}^{n} w_k^2}}$

The main idea of *modularity-based algorithms* is to maximise the value of modularity, and most of these algorithms combines heuristics in community detection

process. In 2001, based on genetic algorithm, Boettcher and Percus proposed a extremal optimisation to solve hard optimisation problem by maximising modularity [57]. In [58], based on spectral information, eigenvalues and eigenvectors of modularity matrix were optimised. Newman proposed a greedy optimisation, which was an agglomerative algorithm by merging nodes to larger communities according to the increase of modularity or less reduction of modularity [56]. Modularity-based algorithms provide good ways to compare different partitioning results, and they are effective to solve NP-hard (non-deterministic polynomial hard) community detection problems [59]. Comparing to the other modularity-based algorithms, greedy optimisation method has a specific feature, which refers to detecting optimal solutions for a variety number of communities, so flexible solutions can be provided.

Although many algorithms are applied to detect communities in complex networks, most of them are based on pure topological analysis, which means either the analysis of geodesic distance between nodes or density distribution of physical connection is considered. For electrical networks, straight application of pure topological analysis cannot reflect characteristics of electrical networks. It is necessary to consider specific electrical characteristics, i.e. distance and capacity, to detect communities (VMs) in CDNs. Based on the theories discussed in this section, a hierarchical partitioning method for CDNs is proposed and explained in Chapter 4.

3.2 A Review of Optimisation Technologies

Optimisation is a practical mathematical tool that is widely used to obtain optimal solutions in many areas, such as mechanics, civil engineering, control engineering, and electrical engineering. Defining objective functions is an important step for any optimisation problem. Accordingly, optimisation can be seen as a process of minimising or maximising objective functions, and related objective functions are called loss/cost functions (minimization) or utility/fitness functions (maximisation). Taking loss functions as examples, an optimisation problem can be expressed as

$$\min \ f(x) = \min \ \left(f_1(x), f_2(x), ..., f_n(x)\right), \qquad x \in \Omega \tag{3.16}$$

$$g(x) = 0 \tag{3.17}$$

$$h(x) \leq 0 \tag{3.18}$$

where *f(x)* is the objective function, and it can have single or multiple objectives. *x* is a decision (control) variable, and it is possible solutions belonging to *Ω*. *Ω* is called searching space or choice set. *g(x)* and *h(x)* are equality and inequality constraints. All candidate solutions of optimisation must satisfy these constraints.

The problem formulation for optimisation is based on following steps [60].

- Choosing variables;
- Formulating constraints and variable limits;
- Formulating objective functions;
- Choosing algorithms to solve optimisation problems; and
- Solving problems to get optimal solutions.

Based on different optimisation mechanisms, there are a number of algorithms which can be used to solve optimisation problems, and different algorithms are only suitable to solve certain problems. Optimisation algorithms are always classified to three categories, and they are analytical methods, numerical methods and heuristic methods. To find a suitable optimisation algorithm to determine optimal allocation of DGs in the two-phase strategy, a review of related algorithms is given in this section.

3.2.1 Analytical Methods

In general, analytical methods are based on mathematical analysis, and they are applied to solve the problems with assumed conditions. Analytical methods are classified into two categories [60]. One is to verify candidate solutions to see if they can meet specific conditions. The other one is to find optimal solutions based on derived equations which are satisfied with optimality criteria. Compared to the other two kinds of optimisation methods (numerical methods and heuristic methods), the

optimisation process of analytical method is simpler, so it is easy to apply this kind of methods to solve problems if the problems have candidate solutions or optimal equations can be derived. The computation time of analytical methods is commonly less than other optimisation methods [61]. However, by using analytical methods, results obtained are not necessarily optimal. In addition, they are not general methods as they are only effective to solve certain problems. It has some limitations to solve more complex optimisation problems.

3.2.2 Numerical Methods

Numerical method is a kind of searching method. Taking the optimisation problem with lost functions as an example, general optimisation process of numerical methods can be summarised as [60]:

Step 1: Based on either random or common sense, an initial trial solution is selected, then the objective function is evaluated.

Step 2: According to certain movement principle, the second trial solution is obtained, and then the objective function is evaluated again.

Step 3: If the objective function in step 2 is smaller than that in step 1, a new movement is made.

Step 4: Repeat the process of step 2 and step 3 until a solution with the minimum objective function is found.

Gradient search is one kind of numerical methods. According to opposite searching mechanisms, gradient search is classified to gradient descent and gradient ascent. Gradient descent is to find the local minimum while gradient ascent is to find the local maximum. Assuming *F(x)* is a multi-objective function, gradient descent can be explained by

$$x_{n+1} = x_n - \gamma \nabla F\left(x_n\right) \tag{3.19}$$

where $-\nabla F(x_n)$ represents that the direction of search is in the negative direction of gradient. γ is the step size. Selecting a reasonable step size is very important. If step size is too large, it will lead to an iterative too fast and the optimal solution may be missed. If step size is too small, iterative time becomes very slow. Determining the direction of movement, and new trial solutions are two important issues for gradient search. A disadvantage of gradient search is that it is not convergent for the network with few number of nodes [62].

Linear programming is another kind of numerical method, and it is used to solve linear objectives with linear equality and linear inequality constraints. It is to find the point with a minimum or maximum objective in the feasible region of a convex polytope. Linear programming is suitable to solve complex problems, but some errors may occur during the process of linearization since linearization results are approximate values but not exact values. Moreover, this kind of methods are only effective to deal with the problems with linear objectives and constraints. To optimise the problems with non-linear objectives and constraints, applying *non-linear programming* is an effective method. Although non-linear programming can solve non-linear optimisation problems, the computation time of some problems is very long due to numerous number of variables [63].

Dynamic programming was first introduced by Richard Bellman in the 1950s. It is used to solve problems with dynamic nature. Using this kind of method, a complicated problem is divided to many inner smaller problems, and these smaller problems are recursive. Other numerical algorithms, such as sequential quadratic programming [64] and ordinal optimisation [65], are also applied to solve optimisation problems. Compared to analytical algorithms, numerical algorithms are based on numerical calculation but not mathematical analysis. They are more complicated, and more computation time is needed due to searching process is needed. Thanks to the development of computer technologies, it makes numerical methods efficient and feasible. However, it also has several limitations. Numerical methods may only find local optima but not global optimal results. Another drawback is that the feasibility of

dynamic programming has an important premise, which means that a clear objective function must be given. It is inefficient to solve some real-world problems as it is impossible to generate explicit objective functions in some cases [60].

3.2.3 Heuristic Methods

Comparing to analytical and numerical methods, heuristic-based methods provide possible ways to solve more complex and large-scale problems, which are impossible to be solved by using the technologies mentioned above. It is a kind of 'trial-and-error' method, which is to find optimal results by trials and errors, so it cannot guarantee to get the best solution, but it provides an effective and fast way to find a satisfactory solution. Until now, many heuristic methods are proposed and widely used to solve optimisation problems in different aspects, and most of these methods are named after the mechanism of related algorithms, which are based on animals' or humans' behaviors. In this subsection, some popular heuristic algorithms are introduced.

Harmony search is a metaheuristic method, which simulates the improvisation of jazz musicians. This optimisation algorithm was proposed by Zong Woo Geem in 2001 [66]. It is to find a perfect harmony (the optimal result) based on aesthetic standards (objective functions) from various combination of pitches (variables). The optimisation process of harmony search includes four steps:

Step 1: Initialize harmony memory (HM) which contains a given number of possible solutions.

Step 2: Based on harmony memory considering rate and pitch adjusting rate, a new harmony is generated. (Harmony memory considering rate is the probability of choosing a member from present harmony memory and pitch adjusting rate is the mutation rate of the chosen member.)

Step 3: Update harmony memory. If the new harmony formed in step 2 is better than the worst harmony in HM, it will replace the worst one. Otherwise, it is eliminated.

Step 4: Repeat the procedure of step 2 and step 3 until a termination criterion is met.

Particle swarm optimisation is inspired by behaviours of a bird flock or fish school in nature. It was proposed by Kennedy and Eberhart in 1995 [67]. This method is to guide particles (candidate solutions) to move towards the best position in searching space based on position and velocity. New velocity v'_i and new position x'_i are expressed as

$$v'_i = v_i + a\varepsilon_1\left(x_i - g^*\right) + b\varepsilon_2\left(x_i - x_i^*\right) \tag{3.20}$$

$$x'_i = x_i + v_i \tag{3.21}$$

where v_i and x_i is the velocity and position of particle *i*. g^* is the current global best of all particles, and x_i^* is the individual best solution of particle *i* obtained so far. ε_1 and ε_2 are acceleration random vectors, which pull particles toward the best solution. *a* and *b* are called learning factors, which are constant. As particles are closer to optima, the motion and randomness of *a* and *b* decrease [68].

It can be found that there are two important parameters in this algorithm, i.e. global best g^* and local best known x_i^*. Both of them guide particles approach the best solutions. Besides, there is another key parameter, the maximum velocity v_{max}, which limits the variation of v_i' and it should be carefully selected. If v_{max} is too big, optimisation will converge too quickly. The optimal solution may be missed. If v_{max} is too small, optimisation will converge too slowly due to huge searching space. It leads to a long computing time.

Artificial bee colony was proposed by Karaboga in 2005 [69]. It is inspired by the foraging behavior of honey bees. There are three roles in this method: employed bees, onlookers and scouts. Employed bees are responsible for looking for food sources (candidate solutions). According to information of nectar (fitness) from employed bees, onlookers choose a food source. The food source with high quality has a big chance to be selected by onlookers. When the food resource found by employed bees is

abandoned, employed bees become scouts, then scouts begin to explore and search for new food sources.

The procedure of artificial bee colony can be explained as: Firstly, generating initial population with N food sources. N is swarm size. Based on memories, each employed bee goes to food sources and chooses the closest food source, then it sends this message to onlookers through dancing. Secondly, each onlooker selects a food source and goes to that source. Thirdly, neighborhood food sources v_{ik} are found according to previous memories,

$$v_{ik} = z_{ik} + \phi_{ik}\left(z_{ik} - z_{mk}\right) \tag{3.22}$$

where z_{ik} is the ith solution of the swarm with a dimension of D. $m \in [1, 2, ..., N]$, and $k \in [1, 2, ..., D]$ are two random selected indexes, and m must be different from i. z_m is a randomly selected solution. ϕ_{ik} is a random number within [-1,1]. When solutions approach to optimal solutions, the difference between z_{ik} and z_{mk} becomes smaller. Accordingly, the step length of search decreases.

Fourthly, onlooker bees evaluate nectar amount of food sources, and then select food sources which need to be abandoned. The abandoned food sources are selected based on the value of p_i, and p_i is defined as

$$p_i = \frac{f_i}{\sum_{n=1}^{N} f_n} \tag{3.23}$$

where f_i is the fitness of solution i, N is the total number of food sources, which is equal to the number of employed bees.

Fifthly, some employed bees become scouts, and they start to find new sources to replace the ith solution according to

$$x_{ik} = lb_k + rand\,(0,1)\cdot(ub_k - lb_k) \tag{3.24}$$

where lb_k and ub_k are lower and upper boundaries of kth dimension. Based on the normal distribution, *rand* (0,1) is a random number between [0,1].

Sixthly, update the best solution obtained so far. The process except initialization is repeated until a terminating condition is met.

Genetic algorithm (GA) is another popular heuristic method, and it is based on evolutionary of natural selection and genetics [70]. In GA, each possible solution is named as a chromosome. Each variable is a gene of the chromosome. The number of genes is always equal to the number of variables. There are several steps for implementation of GA. Firstly, initial population is generated, which refers to randomly generating a number of chromosomes (the number of chromosomes is always 30 or 100), the number of chromosomes is called population size in GA. Secondly, calculating fitness for each chromosome. Thirdly, a new population, which is named as offspring population is generated based on selection, crossover and mutation operators. There are many ways to implement these three operators. Generally, the chromosome with a better fitness has higher probability to be selected in selection operator. The chromosome diversity increases in crossover and mutation operators, but crossover and mutation do not happen for each chromosome. Distinct settings of crossover and mutation rates are defined as follows [71]:

- For a small population size, such as 30, crossover and mutation rates can be set to 0.9 and 0.01 respectively;
- For a large population size, such as 100, crossover and mutation rates can be set to 0.6 and 0.001 respectively.

All these steps discussed above can be seen as an iteration, and it is called a generation in GA. This process is repeated until a terminating condition is reached. Common terminating conditions include: computation time limits, the maximum generation number, fitness criteria and so on [71].

Comparing to numerical methods, GA has many advantages:

- It is more efficient as it can search multiple points in parallel instead of one point;
- It has a greater probability to find the local optimal result due to the randomness of initial population and the diversity of population during searching process;
- It is more versatile, which means it can be applied to solve many kinds of complex optimisation problems, especially for the problems which do not have full information of objective functions, as it only uses fitness information to measure the performance without derivatives or other information in searching process.
- It uses probabilistic transition instead of deterministic rules, the search is multidirectional and there is no unified connection between generations. Base on crossover and mutation in searching process, random transition is used as a tool to ensure improvement among iterations.
- It expresses variable sets as fixed-length chromosomes and it works in coded form instead of solving parameters, so it has good operability for solving different problems.

To solve the DG allocation problem with many variables and complicated objective functions, GA is a good candidate method. Although GA is easy to be implemented as it has inherent parallelism, it also has several drawbacks. For example, the execution time of GA is very long, but for DG planning, this issue is not very important. Although it cannot guarantee to find the local best solution but it tends to converge towards good regions with high fitness [60]. It is found that GA is one of the most popular optimisation methods for DG allocation [61]. Moreover, some studies state that the population-based heuristic algorithms, such as GA, are more efficient for solving multiobjective and multimodal problems due to parallel searching characteristics [68].

Suitable algorithms are very important tools to solve optimisation problems as they affect the efficiency of calculation as well as the effectiveness and accuracy of solutions. As discussed at the beginning of this section, in addition to optimisation algorithms, variables selection, constraint setting and objective formulation are also

vital steps in the optimisation, but these steps should be chosen and set according to specific optimisation problems. The problem formulation for DG allocation is detailed discussed in Chapter 5.

3.3 Summary

To solve the two-phase strategy proposed in Chapter 2, a review of related techniques is discussed in this chapter, including complex network theories and optimisation methodologies.

Complex network theories are applied to analyse many networks by simplifying networks to a number of nodes connecting with edges. For most of complex networks, topological information or weight distribution is used to describe characteristics of networks. However, these representations cannot reflect special characteristics of electrical networks. For electrical networks, both distance and capacity should be considered as weight. By analysing different concepts which have been used to describe distance and capacity respectively, the definition of net-ability gives a good way to express the relationship between equivalent impedance (distance) and power transmission capacity (capacity) in electrical networks, which is the basic idea to define ECS in Chapter 4. To find a suitable method to determine boundaries of VMs, a variety of community detection methods are introduced. Comparing to partitional clustering and hierarchical clustering methods, modularity-based methods, especially the greedy optimisation method proposed by Newman, are more effective to partition electrical networks and give accurate and flexible solutions.

Optimisation technologies are popular tools to find the optimal solutions according to specific objective functions. To select a suitable optimisation method to solve DG allocation problem, three kinds of optimisation algorithms are discussed, including analytical methods, numerical methods and heuristic methods. Among these three kinds of algorithms, heuristic algorithms are more effective than the other two kinds of algorithms considering the scale and complexity of optimisation problems in electrical networks. Among heuristic algorithms, GA is one of the most popular

methods, and it has inherent parallelism based on efficient parallel searching. What is more, crossover and mutation operators can guarantee the variety and improvement of solutions in optimisation process. Based on GA, an optimisation method for optimising DG allocation is explained in Chapter 5.

Chapter 4
Hierarchical Partitioning of Virtual Microgrids Based on Structure Information

4.1 Introduction

To develop CDNs to SDNs, constructing VMs is a good way to integrate DGs and improve the flexibility and efficiency of power systems. According to the two-phase strategy which is proposed in Section 2.3.3, phase 1 is to partition CDNs, and determine VM boundaries. Therefore, selecting a suitable partitioning method for CDNs is very important.

Community detection technologies in complex networks can be applied to partition electrical networks, and Section 3.1 reviewed many methods for community detection. Some partitioning methods are also proposed to partition distribution networks, which is discussed in Section 4.2. Although many partitioning methods are proposed to partition electrical networks, until now, there is no widely accepted standard approaches for partitioning and operation of VMs. Based on partitioning methods for community detection, in this chapter, a structural and hierarchical partitioning method is proposed. By using this partitioning method, not only boundaries for VMs but also dynamic boundaries can be detected.

4.2 Partitioning Methods for Distribution Networks

To upgrade CDNs and improve the function of distribution networks, several partitioning methods for distribution networks have been proposed. An optimal construction was proposed in [72], this construction was based on minimising power imbalance between generations and loads by considering the probabilistic nature of DGs, distributed energy storage resources (DGRs), and distributed reactive sources. Besides these factors, in [30], the reliability and supply-security were also taken into

consideration to optimise the construction of distribution networks. Using non-dominated genetic algorithm-Ⅱ, Haddadian and Noroozian presented a two-step partitioning method [26]. Firstly, energy storage devices were used to determine boundaries of multi-microgrids, and then operation quality was tested by considering several technical indices, including adequacy, efficiency, voltage and reliability. Buayai, Ongsakul and Mithulananthan [73] proposed a two-stage multi-objective partitioning method. The optimal detection of partitioned units was based on analysing the loss sensitivity factor firstly, and then optimising the size and location of DGs by Pareto-based non-dominated sorting genetic algorithm II. Kirthiga *et al.* in [74] introduced a method to develop autonomous microgrids based on particle swarm optimisation and genetic algorithm. In this method, the location and size of DGs were determined firstly, then virtual boundaries of microgrids were identified by the analysis of power flow. In order to improve self-adequacy of distribution networks, dynamic boundaries of microgrids were used as variables in [75]. In this paradigm, the size and location of DGs were given, and dynamic boundaries of microgrids were determined based on the transmission lines with the lightest power flow according to different scenarios.

The main function of conventional distribution networks is to distribute electrical power to customers, therefore, for most of existing distribution networks, there is no resource allocation of DGs. Although there are many partitioning methods which are already proposed for partitioning distribution networks [26], [30], [72]–[75], in these models, resource allocation of DGs is assumed to be given, and these methods are based on analysing operating states. In fact, besides resource allocation, another important factor which determines operating states is network structure. In addition, special characteristics of VMs are also very important for constructing VMs. For example, VMs are self-sufficient and autonomous systems. Therefore, VMs should have some features from the structural point of view, which refers to dense electrical connection inside their own systems while relatively sparse electrical connection between VMs. This feature can also meet the goal of power transmission, which refers

to transmitting the maximum power with the least losses. What is more, for CDNs, network structure is already formed, and it is unlikely to be changed much, but resource allocation of DGs is an evolutionary process. Hence, it is more reasonable to partition VMs based on the analysis of inherent characteristics of network structure, and it is more feasible to upgrade CDNs in which resource allocation of DGs is not performed yet. Therefore, rather than analysing operating states based on given resource allocation, network structural characteristics are used to identify boundaries of VMs in phase 1. ECS is defined to describe structural characteristics and identify boundaries of VMs. Based on partitioned networks, in the next chapter, the optimisation method of DG allocation for phase 2 is discussed.

4.3 Electrical Coupling Strength

As the partition based on structural characteristics is more reasonable and meaningful, it is necessary to find a suitable way to describe structural characteristics and electrical connection of distribution networks in terms of following three problems.

- *In complex networks, adjacent matrix is used to describe the characteristics of connection. But for distribution networks, what quantities should be considered for the definition of weight index?*
- *If the number of quantities for weight index is more than one, how to define the composite weight index?*
- *To incorporate the characteristics of electrical networks where power flows through different routes between two buses, how to describe and define the equivalent weight index?*

In following parts, these problems are discussed and solved one by one.

- *In complex networks, adjacent matrix is used to describe the characteristics of connection. But for distribution networks, what quantities should be considered for the definition of weight index?*

As discussed in Section 3.1, for many complex networks, community detection methods are always based on topological analysis. It is not reasonable to straight apply these methods to partition distribution networks. For distribution networks, both electrical distance and transmission capacity should be important quantities to define the weight index. The smaller electrical distance is, the less voltage drop and power losses are. The larger transmission capacity is, the more power lines can transmit. Therefore, the definition of weight index should be based on these two quantities, i.e. electric distance and transmission capacity, to realise the goal to transmit the maximum power with the least losses.

- *If the number of quantities for weight index is more than one, how to define the composite weight index?*

So far, most of weight indexes in complex networks usually consider one quantity, for example the interpersonal relationship in social networks, the energy between predators and preys in food chain networks [45]. However, for the partition of distribution networks, two quantities should be taken into account at the same time.

As introduced in Section 3.1.1, net-ability provides a good way to describe the inversely proportional relationship between capacity and distance. The bigger the capacity is and the smaller the distance is, the electrical connection is stronger. However, it only considers the paths between generation nodes and load nodes. For most of CDNs without DG allocation, all nodes can be seen as candidate nodes for DG installation. What is more, the scale difference between these two quantities should be considered as it may result in the value of electrical connection being only sensitive to C^d_g or Z^d_g. Therefore, considering the electrical connection between any pair of nodes, these two quantities are redefined by normalising their values based on average,

$$\overline{C}_{vw} = \frac{C_{vw}}{\overline{C}} \qquad v, w \in \mathrm{B} \tag{4.1}$$

$$\overline{Y}_{vw} = \frac{Y_{vw}}{\overline{Y}} = \frac{1/Z'_{vw}}{\overline{Y}} \qquad v, w \in \mathrm{B} \tag{4.2}$$

where C_{vw} is transmission capacity between any two nodes, i.e. node v and node w. Z'_{vw} is the electrical distance between node v and node w, and Y_{vw} is the reciprocal of Z'_{vw}. $\overline{C}$ and $\overline{Y}$ are average values of the total transmission capacity and total electrical distance in the same network. B refers to all the buses in the network.

In order to obtain different partitioning results according to different purposes and improve the flexibility of upgrading strategies, the weight proportions of the two quantities can be changeable, thus, the composite weight index $\overline{E}_{vw}$ is defined as

$$\overline{E}_{vw} = \left| \alpha \overline{Y}_{vw} + j\beta \overline{C}_{vw} \right| \qquad v, w \in \mathrm{B} \tag{4.3}$$

where α and β are proportion coefficients, and $\alpha + \beta = 1$. B is the set of nodes. The relationship for different values in this equation can be clearly seen in Fig. 4.1, which is similar to the relationship of impedance, resistance and reactance.

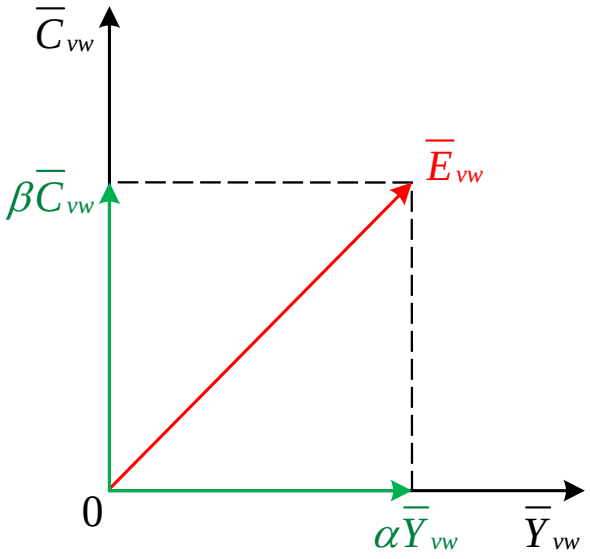

Fig. 4.1 The relationship of different values in the composite weight index.

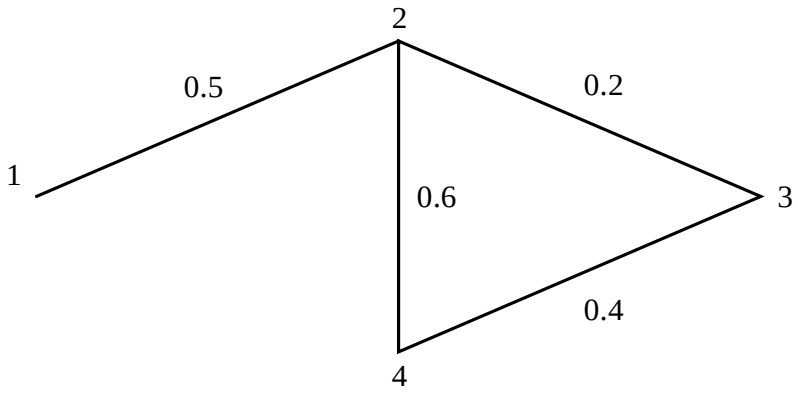

Fig. 4.2 A simple distribution network.

- *To incorporate the characteristics of electrical networks where power flows through different routes between two buses, how to describe and define the equivalent weight index?*

In complex networks, sometimes, it is necessary to analyse weighted networks, but only directly connected lines are considered [45], [76]. It is different from distribution networks due to specific electrical characteristics. For distribution networks, the power flows on not only directly connected transmission lines but also indirectly connected transmission lines. Taking the network shown in Fig. 4.2 as an example, the numbers on transmission lines are impedance values. Assuming transmission capacity for all lines are identical, if certain amount of power is injected from bus 2 and it withdraws from bus 4, the power will not only flow on the directly connected transmission line $l_{2\text{-}4}$ but also on the indirectly connected lines $l_{2\text{-}3}$ and $l_{3\text{-}4}$. Consider the impact from $l_{2\text{-}3}$ and $l_{3\text{-}4}$, it can be easily seen that the parallel impedance between bus 2 and bus 4 ($\frac{0.6*(0.2+0.4)}{0.6+(0.2+0.4)}=0.3$) is smaller than the impedance directly connecting bus 2 and bus 4 (0.6), so the value of ECS between bus 2 and bus 4 is bigger than that just considering directly connecting line $l_{2\text{-}4}$. It has a great impact on the evaluation of electrical connection between these two buses. Therefore, when calculating the composite weight index between any two buses, all possible lines for power

transmission should be considered, so it is better to use equivalent values of electrical distance Z'_{vw} and transmission capacity C_{vw}.

In electrical theories, equivalent impedance is an importance concept which can be used to measure the impedance between any two buses, including all transmission lines no matter they are directly connected or indirectly connected. Some studies use this concept to represent electrical distance [41], [77].

Imaging there are n buses in an electrical network, the network can be expressed as

$$\begin{bmatrix} \dot{U}_1 \\ \dot{U}_2 \\ \vdots \\ \dot{U}_v \\ \vdots \\ \dot{U}_w \\ \vdots \\ \dot{U}_n \end{bmatrix} = \begin{bmatrix} Z_{11} & Z_{12} & \cdots & Z_{1v} & \cdots & Z_{1w} & \cdots & Z_{1n} \\ Z_{21} & Z_{22} & \cdots & Z_{2v} & \cdots & Z_{2w} & \cdots & Z_{2n} \\ \vdots & \vdots & & \vdots & & \vdots & & \vdots \\ Z_{v1} & Z_{v2} & \cdots & Z_{vv} & \cdots & Z_{vw} & \cdots & Z_{vn} \\ \vdots & \vdots & & \vdots & & \vdots & & \vdots \\ Z_{w1} & Z_{w2} & \cdots & Z_{wv} & \cdots & Z_{ww} & \cdots & Z_{wn} \\ \vdots & \vdots & & \vdots & & \vdots & & \vdots \\ Z_{n1} & Z_{n2} & \cdots & Z_{nv} & \cdots & Z_{nw} & \cdots & Z_{nn} \end{bmatrix} \begin{bmatrix} \dot{I}_1 \\ \dot{I}_2 \\ \vdots \\ \dot{I}_v \\ \vdots \\ \dot{I}_w \\ \vdots \\ \dot{I}_n \end{bmatrix} \tag{4.4}$$

where $\dot{U}_1, \dot{U}_2, \cdots, \dot{U}_v, \cdots, \dot{U}_w, \cdots, \dot{U}_n$ are node voltage; $Z_{11}, Z_{12}, \cdots Z_{nn}$ are elements in the impedance matrix. $\dot{I}_1, \dot{I}_2, \cdots, \dot{I}_v, \cdots, \dot{I}_w, \cdots, \dot{I}_n$ are injection current at nodes.

If one unit of current is injected at node v and withdraws from node w, Equation (4.4) can be updated to

$$\begin{bmatrix} \dot{U}_1 \\ \dot{U}_2 \\ \vdots \\ \dot{U}_v \\ \vdots \\ \dot{U}_w \\ \vdots \\ \dot{U}_n \end{bmatrix} = \begin{bmatrix} Z_{11} & Z_{12} & \cdots & Z_{1v} & \cdots & Z_{1w} & \cdots & Z_{1n} \\ Z_{21} & Z_{22} & \cdots & Z_{2v} & \cdots & Z_{2w} & \cdots & Z_{2n} \\ \vdots & \vdots & & \vdots & & \vdots & & \vdots \\ Z_{v1} & Z_{v2} & \cdots & Z_{vv} & \cdots & Z_{vw} & \cdots & Z_{vn} \\ \vdots & \vdots & & \vdots & & \vdots & & \vdots \\ Z_{w1} & Z_{w2} & \cdots & Z_{wv} & \cdots & Z_{ww} & \cdots & Z_{wn} \\ \vdots & \vdots & & \vdots & & \vdots & & \vdots \\ Z_{n1} & Z_{n2} & \cdots & Z_{nv} & \cdots & Z_{nw} & \cdots & Z_{nn} \end{bmatrix} \begin{bmatrix} 0 \\ 0 \\ \vdots \\ 1 \\ \vdots \\ -1 \\ \vdots \\ 0 \end{bmatrix} \tag{4.5}$$

The equivalent impedance between node v and node w Z'_{vw} can be derived from Equation (4.5)

$$Z'_{vw} = Z_{vv} + Z_{ww} - 2Z_{vw} \tag{4.6}$$

Therefore, for a given electrical network, the equivalent impedance between any two nodes can be calculated. In this thesis, equivalent impedance is used to represent equivalent electrical distance between nodes. C_g^d

As discussed in Section 3.1.1, real power transmission capacity C_g^d is a good way to represent the capacity between any two nodes, however, it only considers the power transmission between generator nodes and load nodes. If ignoring bus types, which means any bus can be either a generator node or a load node, for any pair of nodes in a network, C_g^d can be updated to

$$C_{vw} = \min\left(\frac{p^l_{\max}}{|f^l_{vw}|}\right), \qquad v, w \in \mathrm{B},\ l \in \mathrm{L} \tag{4.7}$$

where L is the set of lines. $p^l_{\max}$ is the transmission limit on line l. f^l_{vw} is the power change on line l when a unit of power is injected to node v and withdraws from node w, and it can be calculated based on Power Transfer Distribution Factors (PTDF), which is a $N_L \times N_B$ matrix and measures the sensitivity of power change on lines when a unit of power is injected to a couple of buses and withdraws from the reference bus. Thus, each element f_{lv} in the PTDF means the power change on line l when a unit power is injected to bus v and withdraws from the reference bus. f^l_{vw} can be expressed as [48]

$$f^l_{vw} = f_{lv} - f_{lw}, \qquad l \in L \tag{4.8}$$

Based on the discussion above, ECS matrix is defined to describe electrical connection from the structural point of view, and the element in the ECS matrix A_{vw}^{E} is expressed as

$$A_{vw}^{E} = \bar{E}_{vw} \tag{4.9}$$

4.4 Partitioning Based on Electrical Modularity

As discussion in Section 3.1.2, the buses within VMs have stronger electrical connection from the structural perspective, which is similar to structural characteristics of communities. Considering the merits of modularity-based community detection methods, in this chapter, Newman Fast Algorithm (the greedy optimisation method) which is based on modularity [56] is chosen to solve VM partitioning. Modularity is further improved by proposing the electrical modularity which is more suitable for distribution networks.

4.4.1 Electrical Modularity

For community detection in complex networks, Newman proposed to use modularity to judge the quality of partitioning [76]. If modularity is bigger, it means the nodes which are in the same community are densely connected with each other, while the nodes which are in different communities have sparse connection with each other. Therefore, the bigger the modularity is, the better the partition is. The definition of modularity Q is defined in Equation (3.15). However, this modularity index can only be applied to unweighted networks, and it is unsuitable for partitioning weighted distribution networks. In [45], Newman proposed an algorithm for weighted network, but it is not suitable for describing the electrical characteristics as discussed in Section 4.3. Therefore, according to the definition of ECS and modularity, electrical modularity Q_e is proposed to judge the partitioning quality of CDNs, and it is expressed as

$$Q_e = \sum_{v,w \in B} \left[\frac{A_{vw}^E}{2M} - \frac{A_v^E}{2M} \cdot \frac{A_w^E}{2M} \right] \delta(C_v, C_w) \tag{4.10}$$

$$A_v^E = \sum_{i \in B} A_{vi}^E \tag{4.11}$$

$$M = \frac{1}{2} \sum_{vw} A_{vw}^E \tag{4.12}$$

where A_v^E is defined as the ECS degree of bus v, and it is equal to the sum of ECS connecting to bus v. Similarly, A_w^E is the ECS degree of bus w. M is the sum of ECS in the whole distribution network.

The meaning of electrical modularity can be explained as: for a given network G, if one unit of ECS is randomly taken from it, the probability of this unit of ECS connecting between bus v and bus w can be explained by considering the following two events:

(1) One side of the unit of ECS is connected with bus v.

(2) The other side of this unit of ECS is connected with bus w.

The probability for event (1) should be $\frac{A_v^E}{2M}$. As in the given network G, the ECS A_{vw}^E between bus v and bus w is already known, so event (2) is not independent from event (1). When event (1) is true, the probability of event (2) is $\frac{A_{vw}^E}{A_v^E}$. Therefore, the probability of the selected unit of ECS connecting bus v and bus w is equal to $\frac{A_v^E}{2M} \cdot \frac{A_{vw}^E}{A_v^E} = \frac{A_{vw}^E}{2M}$.

Similarly, imaging there is a benchmark network R. In this network, the number of buses, ECS degree and total ECS are exactly the same with those in G, however, the distribution of ECS is random. If one unit of ECS is randomly taken from this network,

the probability of event (1) is also equal to $\frac{A_v^E}{2M}$. However, as the distribution of ECS is random, event (2) and event (1) are independent, so the probability of event (2) is $\frac{A_w^E}{2M}$. Therefore, the probability for the selected unit of ECS connecting bus v and bus w is $\frac{A_v^E}{2M} \cdot \frac{A_w^E}{2M}$.

Consequently, according to the definition in Equation (4.10), the electrical modularity is based on calculating the probability difference of the randomly selected units of ECS between the given network G and the benchmark network R. The stronger the electrical connection between nodes is, the higher the probability in the given network G is compared to the corresponding probability in the benchmark network R (the bigger the probability difference Q_e is). Therefore, the optimal partitioning can be determined by seeking the partitioning results with the maximum Q_e. In the following section, a detailed explanation for bus grouping is given.

4.4.2 Hierarchical Partitioning for Boundary Detection

As discussed in Section 4.4.1, although Newman Fast Algorithm is popular, it is not suitable for partitioning distribution networks considering electrical characteristics, so Equation (3.15) is developed to Equation (4.10). According to main steps of the partitioning method proposed in [76], partitioning process is improved by replacing modularity Q by electrical modularity Q_e, and it is more suitable for partitioning electrical networks. The overall partitioning process is shown in Fig. 4.3. In the updated algorithm, one step (the last step) is added to determine dynamic boundaries in order to maintain self-adequacy, detailed characteristics of dynamic boundaries are discussed in [75]. According to practical engineering conditions and constraints, a possible acceptable range of VM number is assumed to be the value between N_a and N_b ($1 < N_a < N_b < N$), N is a variable number being the VM number in each step, and

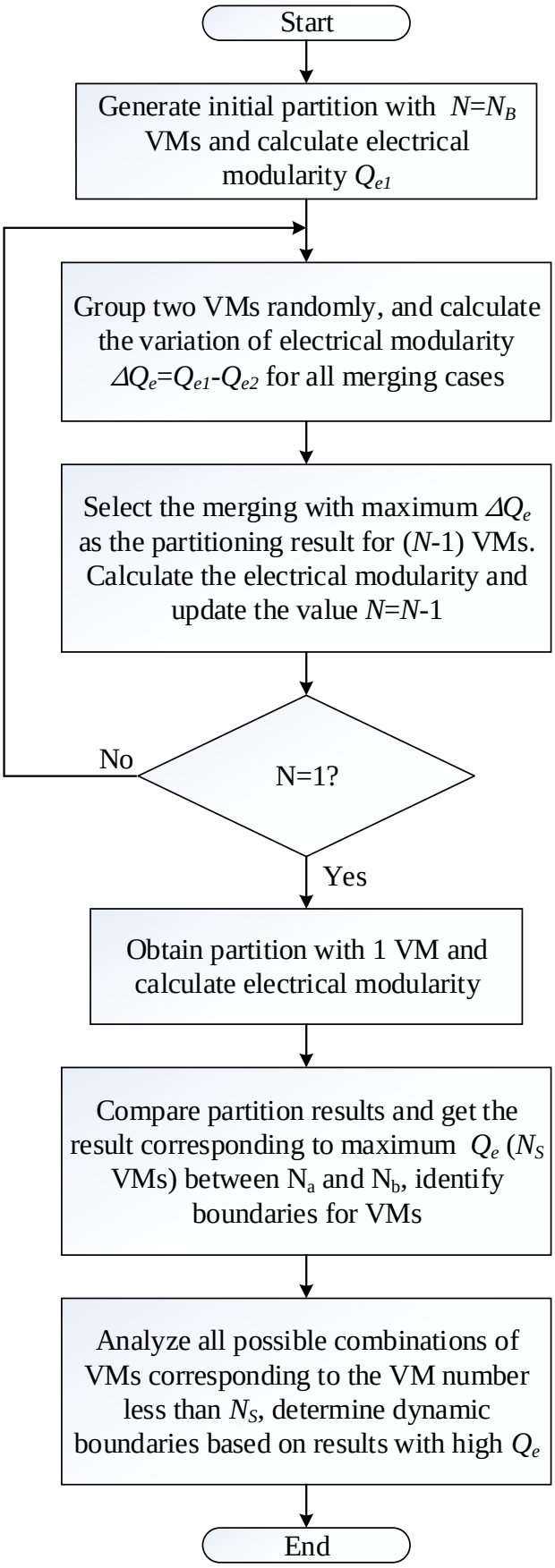

Fig. 4.3 The partitioning process based on electrical modularity.

N_B is the total bus number in a distribution network. Q_e is calculated based on Equation (4.10).

4.5 Results and Discussions

In this section, the hierarchical partitioning method based on electrical modularity is applied to several networks, including IEEE 33-bus distribution network [35], 94-node Portuguese distribution network [78] and PG&E 69-bus distribution network [36], in MATLAB based on Octave toolbox [79]. Here, the weight proportions for electrical distance and transmission capacity (α and β) are equal to 0.5, and the calculation of electrical distance is on the basis of reactance but ignore resistance as resistance is much less than reactance for transmission lines. For each distribution network, power limit of all transmission lines is assumed to be the same, which is a common assumption for real distribution networks.

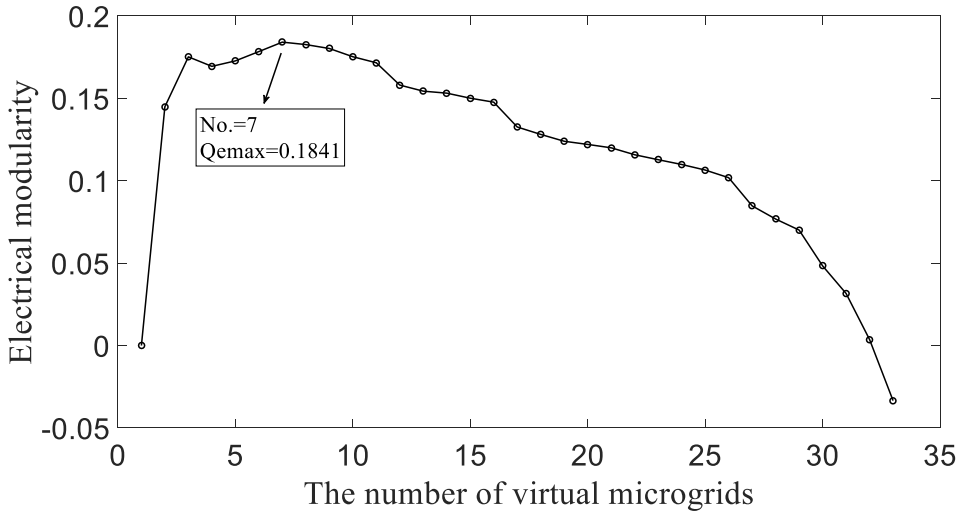

Fig. 4.4 The value of electrical modularity with different numbers of VMs in IEEE 33-bus distribution network.

4.5.1 IEEE 33-bus Distribution Network

Before applying the partitioning method to IEEE 33-bus distribution network, ECS is calculated using Equation (4.9). After that, electrical modularity is calculated for all possible numbers of VMs as shown in Fig. 4.4. From Fig. 4.4, it can be seen that the electrical modularity reaches to its maximum value (0.1841) when the number of VMs is equal to 7. It is regarded as the best partition result, and this result is used to determine boundaries of VMs as shown in Fig. 4.5 (a).

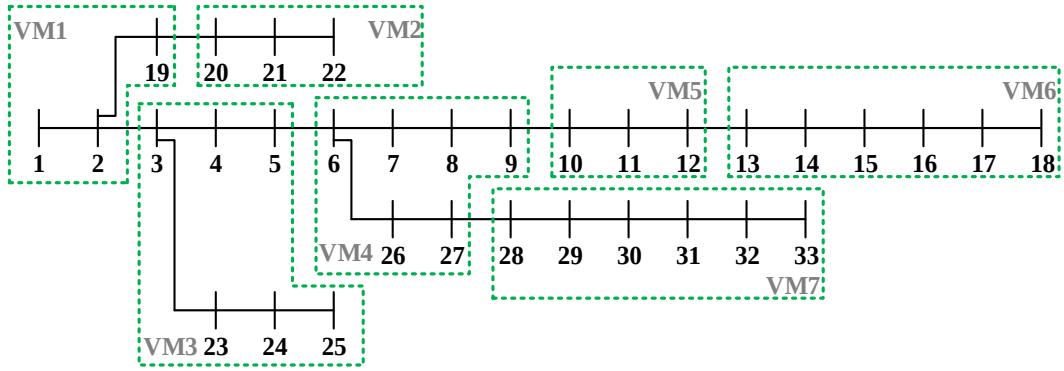

(a)

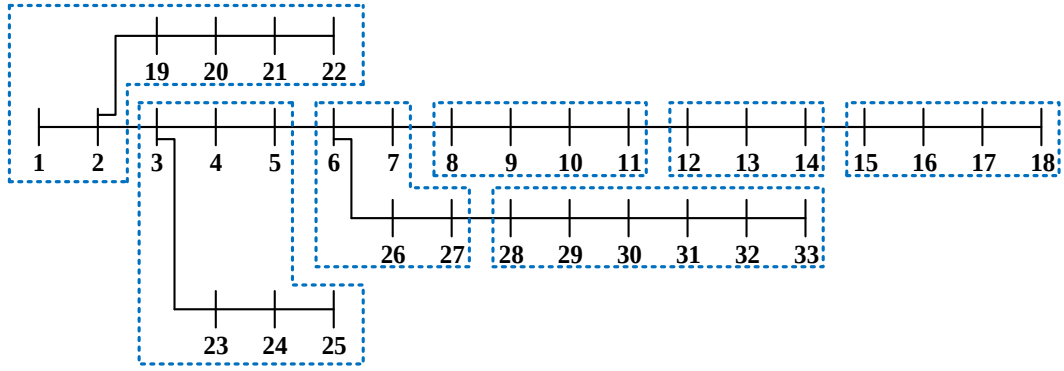

(b)

Fig. 4.5 Partitioning results of IEEE 33-bus distribution network. (a) Results based on the hierarchical partitioning method (Q_e = 0.1841); (b) Results based on the partitioning method in [26] (Q_e = 0.1519).

Power transmission should happen on transmission lines with strong electrical connection in order to reduce losses and improve efficiency. Because the maximum power limit of transmission lines is same, so electrical connection is mainly

determined by reactance, and transmission lines with big reactance should be determined as boundaries. Comparing partitioning results based on the hierarchical partitioning method in this chapter with that using the partitioning method in [26], several boundary differences of VMs can be seen clearly. Taking $l_{19\text{-}20}$ which is the boundary between VM1 and VM2 as an example, it is a line with big reactance (0.0112) and small ECS value, so $l_{19\text{-}20}$ is reasonable to be identified as the boundary between VM1 and VM2, but $l_{19\text{-}20}$ is not determined as the boundary in Fig. 4.5 (b). Other boundary differences can be found near VM5 and VM6. $l_{9\text{-}10}$ and $l_{12\text{-}13}$ are boundaries in Fig. 4.5 (a) while $l_{11\text{-}12}$ and $l_{14\text{-}15}$ are boundaries in Fig. 4.5 (b). Comparing the reactance value of these lines, the reactance of $l_{9\text{-}10}$ (0.0061) and $l_{12\text{-}13}$ (0.0095) is obviously bigger than that of $l_{11\text{-}12}$ (0.0010) and $l_{14\text{-}15}$ (0.0043), and the ECS of $l_{9\text{-}10}$ and $l_{12\text{-}13}$ is smaller than that of $l_{11\text{-}12}$ and $l_{14\text{-}15}$. Finally, the quality of the partition is analysed by comparing the value of electrical modularity. After calculation, the electrical modularity in Fig. 4.5 (a) is 0.1841 while the electrical modularity in Fig. 4.5 (b) is 0.1519, so it can be concluded that the partitioning result based on hierarchical partitioning method is more reasonable from structural point of view.

Table 4.1 Data of IEEE 33-bus distribution network

From Bus	To Bus	Reactance (p.u.)	ECS
19	20	0.0112	0.8146
9	10	0.0061	1.2796
11	12	0.0010	7.0582
12	13	0.0095	0.9053
14	15	0.0043	1.7309

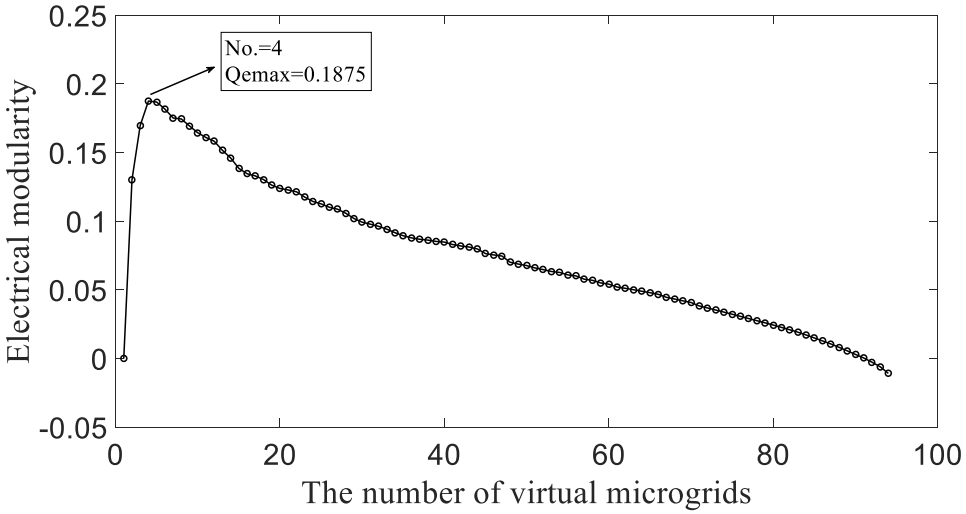

Fig. 4.6 The value of electrical modularity with different numbers of VMs in 94-nodes Portuguese distribution network.

4.5.2 94-node Portuguese Distribution Network

The partitioning method is also applied to 94-node Portuguese distribution network, and Fig. 4.6 shows electrical modularity with different VM numbers in the whole partitioning process. It can be seen that the maximum Q_e is obtained when there are 4 communities, and corresponding VM boundaries are drawn in Fig. 4.7 (a). Fig. 4.7 (b) shows another partitioning result which is based on the analysis of operating states, including power flow, voltage, etc. [26]. Taking the longest line from node 1 to node 33 as an example, the difference between these two results is analysed. The reactance and ECS on VM boundaries are listed in Table 4.2. In Fig. 4.7 (a), $l_{9\text{-}10}$, $l_{10\text{-}11}$ and $l_{17\text{-}18}$ are determined as boundary lines, while in Fig. 4.7 (b), $l_{11\text{-}12}$, $l_{18\text{-}19}$, $l_{24\text{-}25}$ and $l_{26\text{-}27}$ are boundary lines. It can be found that the boundaries in Fig 4.7 (a) have smaller ECS values (1.4550, 0.9188 and 1.7035) compared to those in Fig. 4.7 (b) (6.2647, 5.4775, 4.4861 and 6.1212). Considering the characteristic of electrical connection, it is better to determine the lines with a weak connection (small ECS values) as boundaries. What is more, the electrical modularity in Fig. 4.7 (b) is 0.1458, which is lower than that in Fig. 4.7 (a) (0.1875). Hence, the partitioning result in Fig. 4.7 (a) can better reflect structural characteristics of the network.

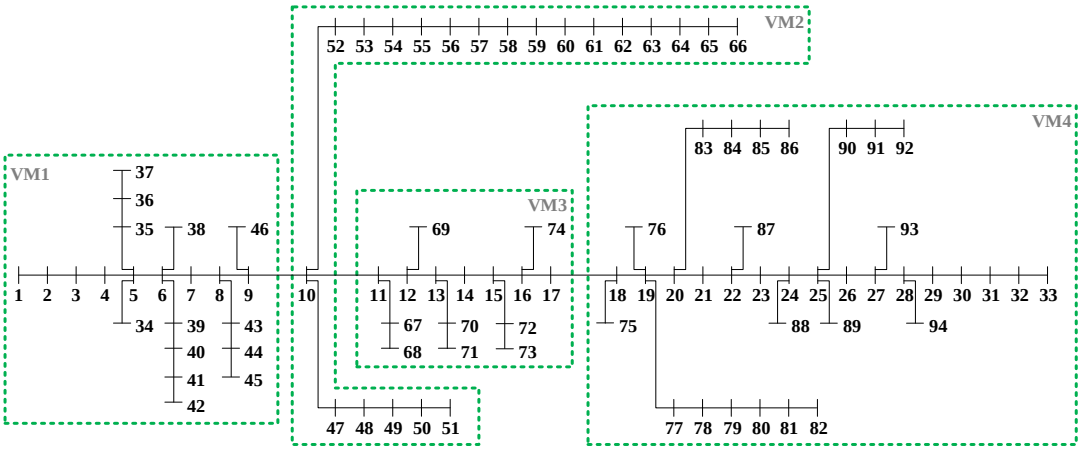

(a)

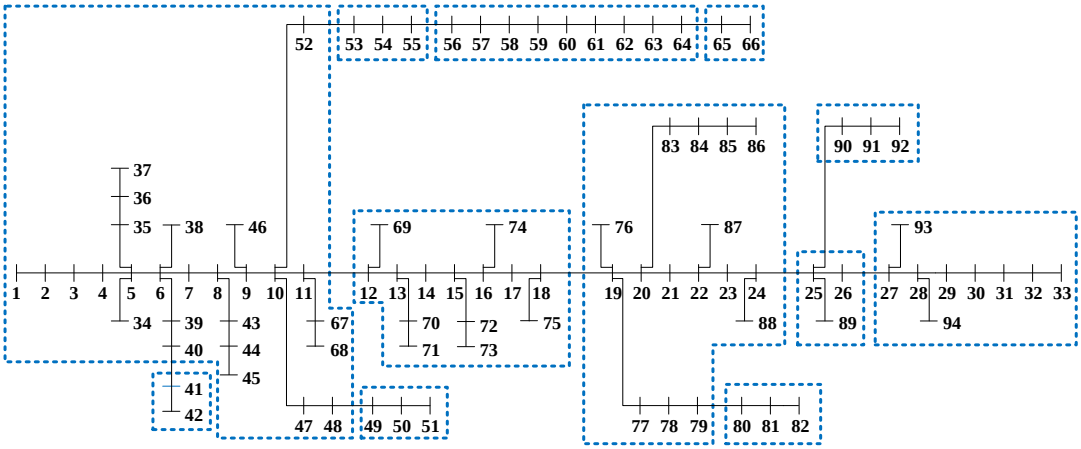

(b)

Fig. 4.7 Partitioning results of 94-node Portuguese distribution network. (a) Results based on the hierarchical partitioning method (Q_e = 0.1875); (b) Results based on the partitioning method in [26] (Q_e = 0.1458).

As discussed in Section 4.2, there are two goals for power transmission. One goal is to transmit electrical power with the least losses, which is mainly determined by electrical distance. The other goal is to transmit as much power as possible, which is mainly determined by transmission capacity. To analyse the impact of transmission capacity on ECS values and partitioning results, the transmission limit on $l_{7\text{-}8}$ is changed from 990 kVA to 9.9 kVA. Corresponding results are shown in Fig. 4.8 and Fig. 4.9. Due to the reduction of transmit limit, the ECS on $l_{7\text{-}8}$ changes from 2.3852 to 2.3323. As the electrical connection between node 7 and node 8 becomes weaker,

$l_{7\text{-}8}$ is detected as a boundary as shown in Fig. 4.9. It can be found that the maximum Q_e is 0.1946 with 6 VMs in this case. As mentioned before, the definition of ECS considers the electrical connection between any pair of nodes, so the change of transmit limit affects the ECS not only on $l_{7\text{-}8}$ but also on other lines with one side connected to node 7 and node 8. ECS variation is presented in Fig. 4.10. That is the reason why there are many boundary changes in Fig. 4.9. It can be seen that not only the value of electrical distance but also the value of transmission capacity affect partitioning results.

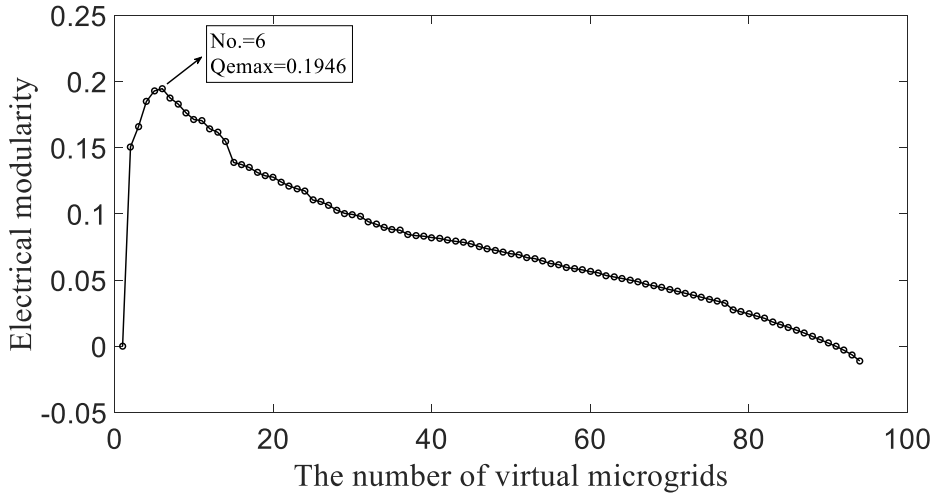

Fig. 4.8 The value of electrical modularity in 94-nodes Portuguese distribution network with different transmission limit on $l_{7\text{-}8}$.

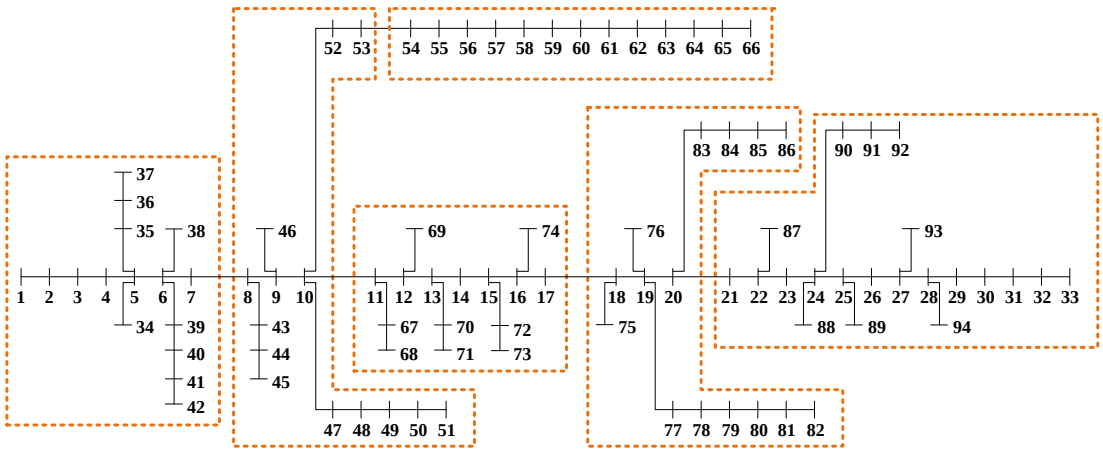

Fig. 4.9 Partitioning results of 94-node Portuguese distribution network with different transmission limit on $l_{7\text{-}8}$.

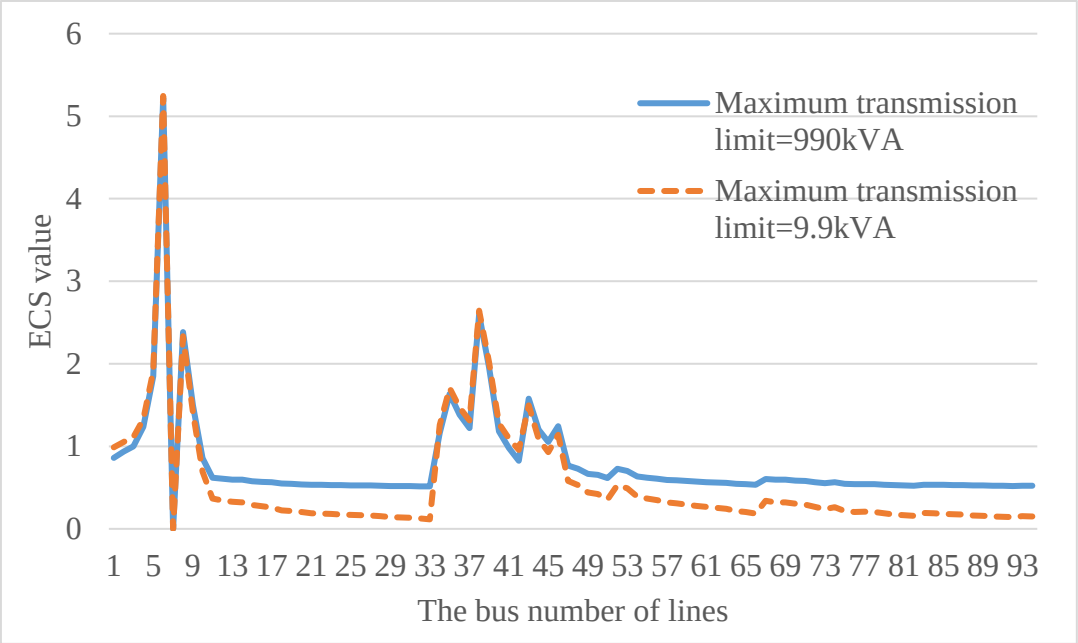

(a)

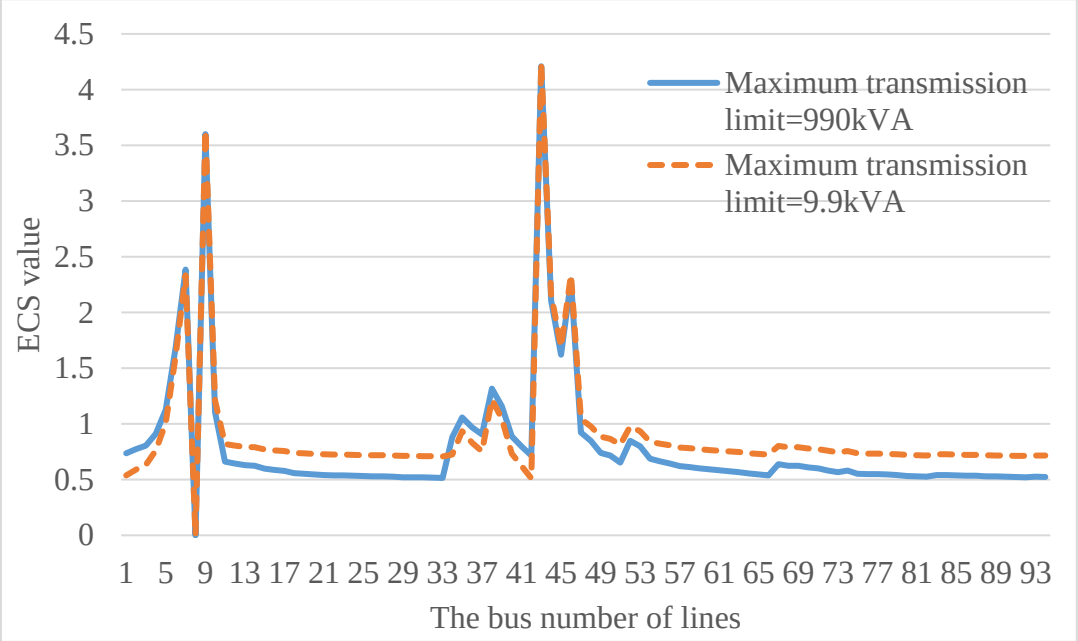

(b)

Fig. 4.10 The variation of ECS with different transmission limit on $l_{7\text{-}8}$. (a) ECS of lines with the other side connecting to bus 7; (b) ECS of lines with the other side connecting to bus 8.

Table 4.2 Data of 94-nodes Portuguese distribution network

From Bus	To Bus	Reactance (p.u.)	ECS
9	10	0.0038	1.4550
10	11	0.0067	0.9188
11	12	0.0008	6.2647
17	18	0.0032	1.7035
18	19	0.0009	5.4775
24	25	0.0012	4.4861
26	27	0.0008	6.1212

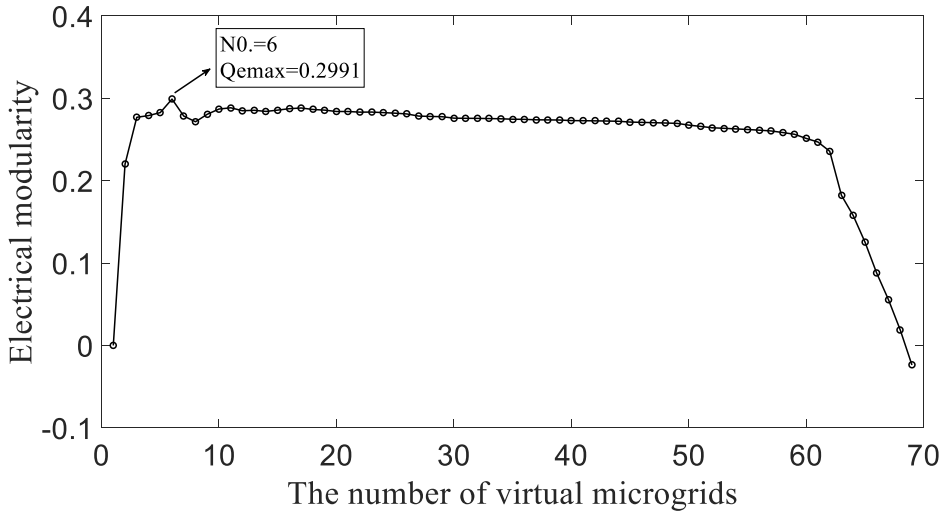

Fig. 4.11 The value of electrical modularity with different numbers of VMs in PG&E 69-bus distribution network.

4.5.3 PG&E 69-bus Distribution Network

Table 4.3 presents the value of electrical modularity with different number of VMs for PG&E 69-bus distribution network. Comparing to the electrical modularity shown in Fig. 4.4, it can be seen that the curve in Fig. 4.11 is slighter and most of electrical modularity in Fig. 4.11 is bigger especially when the number of VMs varies from 3 to

57. Therefore, by using this kind of hierarchical method, it is easier to find out which network has a stronger community structure.

Table 4.3 Electrical modularity of PG&E 69-bus distribution network

No. of VMs	Q_e	No. of VMs	Q_e	No. of VMs	Q_e
1	0	24	0.2826	47	0.2704
2	0.2201	25	0.2819	48	0.27
3	0.277	26	0.281	49	0.2696
4	0.279	27	0.2784	50	0.2674
5	0.2826	28	0.278	51	0.2659
6	0.2991	29	0.2777	52	0.2642
7	0.2784	30	0.2759	53	0.2636
8	0.2715	31	0.2757	54	0.2629
9	0.2806	32	0.2756	55	0.2621
10	0.2869	33	0.2754	56	0.2613
11	0.2885	34	0.2751	57	0.2604
12	0.2849	35	0.2746	58	0.2584
13	0.2854	36	0.2745	59	0.2563
14	0.2841	37	0.2739	60	0.2513
15	0.2856	38	0.2738	61	0.2469
16	0.2874	39	0.2736	62	0.2357
17	0.2882	40	0.2729	63	0.1822
18	0.2864	41	0.2728	64	0.1577
19	0.2856	42	0.2726	65	0.1255
20	0.284	43	0.2724	66	0.08782
21	0.2839	44	0.2721	67	0.05564
22	0.2832	45	0.2711	68	0.019
23	0.2833	46	0.2708	69	-0.02367

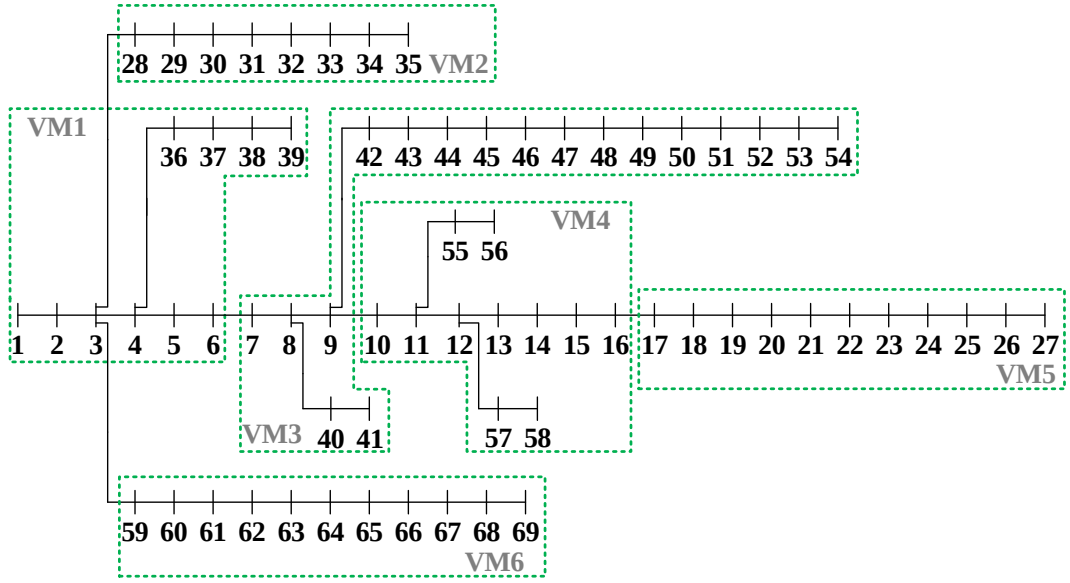

(a)

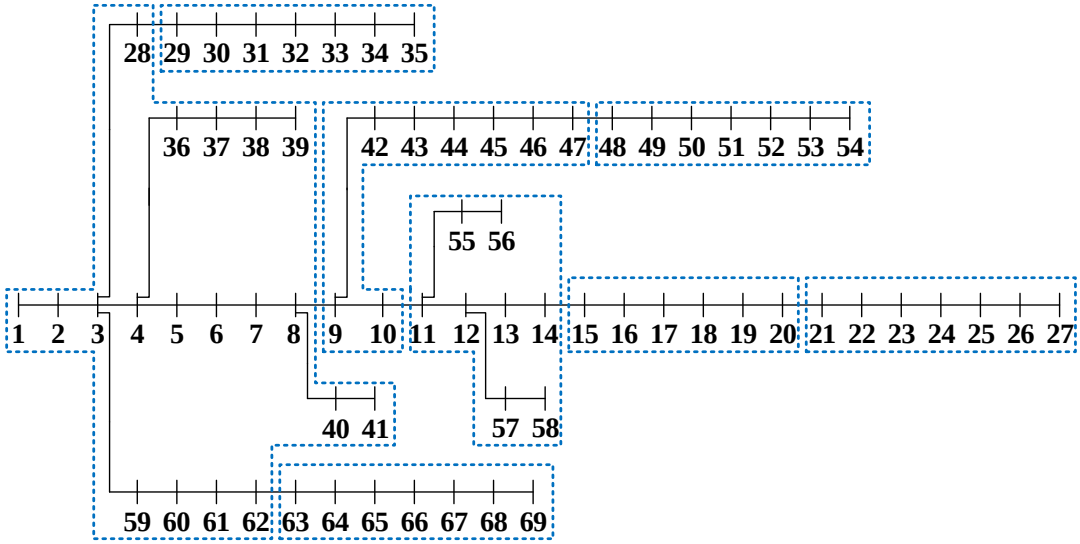

(b)

Fig. 4.12 Partitioning results of PG&E 69-bus distribution network. (a) The results based on the hierarchical partitioning method (Q_e = 0.2991); (b)The results based on analysis of operating states in [72] (Q_e = 0.0726).

The partitioning result with the maximum electrical modularity (0.2991) is selected to determine VM boundaries of this distribution network, and this result is compared with the partition result based on operating states in [72]. Green lines in Fig. 4.12 (a) are boundaries of VMs based on structural analysis while blue lines in Fig. 4.12 (b) are boundaries of VMs based on operating states. Comparing the data of Fig. 4.12 (a)

and Fig. 4.12 (b) as shown in Table 4.4, it can be easily found that the reactance of $l_{6\text{-}7}$ (0.0121) and $l_{9\text{-}10}$ (0.0169) is bigger than that of $l_{8\text{-}9}$ (0.0016) and $l_{10\text{-}11}$ (0.0039) while the ECS on $l_{6\text{-}7}$ and $l_{9\text{-}10}$ is larger, so it is reasonable to select $l_{6\text{-}7}$ and $l_{9\text{-}10}$ as boundaries for this area as shown in Fig. 4.12 (a). For bottom lines in this network, since the reactance on $l_{62\text{-}63}$ (0.0001) is very small, it is unsuitable to select this line as a boundary in Fig. 4.12 (b). What is more, in general, as the electrical modularity in Fig. 4.12 (a) is 0.2991, which is larger than that in Fig. 4.12 (b) (the electrical modularity is 0.0726), so the partitioning result in Fig. 4.12 (a) is more reasonable for this distribution network.

Table 4.4 Data of PG&E 69-bus distribution network

From Bus	To Bus	Reactance (p.u.)	ECS
6	7	0.0121	0.7692
8	9	0.0016	4.5473
9	10	0.0169	0.6524
10	11	0.0039	1.8997
62	63	0.0001	54.0234

If the design requirement is that electrical modularity should be no smaller than 0.28, and the results of Q_e = 0.2854 (VM No. = 13) is used to determine VM boundaries as the dashed green lines presented in Fig. 4.12 (a). It can be found that there are 5 possible combinations to determine dynamic boundaries (when VM No. is 5, 9, 10, 11, 12 as shown in Table 4.3). Here, the partitioning result with 9 VMs is selected as an example to explain dynamic boundaries. In Fig. 4.13 (a), the VMs that are filled with the same color represent combined results. One possible operating scheme with dynamic boundaries in [75] are also shown in Fig. 4.13 (b).

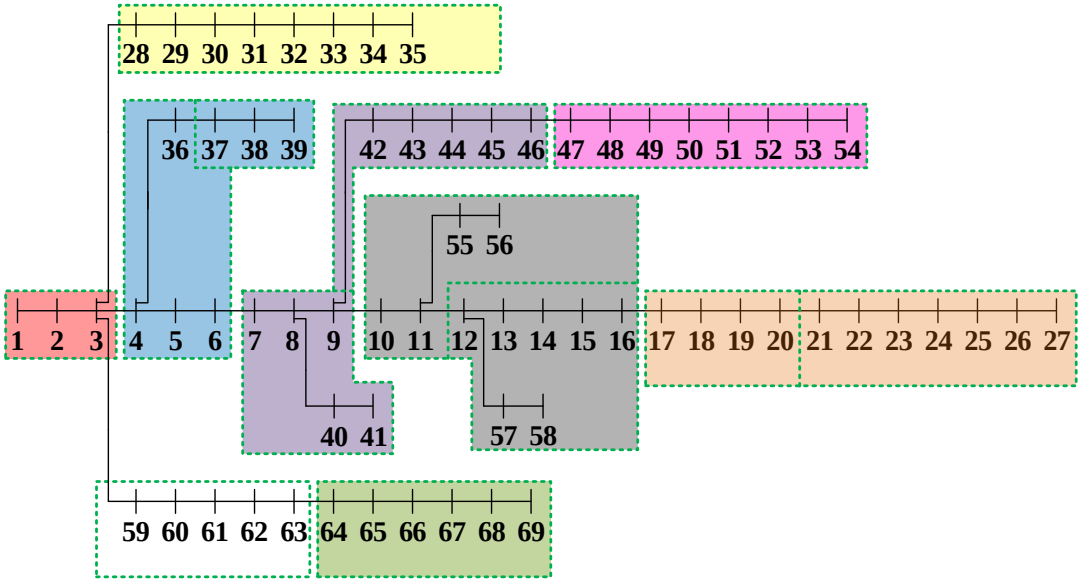

(a)

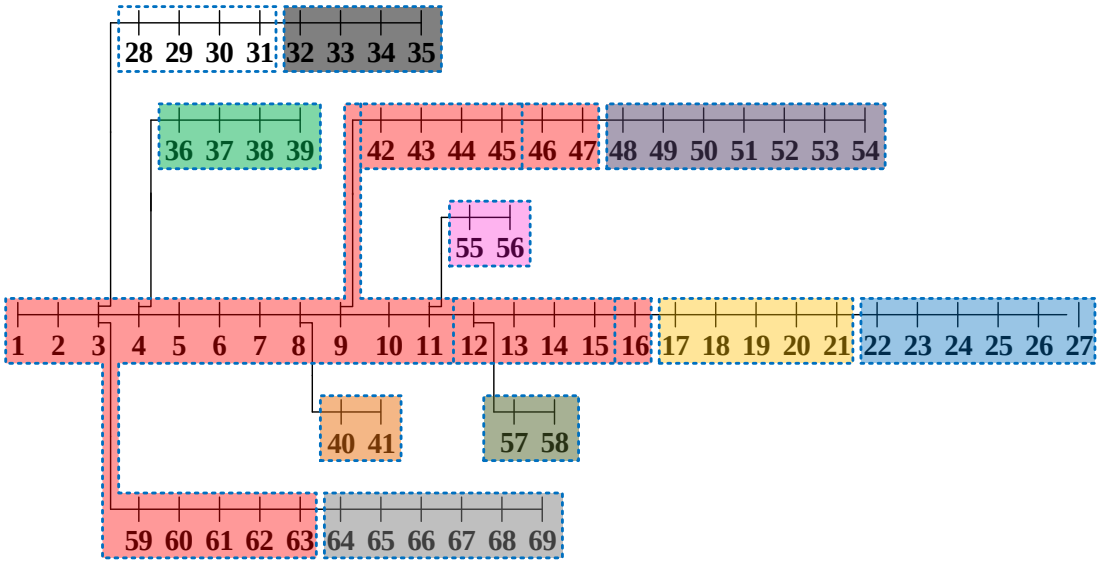

(b)

Fig. 4.13 Possible dynamic boundaries of PG&E 69-bus distribution network. (a) Dynamic boundaries based on hierarchical partitioning method (Q_e = 0.2806); (b) Dynamic boundaries based on analysis of operating states in [75] (Q_e = 0.2379).

In Fig. 4.13 (b), the determination of dynamic boundaries is based on transmission lines with the lightest power flow in different operating states, and resource allocation of DGs in this network is given, but the resource allocation of this network is not in accord with electrical connection in the network structure, and the location

of dynamic boundaries does not fit naturally structural characteristics. This can be verified by the comparison of electrical modularity. Generally, the electrical modularity in Fig. 4.13 (b) (0.2379) is lower than that in Fig. 4.13 (a) (0.2806). Hence, it is more reasonable to design the resource allocation after structural analysis. What is more, as discussed before, the resource allocation of DGs for real distribution networks is not determined and performed yet, so it is unreasonable to analyse a network based on assumed conditions of DG allocation. In Fig. 4.13 (b), it can be found that there are many VMs contain very little number of buses, especially for bus 16, there is only one bus in this VM if it is not combined with other VMs. It is not reasonable for the operation in real cases. On the contrary, if the partition is based on structural analysis in this chapter, these problems can be solved. Therefore, the identification scheme in this chapter is a good choice for the application to real power grids, and more optional schemes for the determination of dynamic boundaries can be provided, so operating modes of upgraded distribution networks can be more various and flexible.

4.6 Summary

As the boundary identification of VMs is a fundamental and important step for upgrading CDNs, in this chapter, a hierarchical partitioning method is proposed, and this method is based on ECS which is defined as a composite weighted factor for the analysis of electrical connection. Then electrical modularity based on ECS is proposed and it is used to identify the quality of partitioning results. Through analysing the results for three real distribution networks, it can be concluded that ECS can describe structural characteristics of distribution networks very well, and the partitioning method based on electrical modularity can provide better choices to determine boundaries of VMs. As it is a kind of hierarchical partitioning method, it can not only identify boundaries of VMs but also provide more choices for dynamic boundaries. It is reasonable and feasible to apply this method to real power grids.

In Chapter 5, based on the partitioned distribution network obtained, the resource allocation of DGs is optimized. The partitioning result is used as a constraint, and it is an important part in the objective function.

Chapter 5
Optimal Allocation of Distributed Generation for Partitioned Distribution Networks

5.1 Introduction

With the enhancement of DG technologies, high penetration of DGs to distribution networks becomes a trend in the future vision of power grids. However, there is almost no DG in CDNs. If DG integration is not preplanned well, it may lead to disordered and inefficient in future distribution networks, and it may conflict with the characteristics of SDNs. Therefore, reasonable placement of DGs is an important issue. At the same time, the lack of DGs in CDNs provides a good opportunity to optimise DG allocation.

Currently, DG allocation is a popular topic, and a number of studies have proposed different methods to deal with this problem. El-Khattam *et al.* in [80] introduced a new heuristic approach to optimise the location and capacity of DGs by considering different scenarios of peak demands and market prices. In this model, distribution companies were owners and operators in distribution networks. They purchased power from genco or electricity markets. In addition to location and capacity of DGs, in [81], the location of remote controllable switches was also considered as a variable. With the consideration of controllable switches, faulted areas were isolated and the power supply for other parts of the network were restored. Naderi *et al.* [82] proposed a dynamic method for DG allocation by determining the best installation time in addition to equipment type, location and capacity. The optimisation target was to minimise various kinds of costs, and the growth of load demand was considered in a N-level load duration curve. In [83], a nonlinear bi-level programming was proposed to optimise the location and contract pricing of DGs. In this model, two decision-making agents were considered, namely, DG owners and distribution companies. For DG owners, location and contract price of DGs were optimised with the aim to maximise

their profits from selling energy to distribution companies. For distribution companies, the quantity of energy required was optimised with the aim to minimise costs. In these models, only dispatchable DGs, such as natural gas generators [80], [82], micro turbines [81] were considered, but other DGs with renewable resources were not considered, such as wind turbine generators, solar power generators. Due to the stochastic nature of these renewable resources, they cannot provide constant power, which makes the optimisation of DG allocation become more complex.

As renewable resources are clean and sustainable, based on establishing DG models with renewable sources, several methods for DG allocation are proposed. Atwa and El-Saadany [84] proposed a generation-load model for optimising the allocation of wind turbine generators. In this model, customers were owners of wind turbine generators, and Rayleigh probability density function (PDF) and IEEE-RTS (Institute of electrical and electronics engineers - Request to send) were used to generate the data of wind speed and load variation respectively. Beta distribution and Rayliegh distribution were used to estimate solar irradiance and wind speed, and a probabilistic planning techniques was presented in [85]. With the consideration of both dispatchable and non-dispatchable DGs, the optimal allocation of DGs proposed in [86] was based on new indices which were related to voltage and current controllability. Location and capacity of DGs were decided by using Tabu Search and probabilistic power flow. To find optimal contract price, capacity and location of DGs, Kalkhambkar *et al.* [87] proposed a joint optimal allocation method for minimising the cost of distribution companies while ensuring the benefit of DG owners. In these models, either one or several kinds of renewable-based DGs were considered, but DG allocation was based on candidate buses, so the number and location of DGs were limited to a certain range.

Although many methods have been proposed to optimise DG allocation, most of them are based on a unique monopoly control unit by centralized decision-making and hierarchical control. They may not be fully appropriate with consideration of trend in fully decentralised control for future SDNs. In this chapter, based on the operating mechanism of VMs, a bi-level method for DG allocation is put forward. The

partitioning results obtained in Chapter 4 are important constraints in the optimisation, and both structure characteristics and operating states are considered for DG allocation. The feasibility of this method is tested by applying it to PG&E 69-bus distribution network.

5.2 Bi-level Optimisation Method

For most of the studies related to DG allocation, economic and technical issues are always considered in the optimization. Since these two issues are very different in scales and units, many studies only consider one of them as an optimisation target. However, considering the long-term development of electrical networks, both economic and technical issues are important for saving costs and improving the performance of power systems.

In this chapter, a bi-level optimization method consisting of an outer optimisation and an inner optimisation is proposed. The relationship between them can be seen from Fig. 5.1. An important feature of this method is that the solutions achieved by outer optimisation rely on the results of inner optimisation. On the one hand, possible solutions (variables) are generated in the outer optimisation, and the optimal operating states of each possible solution are determined through the optimisation in inner optimisation. On the other hand, the optimal solutions in outer optimisation are determined based on the result of optimal operating states from inner optimisation.

As shown in Fig. 5.1, technical objectives are considered in the outer optimisation while economic objectives are considered in the inner optimisation. Since power systems will finally develop to decentralised systems, in the outer optimisation, the optimal DG allocation (DG type, DG location, DG number and DG capacity) is determined with the aim to realise the self-sufficient function of VMs by minimising the power flow on boundaries, which is the long-term goal for planning. As discussed in Chapter 4, the determination of VM boundaries is based on structural information. By minimising power flow on boundaries, the function of VMs can be further optimised with the consideration of operating states. In addition, power loss

minimization is also considered in the outer optimisation as it is an important index to measure the operating performance of systems. In the inner optimisation, optimal operating states of systems are determined by minimising operating costs of networks, which enhance the ability of active energy management of SDNs. An effective way to solve this optimisation problem is by means of AC optimal power flow. Moreover, since operating costs of renewable DGs are always cheaper than DGs with other resources, minimization of operating costs also contributes to increasing the deployment of renewable DGs. Accordingly, the outer optimisation considers the long-term goal of planning, and the inner optimisation is to enhance the performance of operation. By applying this method, the optimal plan of DG allocation can be determined by optimising both economic and technical objectives.

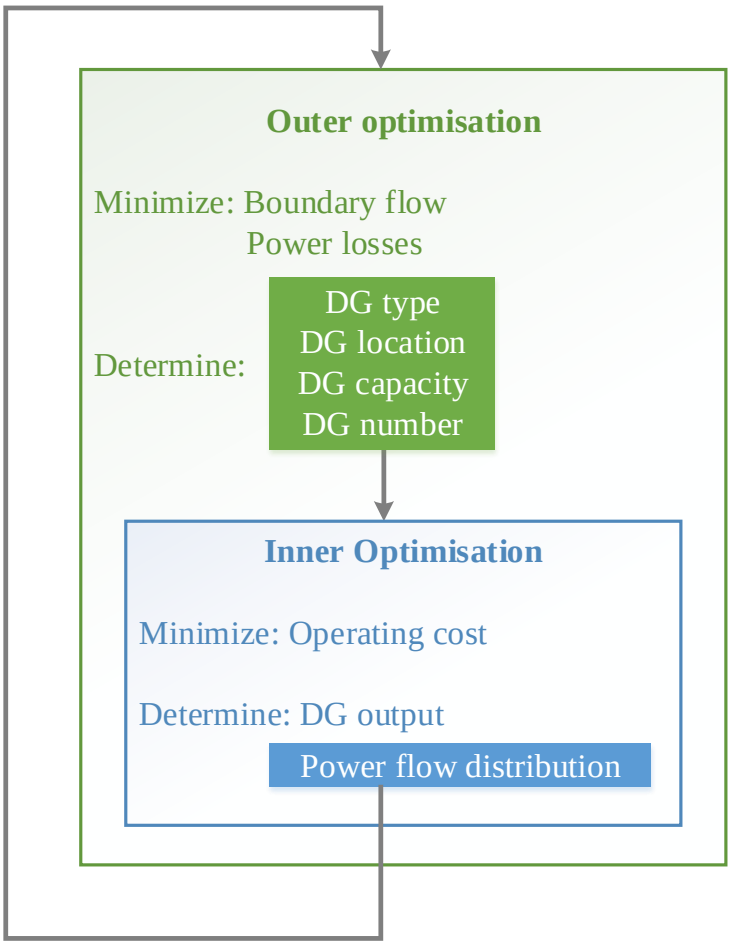

Fig. 5.1 Bi-level optimization method.

The bi-level optimisation method is designed for VM operators, who are responsible for managing the operation of distribution networks. In the following sections, specific technologies which are applied to solve this bi-level optimisation method are explained.

5.3 Modelling of Distributed Generators, Loads and Operating Scenarios

Although high penetration of renewable DGs are expected, some types of renewable DGs, such as wind turbine generators and solar power generators, are non-dispatchable DGs, they cannot provide stable power. In order to ensure stable power supply in networks, especially when VMs operate in islanding mode, not only non-dispatchable DGs but also dispatchable DGs (such as biomass generators, steam turbines) should be considered. Meanwhile, the stochastic nature of non-dispatchable DGs and loads should also be taken into account. In this section, the modeling of loads and DGs, including dispatchable DGs and non-dispatchable DGs, is explained. Based on these models, operating scenarios and relevant probabilities are summarised.

5.3.1 Modelling of Dispatchable DGs

As the power generated by dispatchable DGs can be adjusted, so in this chapter, output power of dispatchable DGs are fully controllable within its capacity limit [30], [72].

5.3.2 Modelling of Non-dispatchable DGs

Wind turbine generators are popular renewable-based DGs, and some methods have been proposed to optimise the allocation of wind turbine generators. Considering the intermittent nature of wind turbine generators, most of the modeling of wind turbine generators is based on PDFs [84], [88]. In this chapter, wind turbines generators are regarded as non-dispatchable DGs. Based on the historical data of wind speed, the output power of wind turbine generators P_w can be calculated according to [89]

$$P_w = \frac{1}{2}\rho\pi R_{tr}{}^2 v^3 C_p(a,b) \tag{5.1}$$

$$C_p(a,b) = (0.44 - 0.0167b)\sin\left(\frac{\pi(a-3)}{15-0.3b}\right) - 0.00184(a-3)b \tag{5.2}$$

$$a = \frac{\omega_r R_{tr}}{v} \tag{5.3}$$

where ρ is the air density, R_{tr} is the radius of turbine rotors, v is the wind speed, $Cp(a,b)$ is the conversion coefficient of wind energy, a is the tip speed ratio and b is the pitch angle, w_r is the rotor speed of turbine rotors.

Then per unit output power of wind turbine generators is generated by using Johnson SB PDF. Johnson SB PDF $f_1(x_1)$ can be expressed as [75]

$$\begin{cases} f_1(x_1) = \dfrac{\delta}{\lambda\sqrt{2\pi}z(1-z)}\exp\left(-\dfrac{1}{2}\left(\gamma + \delta\ln\left(\dfrac{z}{1-z}\right)\right)^2\right) \\ \xi \le x_1 \le \xi + \lambda \\ z = \dfrac{x_1 - \xi}{\lambda} \end{cases} \tag{5.4}$$

where δ and γ are shape parameters; ζ is the location parameter; λ is the scale parameter.

Table 5.1 Parameters of Johnson SB PDF for wind turbine generators

Scenario (Seasons)	W1 (Spring)	W2 (Fall)	W3 (Summer)	W4 (Winter)
γ	0.40832	0.1866	0.48423	-0.0199
δ	0.46673	0.49059	0.55561	0.48906
λ	0.97881	0.98015	0.97956	0.95746
ζ	-0.0765	-0.00616	-0.00874	0.005568
Probability	1/4	1/4	1/4	1/4

As wind speed has seasonal characteristics, four scenarios are considered accordingly, and parameters of Johnson SB PDF [75] with relevant probability of different seasons are listed in Table 5.1. With assumption of same duration for each season, the probability of each season is 1/4.

5.3.3 Modelling of Loads

Similarly, based on historical data of load, Weibull PDF $f_2(x_2)$ is applied to generate load model, and it can be written as [90]

$$f_2(x_2) = \frac{\alpha}{\beta}\left(\frac{x_2-\gamma}{\beta}\right)^{\alpha-1} e^{-\left(\frac{x_2-\gamma}{\beta}\right)^{\alpha}} \tag{5.5}$$

where α is the shape parameter; β is the scale parameter; γ is the location parameter.

Table 5.2 Parameters of Weibull PDF for loads

Season	Scenario	α	β	γ	Probability
Spring	L1 (Weekend)	2.4226	0.09934	-0.08812	5/28
	L2 (Weekday)	1.7979	0.05353	-0.04758	1/14
Fall	L3 (Weekend)	5.247	0.22676	-0.20872	5/28
	L4 (Weekday)	5.1698	0.16188	-0.14876	1/14
Summer	L5 (Weekend)	8.2088	0.21547	-0.20307	5/28
	L6 (Weekday)	17.046	0.29313	-0.28402	1/14
Winter	L7 (Weekend)	8.2088	0.21547	-0.20307	5/28
	L8 (Weekday)	17.046	0.29313	-0.28402	1/14

Based on the load data of IEEE-RTS in [91], not only the difference in seasons but also the difference between weekday and weekend are considered to generate load data. Therefore, 8 scenarios are considered. For each scenario, Weibull PDF represents the deviation of actual load data from mean load values. Parameters of Weibull PDF [90]

and probability are listed in Table 5.2. Assuming that in each week, there are 5 weekdays and 2 weekends, for each season, the probability of weekday is 1/4 × 2/7 = 1/14 while the probability of weekend is 1/4 × 5/7 = 5/28.

Table 5.3 Operating scenarios and probabilities

Scenario			Wind	Load	Probability (T_m)
1	Spring	Weekday	W1	L1	5/28
2		Weekend		L2	1/14
3	Fall	Weekday	W2	L3	5/28
4		Weekend		L4	1/14
5	Summer	Weekday	W3	L5	5/28
6		Weekend		L6	1/14
7	Winter	Weekday	W4	L7	5/28
8		Weekend		L8	1/14

5.3.4 Operating Scenarios

With the stochastic models of DGs and loads mentioned, in this chapter, one year is divided to 4 seasons including 5 weekdays and 2 days of weekend in each week. Therefore, 8 scenarios are considered (4 seasons/year * 7 days/season) as shown in Table 5.3.

5.4 Problem Formulation

In this chapter, two types of DGs are considered, i.e. dispatchable DGs and non-dispatchable DGs. As discussed in Section 5.2, the optimisation of DG allocation is based on a bi-level optimisation method. For the outer optimisation, the optimal allocation of DG type, DG location, DG number and DG size are determined by

minimising power losses and power flow on VM boundaries. The objective function of outer optimisation OF_{outer} can be written as

$$OF_{outer} = \sum_{m=1}^{N_{sc}} \left(P_{boundaries,m} + P_{loss,m} \right) \cdot T_m \tag{5.6}$$

where N_{sc} is the total scenario number. $P_{boundaries,m}$ is the total active power on all VM boundaries in scenario m. $P_{losses,m}$ is the total power losses in scenario m. T_m is probability of scenario m.

For the inner optimisation, operating states of each sampling points are optimised, which refers to determining the optimal output of DGs of sampling points by minimising operating and maintenance costs. The objective function of the inner optimisation OF_{inner} can be expressed as

$$OF_{inner} = \sum_{i=1}^{N_b} (\text{Cost}_{nd\_DG} \cdot Power_{nd\_DG,i}^{real} + \text{Cost}_{d\_DG} \cdot Power_{d\_DG,i}^{real}) \tag{5.7}$$

where N_b is the total bus number. $Cost_{nd\_DG}$ and $Cost_{d\_DG}$ are operating and maintenance costs of non-dispatchable DGs and dispatchable DGs respectively. $Power_{nd\_DG,i}^{real}$ and $Power_{d\_DG,i}^{real}$ are the real output power of non-dispatchable DGs and dispatchable DGs on bus i. If there is no corresponding DGs on bus i, $Power_{nd\_DG,i}^{real} = 0$, and $Power_{d\_DG,i}^{real} = 0$.

In the optimisation process of DG allocation, some assumptions and constraints should be considered to ensure the stable operation of electrical networks. In practice of engineering, investment in planning is often limited by actual conditions and design targets. So this limitation is approximately modeled as a constraint of total capacity in the whole network:

$$\sum_{i=1}^{N_b} C_{DG,i} \leq R \tag{5.8}$$

where $C_{DG,i}$ is the DG capacity on bus i. If there is no DG on bus i, $C_{DG,i} = 0$. R is the total DG capacity limitation.

As most of renewable DGs are non-dispatchable due to their stochastic nature, in this chapter, non-dispatchable DGs are used to represent renewable DGs. Although high penetration level of non-dispatchable DGs can bring many benefits to power systems, so far, there is no solution which can be widely used by the industry to deal with the impact of these DGs on system stability. This is why dispatchable DGs are indispensable. In the case of ensuring that sensitive loads are reliably supplied, to increase the penetration level of non-dispatchable DGs, the capacity of non-dispatchable DGs is set to be bigger than a certain percentage of the total DG capacity.

$$\sum_{i=1}^{N_b} C_{nd\_\mathrm{DG},i} \geq W\% \cdot \mathrm{C}_{tot\_DG} \tag{5.9}$$

where $C_{nd\_DG,i}$ is the non-dispatchable DG capacity on bus i. If there is no DG on bus i, $C_{nd\_DG,i} = 0$. $W\%$ is proportional coefficient. C_{tot_DG} is the total DG capacity, including the capacity of dispatchable and non-dispatchable DGs.

Similar to normal microgrids, VMs also have two operating modes, i.e. grid-connected mode and islanding mode. To guarantee power supply to sensitive loads in islanding mode, the total capacity of dispatchable DGs in each VM should be larger than the total peak value of sensitive loads:

$$\sum_{j=1}^{N_{bVM}} C_{d\_DG,\mathrm{j}} \geq K\% \cdot \mathrm{C}_{tot\_L} \tag{5.10}$$

where N_{bVM} is the total bus number in any VM, $C_{d\_DG,j}$ is the capacity of dispatchable DGs on bus j. If there is no dispatchable DG on bus j, $C_{d\_DG,j} = 0$. $K\%$ is the proportional coefficient, which is the percentage of peak sensitive loads to the total peak loads. $C_{tot\_L,j}$ is the total load in a VM.

Constraints in power flow calculation:

$$\begin{aligned} P_{DG,i} - P_{load,i} &= |V_i| \sum_{k=1}^{N_b} |V_k| \left(G_{ik} \cos\theta_{ik} + B_{ik} \sin\theta_{ik} \right) \\ Q_{DG,i} - Q_{load,i} &= |V_i| \sum_{k=1}^{N_b} |V_k| \left(G_{ik} \sin\theta_{ik} - B_{ik} \cos\theta_{ik} \right) \end{aligned} \tag{5.11}$$

where $P_{DG,i}$ and $Q_{DG,i}$ are active and reactive DG output power on bus i. $P_{load,i}$ and $Q_{load,i}$ are active and reactive loads on bus i. V_i and V_k are voltage on bus i and bus k. G_{ik} and B_{ik} are real and imaginary parts of the ith row and kth column in the admittance matrix. θ_{ik} is the voltage phase angle difference, and $\theta_{ik} = \theta_i - \theta_k$.

Assuming bus 1 is the slack bus, the voltage $V_{m,1}$ and angle $\delta_{m,1}$ on the slack bus are

$$\begin{aligned} V_{\mathrm{m},1} &= 1 \\ \delta_{\mathrm{m},1} &= 0 \end{aligned} \tag{5.12}$$

Bus voltage limitation $V_{m,i}$:

$$V_i^{\min} \le V_{m,i} \le V_i^{\max}, \quad \forall i \in \{1,2,3,...,N_b\} \tag{5.13}$$

where V_i^{min} and V_i^{max} are the minimum and maximum voltage limitation on bus i.

Feeder power flow limitation P_{ik}:

$$P_{ik} \le P_{ik}^{\max} \quad \forall i,k \in \{1,2,3,...,N_b\} \tag{5.14}$$

where P_{ik}^{max} is the maximum power flow limitation on bus i.

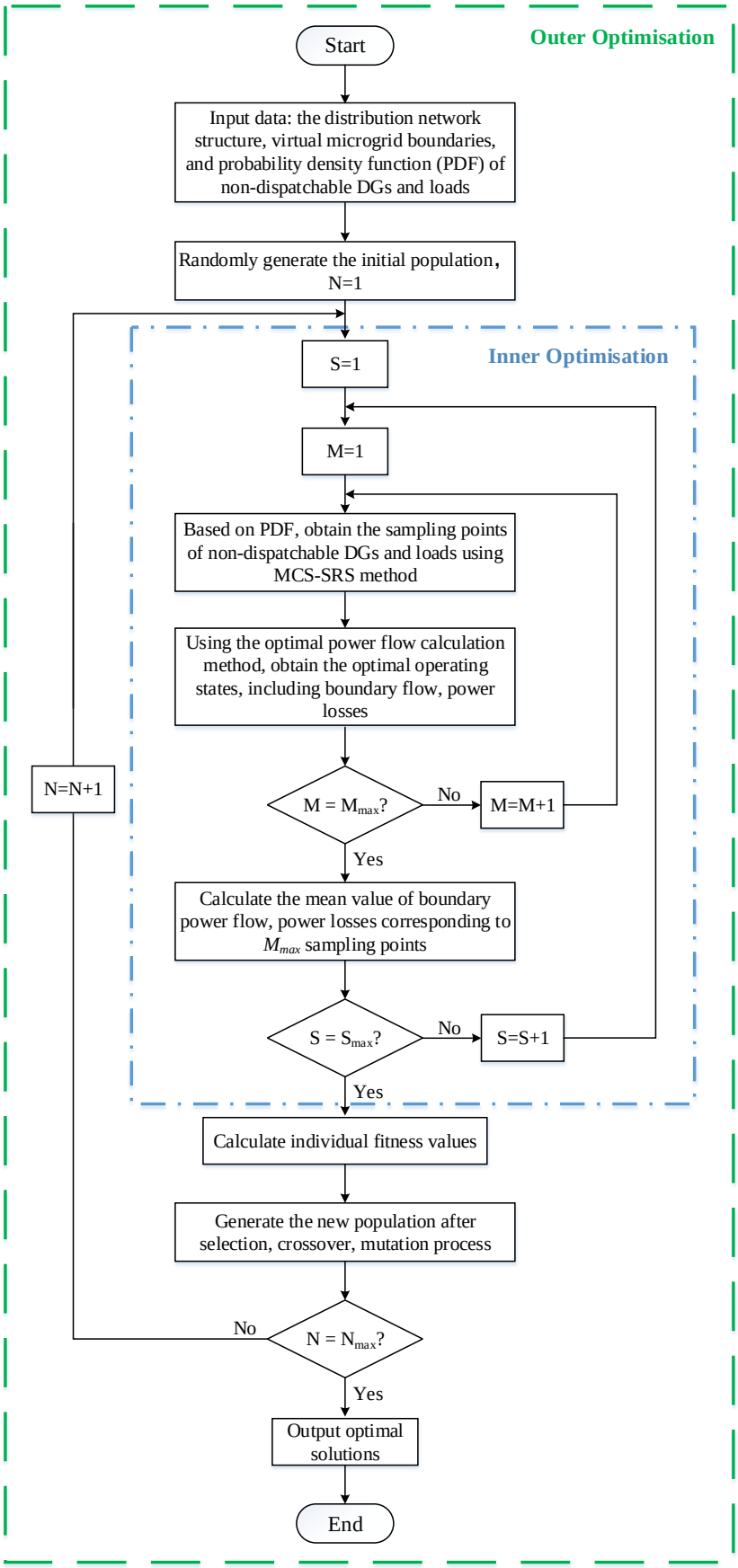

Fig. 5.2 Flowchart of the optimisation for DG allocation.

5.5 Optimisation Algorithm

With large-scale decision variables and their complex relations, the outer planning optimization is performed by Genetic Algorithm (GA). With given allocation of DGs from outer planning decision, the inner operating optimization can be implemented as a probabilistic optimal power flow (POPF) model to determine output power of all DGs. The flow chart of the optimization algorithm is shown in Fig. 5.2. *N* is the total iteration number, *S* is the total number of scenarios and *M* is the number of sampling points for MCS.

5.5.1 Genetic Algorithm

To solve the optimisation problem in the outer optimisation, genetic algorithm is applied, and the optimisation process of GA is discussed in Section 3.2.3. As four variables are considered, including DG location, DG number, DG type and DG capacity, normally, several genes should be used to represent these variables. However, considering scale differences of these variables, in this chapter, three matrices are used to represent each chromosome.

$$\begin{aligned} chromosome = &\left[T_{yDG,1}\ T_{yDG,2}\ \ldots\ T_{yDG,i}\ \ldots\ T_{yDG,Nb}\right]; \\ &\left[\mathrm{C}_{\mathrm{d\_}DG,1}\ \ \mathrm{C}_{\mathrm{d\_}DG,2}\ \ldots\ \mathrm{C}_{\mathrm{d\_}DG,i}\ \ldots\ \mathrm{C}_{\mathrm{d\_}DG,Nb}\right]; \\ &\left[\mathrm{C}_{\mathrm{nd\_}DG,1}\ \ \mathrm{C}_{\mathrm{nd\_}DG,2}\ \ldots\ \mathrm{C}_{\mathrm{nd\_}DG,i}\ \ldots\ \mathrm{C}_{\mathrm{nd\_}DG,Nb}\right] \end{aligned} \tag{5.15}$$

where $T_{yDG,i}$ is the type of DG on bus *i*. Three numbers are used to indicate the type and presence of DGs,

$$T_{yDG,i} = \begin{cases} 0 & \text{There is no DG allocated on bus i} \\ 1 & \text{Dispatchable DG is allocated on bus i} \\ 2 & \text{Non-dispatchable DG is allocated on bus i} \end{cases} \tag{5.16}$$

therefore, three variables are considered in the first matrix in Equation (5.15), including DG number, DG location and DG type. The capacity of dispatchable DGs and non-dispatchable DGs are generated in the other two matrices in Equation (5.15).

Based on Equation (5.15) and Equation (5.16), the initial population can be obtained. According to the basic process of GA, including crossover, mutation and selection, optimal results for DG allocation can be obtained.

5.5.2 Probabilistic Optimal Power Flow (POPF)

The aim of inner optimisation is to obtain optimal operating states for all scenarios generated by the outer optimisation. Based on generator output capacities and load data, the deterministic power flow calculation is a basic and important tool to analyse operating states of electrical networks, but it lacks the ability to analyse the networks with stochastic DGs and variable loads. In 1974, Borkowska first proposed the concept of probabilistic power flow (PPF) and mathematical models to solve the power flow with the consideration of data uncertainty [92]. Since then, many papers were published on this topic [93]–[97]. Generally, Monte Carlo Simulation (MCS) methods, analytical methods, and approximate methods are three main kinds of PPF methods. Among these methods, the MCS based on simple random sampling (MCS-SRS) is one of the most popular and effective PPF methods. It is based on repeating deterministic power flow calculations of sampling points which is randomly selected according to PDFs. As MCS-SRS can provide reliable and accurate results if enough sample points are selected, it is often used to verify the accuracy of other methods [93], [95], [97]. In this chapter, MCS-SRS method is applied to generate sampling points of non-dispatchable DGs and loads according to relevant PDFs, and it is assumed that the selected points of non-dispatchable DGs represent the maximum power they can generate.

To generate M sampling points, a bounded transformation from the common distribution to specific PDF distribution is needed. Based on the parameters in Table 5.1 and Table 5.2, taking one sampling point as an example, bounded transformations

for Johnson SB PDF distribution and Weibull PDF distribution are explained as follows [75]:

(1) For Johnson SB PDF, 3 steps are required for the bounded transformation,

Step 1: Generating a random value R according to normal distribution on [0,1];

Step 2: Calculate $E = e^{\frac{R-\Upsilon}{\delta}}$;

Step 3: Based on $x = \xi + \lambda\left(\frac{E}{1+E}\right)$, calculating the value x which conforms to Johnson SB PDF.

(2) For Weibull PDF, 2 steps are required for the bounded transformation,

Step 1: Generating a random value R according to uniform distribution on [0,1];

Step 2: Based on $x = \Upsilon + \beta\left(-\ln\left(1-R\right)\right)^{\frac{1}{\alpha}}$, calculating the value x which conforms to Weibull PDF.

Based on MCS-SRS method and bounded transformation, for each scenario, M sampling points are obtained, including load demands and the maximum power of non-dispatchable DGs. Using optimal power flow calculations, operating states of each sampling point can be optimised. Since MATPOWER is a popular tool for optimal power flow calculation, it is used to determine the optimal output of DGs (including dispatchable and non-dispatchable DGs) by minimising the objective function in Equation (5.7). As both MCS-SRS method and optimal power flow calculation are applied to determine the optimal operating states, it is a kind of POPF method. By using POPF method, according to different scenarios, VM operators can actively manage power generation and distribution to realise economic operation.

5.6 Results and Discussions

In this section, PG&E 69-bus distribution network is selected as the test system to verify the feasibility of the proposed method. The network data can be found in [98], including impedance of lines and loads. MATLAB is used to calculate results.

5.6.1 Results without DG Allocation

Based on the partitioning results in Fig. 4.12 (a), it is assumed that node 1 is connected to the main grid, thus creating a new boundary $l_{1\text{-}2}$ as shown in Fig. 5.3. Hence, there are totally 6 boundaries, and they are $l_{1\text{-}2}$, $l_{3\text{-}28}$, $l_{3\text{-}59}$, $l_{6\text{-}7}$, $l_{9\text{-}10}$, $l_{16\text{-}17}$. In this subsection, it is assumed that all electrical power is supplied by the main grid, and there is no DG allocated in this network, which is equivalent to the conventional way of power supply in power systems. Based on the load model discussed in Section 5.3.3, MCS is used to generate sampling points of loads, and the classic Newton Raphson Algorithm [99] is used to calculate power losses of the network. Total power losses without DG deployment are 0.0514 kW.

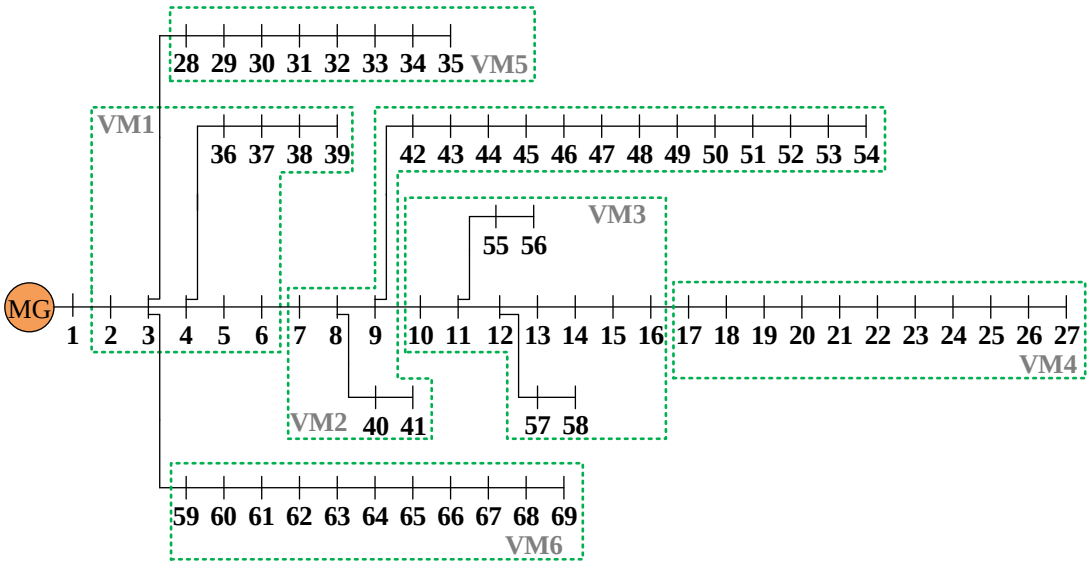

Fig. 5.3 Partitioned results of PG&E 69-bus distribution network.

5.6.2 Optimal DG Allocation Results to Minimise Power Losses without VMs

In this section, the proposed DG allocation method is applied to PG&E 69-bus distribution network. Two types of DGs, i.e. wind turbine generators and biomass generators, are considered, representing non-dispatchable and dispatchable DGs, respectively. It is assumed that all buses can be selected as possible location of DGs. The total capacity limitation of DG allocation R is set to 4000 kW, which is a bit larger than the total peak demand (3802.2 kW) in the network considering stochastic characteristics of non-dispatchable DGs. In each VM, it is assumed that sensitive loads account for 30% (which is the value of K in Equation (5.10)) of the total load demand. The proportional coefficient W is set to 60% to increase the penetration of DGs with renewable resources. Considering different design requirements, these parameters can be changed to different values. The capacities for all DGs can be selected from 4 discrete numbers with a step of 50 kW, and candidate capacities are 50 kW, 100 kW, 150 kW, 200 kW. The parameter settings for optimization are shown in Table 5.4. The maintenance and operating costs of wind turbine generators and biomass generators are 0.01 $/kWh and 0.025 $/kWh [100].

Table 5.4 Parameter settings for optimisation

Population size	Mutation rate	Crossover rate	Iteration	Sampling points
100	0.6	0.001	50	1000

In many studies of DG allocation, minimising power losses is considered as the main objective. Considering the stochastic nature of non-dispatchable DGs and loads, the objective function of minimising power losses OF_L can be expressed as

$$OF_L = \sum_{m=1}^{N_{sc}} P_{loss,m} \cdot T_m \tag{5.17}$$

In this case, DG allocation results with the objective only to minimise power losses are obtained. Optimisation results are shown in Fig. 5.4, in which W stands for wind

turbine generators and G stands for biomass generators. Detailed capacity of wind turbine generators and biomass generators is shown in Table 5.5 and Table 5.6 respectively. Comparing to the result without DG allocation, power losses reduce a lot from 0.0514 kW to 0.003 kW.

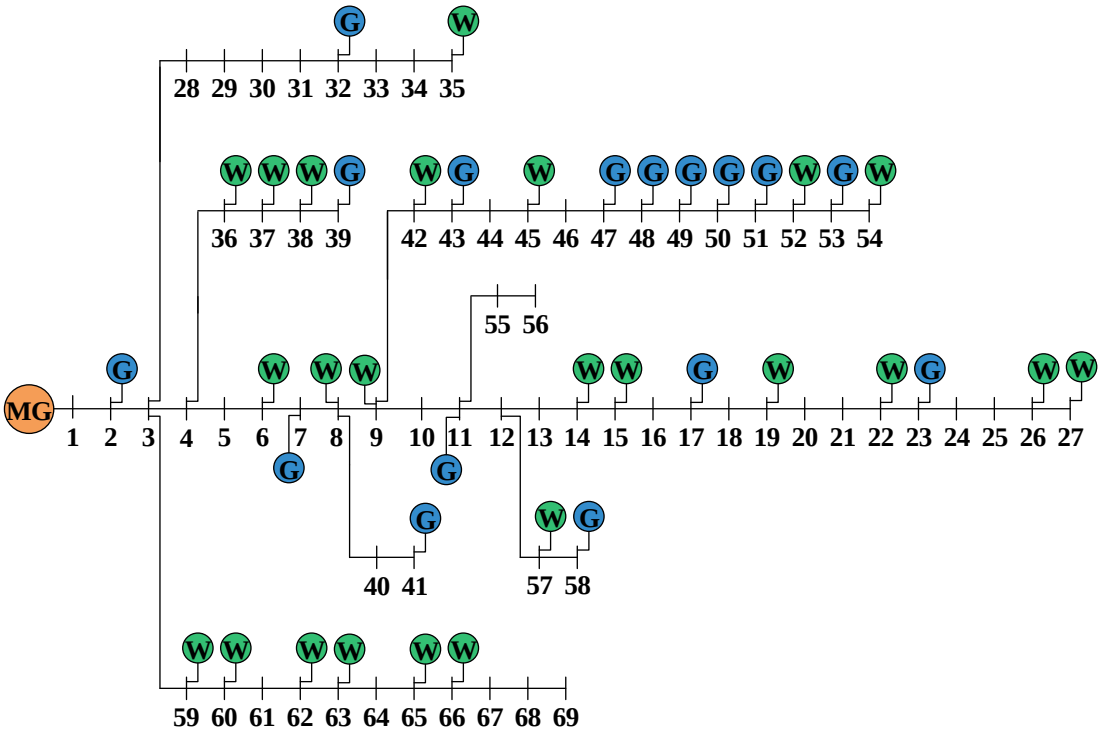

Fig. 5.4 DG allocation results with the objective to minimise power losses.

Table 5.5 The capacity of wind turbine generators with the objective to minimise power losses

Location (bus No.)	6	8	9	14	15	19
Capacity (kW)	100	100	100	50	100	200
Location (bus No.)	22	26	27	35	36	37
Capacity (kW)	50	200	50	100	150	150
Location (bus No.)	38	42	45	52	54	57
Capacity (kW)	50	50	100	100	50	100
Location (bus No.)	59	60	62	63	65	66
Capacity (kW)	100	50	100	100	100	100

Table 5.6 The capacity of biomass generators with the objective to minimise power losses

Location (bus No.)	2	7	11	17	23	32	39	41
Capacity (kW)	50	150	50	50	100	50	100	50
Location (bus No.)	43	47	48	49	50	51	53	58
Capacity (kW)	100	50	150	150	50	200	150	100

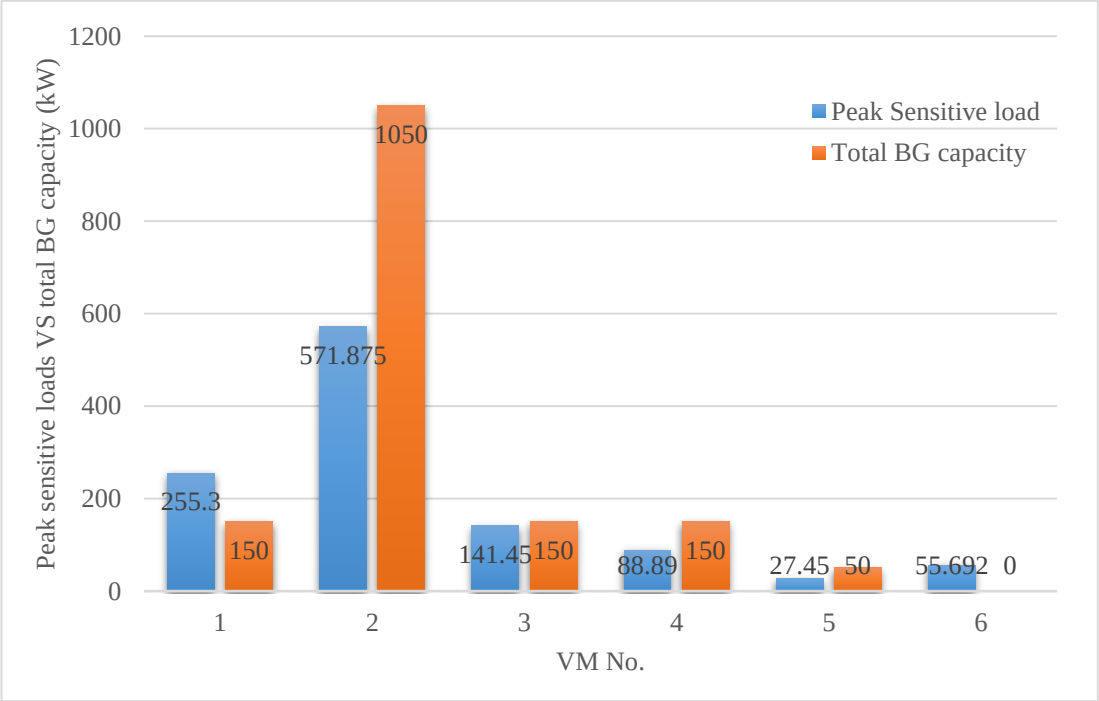

Fig. 5.5 A comparison of peak sensitive loads and total capacity of biomass generators with the objective to minimise power losses.

In this case, the optimization is based on minimising power losses but ignore future decentralized control vision of power systems. If this distribution network will be upgraded to VMs in the future based on the proposed method in this chapter, this optimisation result is not appropriate since it cannot guarantee the power supply when VMs operate in islanding mode. A comparison between peak sensitive loads and biomass generators in VMs can be found in Fig. 5.5. As non-dispatchable DGs (wind

turbine generators) cannot always provide constant power, therefore, it is necessary to configure a sufficient amount of dispatchable DGs (biomass generators) to ensure the power supply to sensitive loads when VMs operate in islanding modes. However, as it is shown in Fig. 5.5, the total capacity of biomass generators in VM1 and VM6 is not big enough to supply sensitive loads. There is even no biomass generator deployed in VM6. Therefore, it is necessary to consider the future vision and change of power networks in the optimization process of DG allocation.

5.6.3 Optimal DG Allocation Results with active energy management by VMs

With the consideration of VM construction, in this section, the proposed bi-level optimization method is applied to PG&E 69-bus distribution network with the same settings as listed in Table 5.4. In this case, the optimization is based on minimising power losses and power flow on VM boundaries as defined in Equation (5.6) and Equation (5.7).

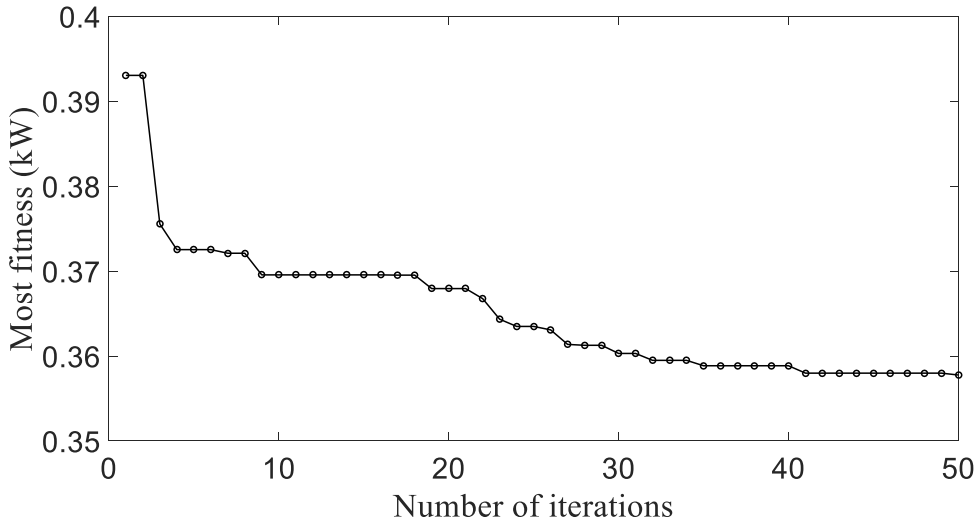

Fig. 5.6 The most fitness value of objectives for different iterations.

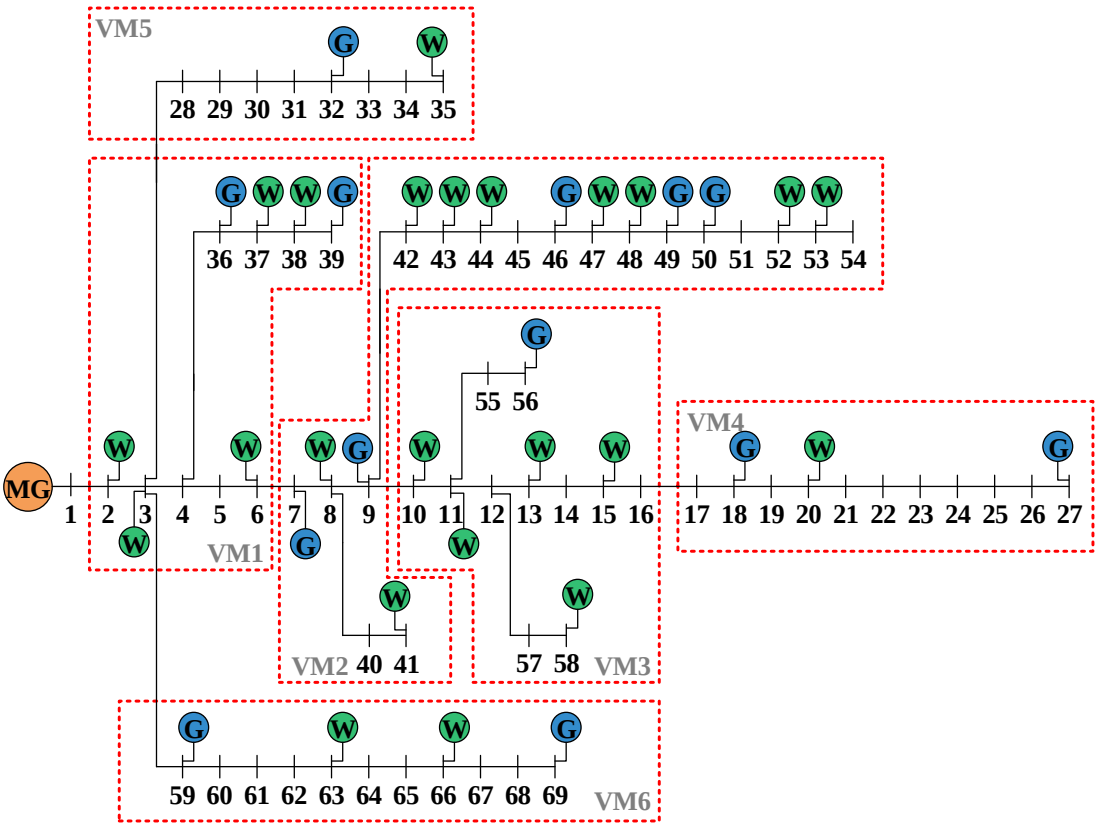

Fig. 5.7 DG allocation results with the consideration of VMs.

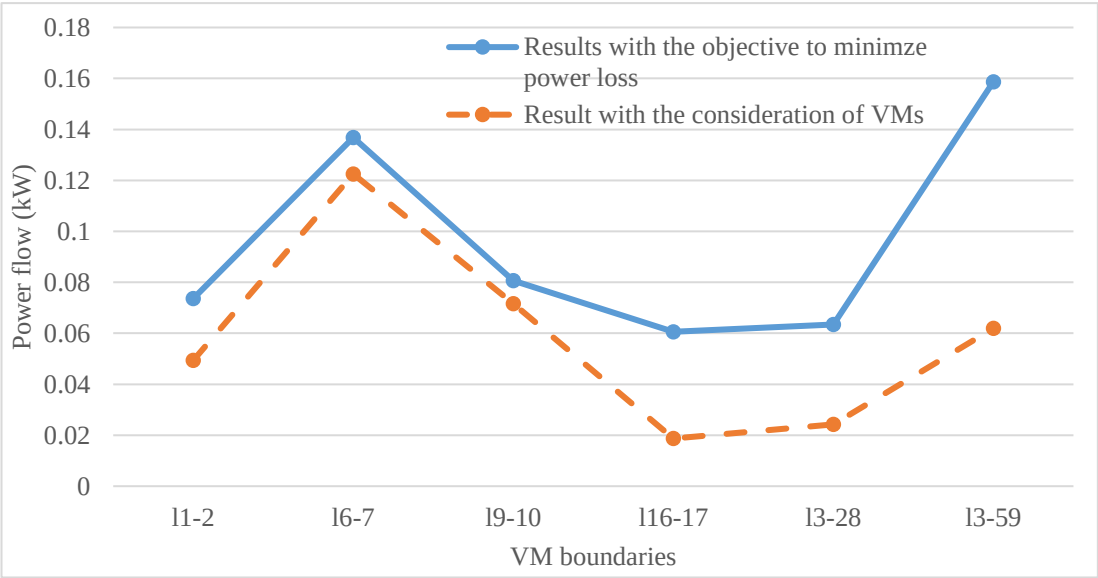

Fig. 5.8 A comparison of power flow on VM boundaries.

Table 5.7 The capacity of wind turbine generators with the consideration of VMs

Location (bus No.)	2	3	6	8	10	11
Capacity (kW)	150	50	100	100	200	150
Location (bus No.)	13	15	20	35	37	38
Capacity (kW)	50	50	50	100	50	150
Location (bus No.)	41	42	43	44	47	48
Capacity (kW)	100	150	100	150	150	50
Location (bus No.)	52	53	58	63	66	
Capacity (kW)	50	150	150	50	100	

Table 5.8 The capacity of biomass generators with the consideration of VMs

Location (bus No.)	7	9	18	27	32	36	39
Capacity (kW)	100	150	150	50	50	200	150
Location (bus No.)	46	49	50	56	59	69	
Capacity (kW)	150	150	50	150	50	150	

Fig. 5.6 shows the change of the most fitness objective in the optimization process, and it can be seen that as the number of iteration increases, the most fitness value continues decreasing, and finally, the curve converges to 0.3578 kW. The optimal DG allocation result is shown in Fig. 5.7, and the capacity of wind turbine generators and biomass generators is listed in Table 5.7 and Table 5.8 independently. The total capacity of DGs, including wind turbine generators and biomass generators, is 3950 kW, which do not exceed the total DG limitation (4000 kW). According to the data in Table 5.7, the total capacity of wind turbine generators is 2400 kW, so the ratio of the capacity of wind turbine generators to the total DG capacity is 60.76%, which is consistent with the constraint in Equation (5.9) as it is bigger than the setting value (60%). Due to another objective is considered, the power losses (0.0093 kW) in this case is not as low as that (0.003 kW) with the objective only to minimise power losses, but power losses in this case are much less than those (0.0514 kW) without DG

allocation. To enhance the ability of self-sufficient of VMs, minimizing power flow on VM boundaries is an important objective in outer optimisation. As shown in Fig. 5.8, the power flow on all boundaries is lower than that in Section 5.6.2 (with the only objective to minimize power losses). What is more, due to the consideration of possible VM construction in the future, it can be found from Fig. 5.9 that the capacity of biomass generators is bigger than the sensitive loads in every VM, hence, the power supply of sensitive loads can be guaranteed even in islanding mode. Therefore, by applying the proposed DG allocation method, the performance of the network is improved, and this DG allocation result can adapt to the future vision of power systems considering decentralised control systems.

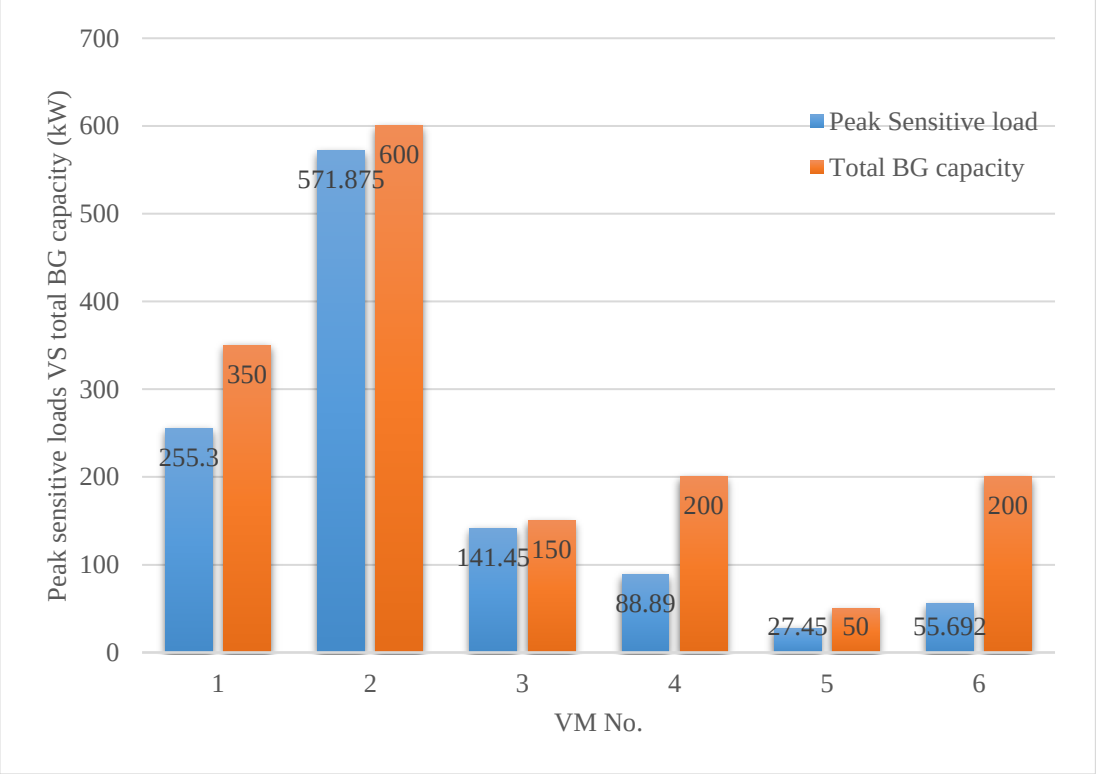

Fig. 5.9 A comparison of peak sensitive loads and total capacity of biomass generators with the consideration of VMs.

5.7 Summary

To adapt to the future vision of power systems, such as high penetration of DGs, decentralised control, in this chapter, a bi-level optimisation method consisting of an outer optimisation and an inner optimisation is proposed to optimise the DG allocation in distribution networks. Based on the partitioning results in Chapter 4, the inner optimisation is to enhance the ability of active energy management by optimising operation states of systems. The outer optimisation considers the long-term goal for planning by minimising power losses and power flow on VM boundaries. Both dispatchable and non-dispatchable DGs are considered, and the stochastic nature of non-dispatchable DGs and loads is taken into consideration by using corresponding PDFs. The feasibility of the proposed method is verified by applying it to PG&E 69-bus distribution network. Comparing to the original distribution network without DG allocation, power losses reduce much with active energy management by DGs. In addition, comparing to the DG allocation results with the objective only to minimize power losses without VMs, the method proposed in this chapter can improve the flexibility and security of SDNs as it is adaptable to developing trends of future power systems.

Considering similarities between microgrids and VMs, in the next chapter, a control and protection scheme for microgrids is introduced with the aim to study operating issues of VMs.

Chapter 6
Control and Protection Schemes from Normal Microgrids to VMs

6.1 Introduction

Although constructing VMs can provide more flexible operating modes, it also causes some problems due to the conflict with existing network configurations. In conventional power systems, fault current is unidirectional and decreases along feeders. The existence of many smaller DG units in VMs increases the possibility of incidents, and these incidents may have more chances, and places, to happen, but they are smaller and local impact [20]. Due to multi-source structure, conventional protection schemes are ineffective in VMs because short-circuit capacity is enlarged and current paths become even reverse. Considering the wide use of inverters to DGs, fault current is limited to 2 times of rated current, which is much lower than the fault current with conventional protection schemes. In addition, VMs show distinct fault characteristics in different operating modes. Furthermore, VMs are open to new DGs due to plug-and-play features. Besides, dynamic output characteristics of DGs are unpredictable. All these add the difficulty in control and protection of VMs.

Currently, VM is still a new concept, and very few studies are directly focus on the research of control and protection schemes of VMs. As the configuration of VMs is similar with microgrids, such as multi-source structure, control and protection of microgrids have great potential to be applied to VM systems. So far, many methods are proposed to ensure normal operation of microgrids. In the control of microgrids, the concept of peer-to-peer is used to ensure no critical components are specified such as master controllers or central storage units [101]. In microgrids, different modes such as grid-connected mode and islanding mode are included, thus, different control strategies such as P-Q control and V-f control are used respectively [102]. The impact of operation mode transitions on critical loads and DGs was discussed in [103].

However, conventional methods for distribution networks show poor flexibility and expansibility in microgrid control, the worst result is system collapse, and similar problems also exist in VMs.

For the protection of microgrids, extra devices or components such as fault current limiters (FCLs) are commonly used. For instance, Static Series Compensators (SSC) were inserted in the main grid side so overcurrent relays could detect the decreased fault current for both grid-connected and islanding modes [104]. Energy storage devices were used to facilitate the fault current detection especially in islanding mode [105]. Considering the coordination problems between fuses and reclosers in microgrids, a microprocessor based recloser was applied [106]. Fault current limiters (FCLs) were connected in series with DGs to restrict fault current [107], [108]. Furthermore, the effects of different arrangements of superconducting fault current limiters (SFCLs) on different fault scenarios in microgrids were analysed [109]. However, additional components are required, which add system costs.

Although many new devices are designed and proposed to improve protection performance of microgrids, currently, these devices are not commercially available in real cases [110]. It should be a possible and effective way to use traditional protection devices, such as directional overcurrent, distance and differential relays, to protect the networks with DGs if they can show good performance. Therefore, several methods focus on analysing fault characteristics of fault current in microgrids and modifying conventional protection schemes. In [111], phase faults in lines, adjacent lines and branch lines were analysed and summarised. The characteristics of fault current of DGs controlled by P-Q and V-f for different modes were presented in [112]. Baran and El-Markabi in [113] introduced an adaptive overcurrent protection for distribution feeders by changing the pickup current of relays. By using a new digital relay with communication channels, Bui *et al.* [114] designed a fast-scalable-adaptable protection algorithm to improve the reliability and adaptability of microgrids. However, these methods are complicated in practical implementation since new functions or relay improvements are required.

In [115], [116], current components were analysed to separate fault current by traditional overcurrent protection. However, this method was ineffective for symmetrical faults. A comparison of directional overcurrent protection with distance protection was conducted in [117]. The research indicated that directional overcurrent protection was preferred since fault current entering feeders and leaving feeders was easily detected and compared. A microgrid system was simulated by using differential relays with either grid-connected or islanding modes for single phase to ground faults [118]. However, the performance of this method for other kinds of faults was not discussed.

Based on control and protection technologies in microgrids, in this chapter, the feasibility of a hybrid control and protection scheme is proposed and tested. This scheme can be applied to ensure the normal and healthy operation of a microgrid system. A discussion of possibilities and issues for applying this scheme to VMs is given in Section 6.5.

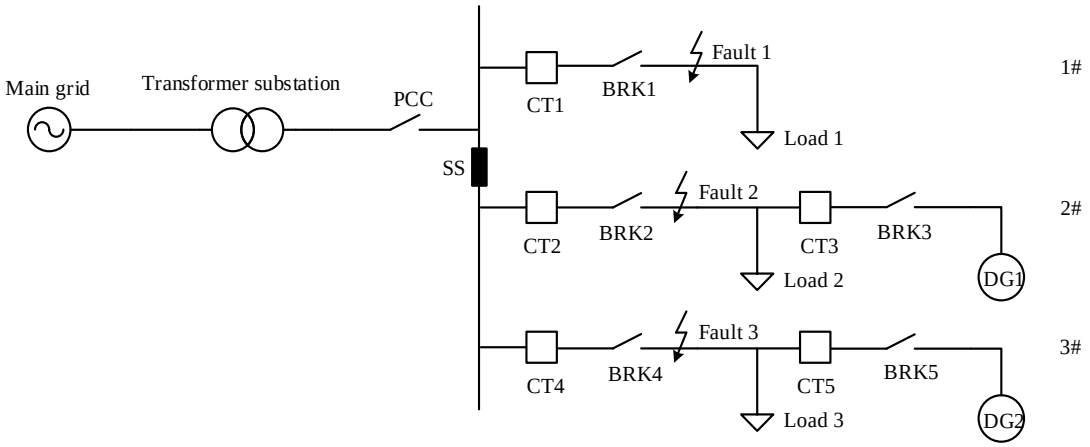

Fig. 6.1 A simple microgrid system.

6.2 Microgrid Control

A microgrid system is shown in Fig. 6.1, which includes two DGs and three loads in this system. This microgrid system can be connected or disconnected from the main grid by changing the state of PCC (Point of Common Couple), and SS (static switch)

is used to change the operating mode of microgrids smoothly. Parameters of this system is presented in Table 6.1.

Table 6.1 Parameter settings of the microgrid

Component	Main grid	Transformer	Load 1
Data	10 kV	25 MVA 10 kV / 0.4 kV	0.18 MW + j0.06 MVar
Component	Load 2	Load 3	
Data	0.06 MW + j0.0195 MVar	0.06 MW + j0.0195 MVar	

In this microgrid system, DG1 is a solar power generator, and DG2 is a micro gas turbine generator. The power generated by solar power generators can be expressed as [85]

$$\begin{cases} T_c = T_A + s_a\left(\dfrac{T_{op}-20}{0.8}\right) \\ I_{ph} = s_a\left[I_{sc} + K_i\left(T_c - 25\right)\right] \\ V = V_{oc} - K_v \times T_c \\ FF = \dfrac{V_{mppt} \times I_{mppt}}{V_{oc} \times I_{sc}} \\ P = N \times FF \times V \times I_{ph} \end{cases} \tag{6.1}$$

where T_c and T_A are cell temperature and ambient temperature; s_a is the solar irradiance; T_{op} is the normal operating temperature of cells; I_{sc} is the short circuit current; V_{oc} is the open circuit voltage; K_i and K_v are current and voltage temperature coefficients; V_{mppt} and I_{mppt} are the voltage and current at the maximum power point; N is the cell number per module.

In this chapter, the solar power generator is controlled by maximum power point tracking (MPPT), then it is connected in series with a battery. Therefore, output power

of the solar power generator can be stored in the battery. Both output power of the solar power generator and the micro gas turbine generator is controllable.

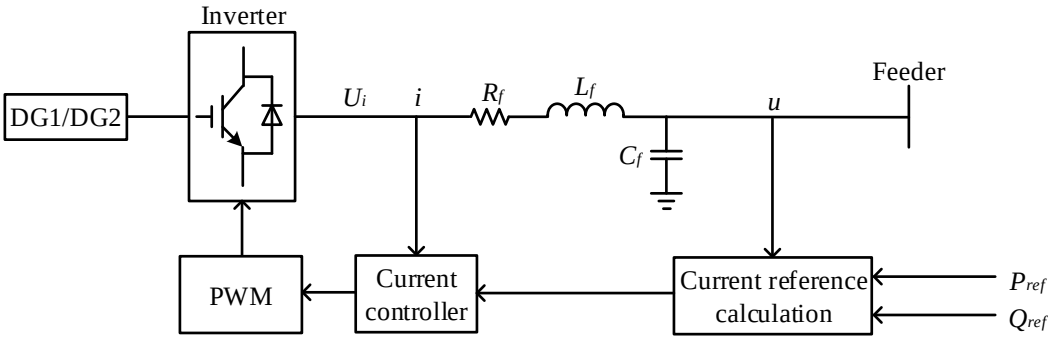

Fig. 6.2 *P-Q* control in microgrids.

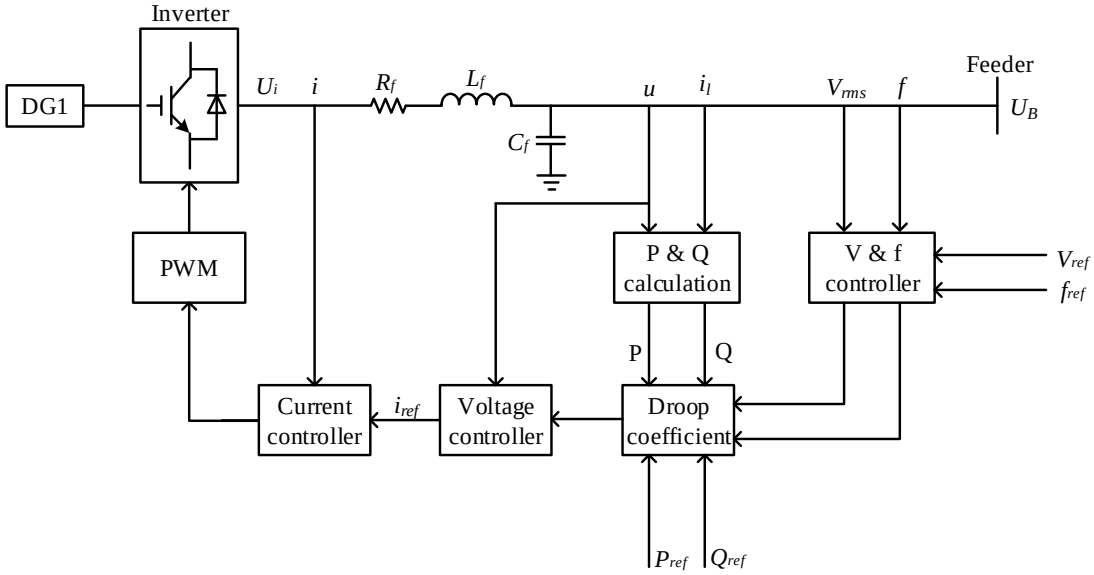

Fig. 6.3 *V-f* control in microgrids.

6.2.1 P-Q and V-f Control Strategies

In grid-connected mode, two DGs are controlled by *P-Q* control method, so active power and reactive power of DGs keeps constant in steady states. Voltage and frequency of systems are regulated by the main grid. When a fault is detected in the main grid, the operation mode of this microgrid is changed to islanding mode. In this case, DG2 is still controlled by *P-Q* method to keep the power balance between

generation and loads, but the control method of DG1 is switched to *V-f* control in order to maintain the stability of voltage and frequency in the microgrid. Detailed control principles of *P-Q* control and *V-f* control are illustrated in Fig. 6.2 and Fig. 6.3 respectively. Fig. 6.4 shows the flow chart of control and protection for the whole system.

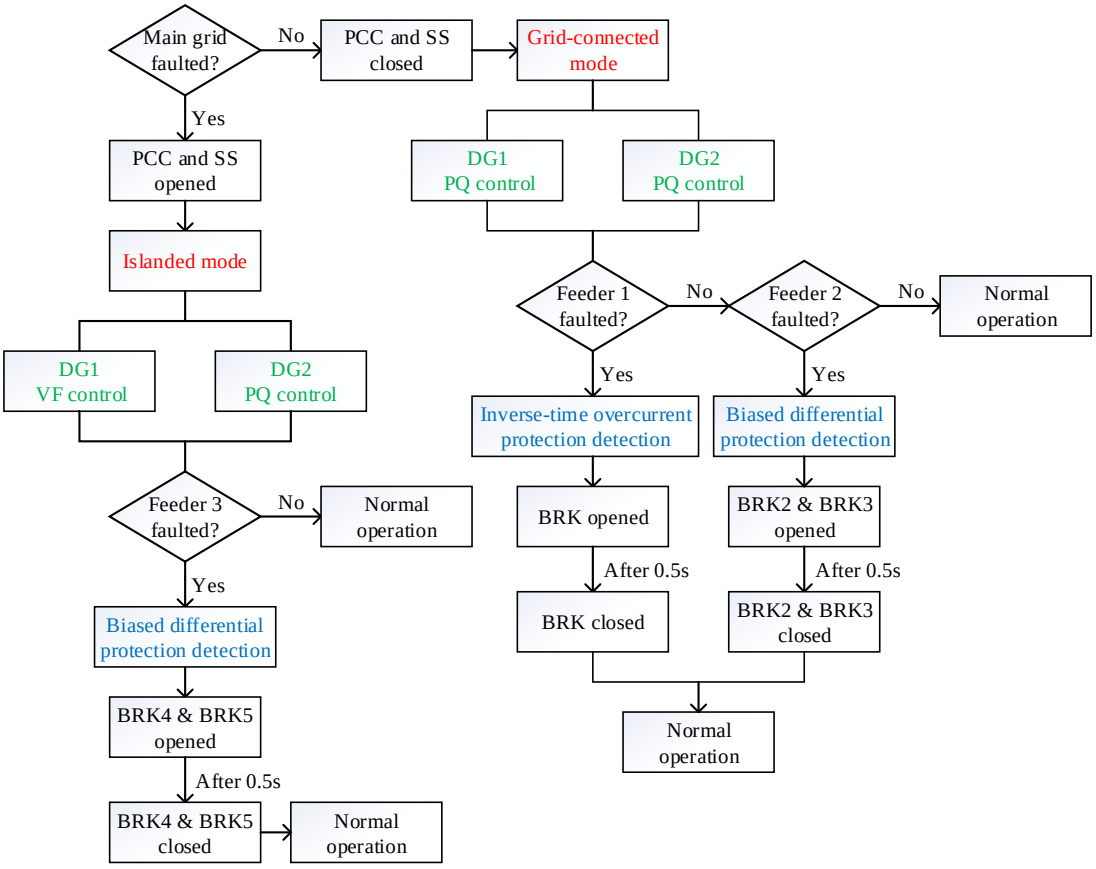

Fig. 6.4 Flow chart of control and protection for the microgrid.

As shown in Fig. 6.2, *P-Q* control strategy relies on calculating reference current and then regulating current to control inverters through pulse-width modulation (PWM) signals. Reference current is obtained from dividing reference active power and reactive power (P_{ref}, Q_{ref}) by actual voltage (u). Comparing to *P-Q* control, *V-f* control is more complicated because more PI controllers are required in outer voltage loop and inner current loop (which is called a dual-loop controller). A block diagram of the dual-loop controller is shown in Fig. 6.5. In Fig.6.5, u_{dref} and u_{qref} are reference input voltage

in d axis and q axis. u_d and u_q are actual voltage in d axis and q axis. k_p and k_i are proportional gain and integral time constant respectively. ω is angular frequency. L_f and C_f are the inductance and capacitance of RLC filter. i_{ld} and i_{lq} are actual current of the grid side in d axis and q axis. i_d and i_q are actual current of the inverter side in d axis and q axis. i_{ldref} and i_{lqref} are reference output current of voltage loop controller in d axis and q axis. u_{idref} and u_{iqref} are output of current loop controller in d axis and q axis.

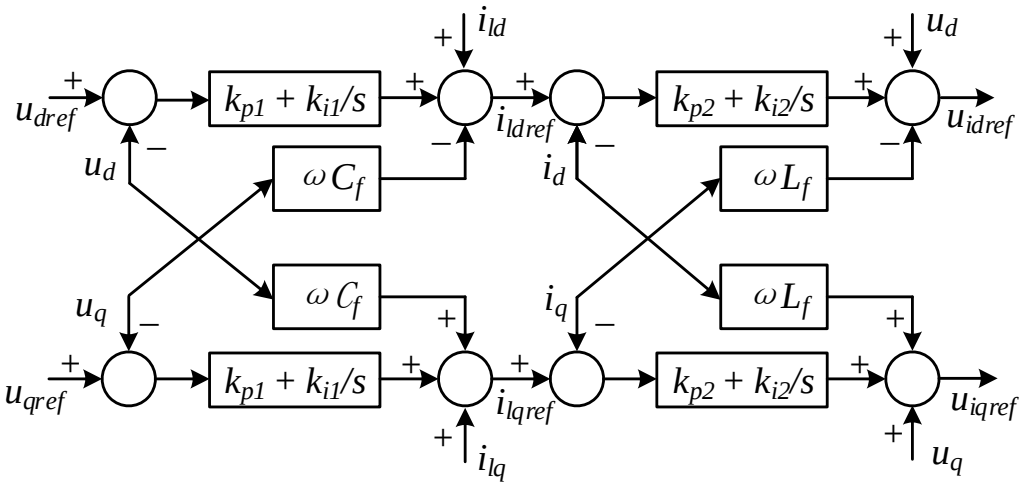

Fig. 6.5 Block diagram of a dual-loop controller.

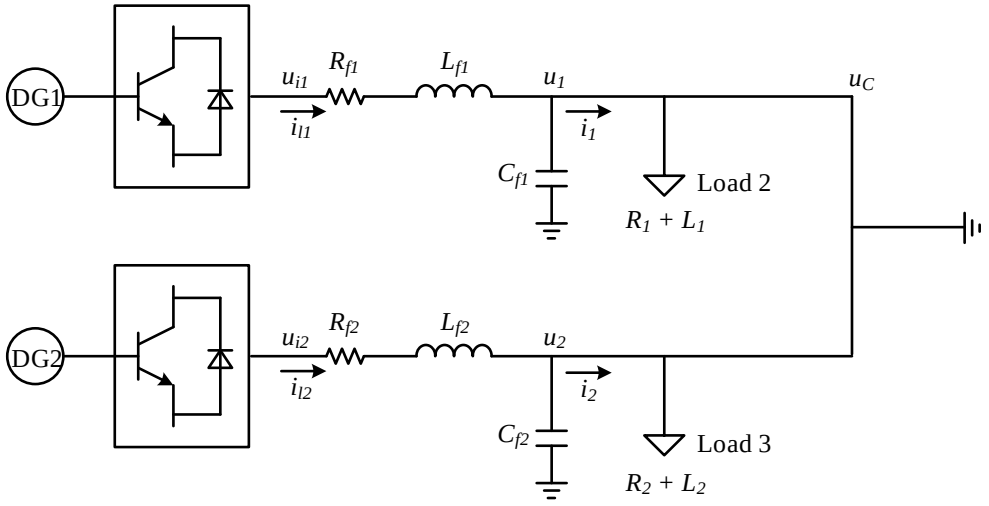

Fig. 6.6 Circuit diagram of a microgrid in islanding mode.

6.2.2 Small-signal Stability Analysis

Comparing to grid-connected mode, microgrids are more likely to loss stability in islanding mode as it cannot get the support from the main grid. In this section, small-signal stability of the microgrid is analyzed, including output harmonics of inverters and filters. A circuit diagram of the microgrid in islanding mode is shown in Fig. 6.6. In this case, load 1 is separated from the network for simplification.

6.2.2.1 Small-signal Modelling for Dual-loop Controller

In order to analyse the stability of V-f control strategy and select suitable parameters for PI controllers, small-signal model of the inverter for DG1 is established after converting original data to d axis and q axis through Park transform. For the dual-loop controller of V-f control strategy in Fig.6.5, to simplify the expression of small-signal equations, φ_d, φ_q, μ_d, μ_q are defined as

$$\begin{cases} \dfrac{d\varphi_d}{dt} = u_{dref} - u_d \\ \dfrac{d\varphi_q}{dt} = u_{qref} - u_q \\ \dfrac{d\mu_d}{dt} = i_{ldref} - i_{ld} \\ \dfrac{d\mu_q}{dt} = i_{lqref} - i_{lq} \end{cases} \tag{6.2}$$

then control equations of the dual-loop controller can be expressed as

$$\begin{cases} i_{ldref} = i_{ld} - \omega C_f u_q + k_{p1}\left(u_{dref} - u_d\right) + k_{i1}\varphi_d \\ i_{lqref} = i_{lq} + \omega C_f u_d + k_{p1}\left(u_{qref} - u_q\right) + k_{i1}\varphi_q \\ u_{idref} = u_d - \omega L_f i_q + k_{p2}\left(i_{ldref} - i_d\right) + k_{i2}\mu_d \\ u_{iqref} = u_q + \omega L_f i_d + k_{p2}\left(i_{lqref} - i_q\right) + k_{i2}\mu_q \end{cases} \tag{6.3}$$

The small-signal state equations of dual-loop controller by adding small signal perturbations are

$$\begin{cases} \left[\Delta\dot{\varphi}_{dq}\right]=\left[0\right]\left[\Delta\varphi_{dq}\right]+B_{u1}\left[\Delta u_{dqref}\right]+B_{u2}\begin{bmatrix}\Delta i_{ldq}\\ \Delta u_{dq}\\ \Delta i_{dq}\end{bmatrix} \\ \left[\Delta\dot{\mu}_{dq}\right]=\left[0\right]\left[\Delta\mu_{dq}\right]+B_{i1}\left[\Delta i_{dqref}\right]+B_{i2}\begin{bmatrix}\Delta i_{ldq}\\ \Delta u_{dq}\\ \Delta i_{dq}\end{bmatrix} \end{cases} \tag{6.4}$$

where $\Delta\varphi_{dq}$ means column vector $\left[\Delta\varphi_d \quad \Delta\varphi_q\right]^{\mathrm{T}}$. Coefficients in Equation (6.4) are

$$B_{u1}=\begin{bmatrix}1 & 0\\ 0 & 1\end{bmatrix},\quad B_{u2}=\begin{bmatrix}0 & 0 & -1 & 0 & 0 & 0\\ 0 & 0 & 0 & -1 & 0 & 0\end{bmatrix}$$

$$B_{i1}=\begin{bmatrix}1 & 0\\ 0 & 1\end{bmatrix},\quad B_{i2}=\begin{bmatrix}0 & 0 & 0 & 0 & -1 & 0\\ 0 & 0 & 0 & 0 & 0 & -1\end{bmatrix}$$

The output equations of dual-loop controller are

$$\begin{cases} \left[\Delta i_{dqref}\right]=C_u\left[\Delta\varphi_{dq}\right]+D_{u1}\left[\Delta u_{dqref}\right]+D_{u2}\begin{bmatrix}\Delta i_{ldq}\\ \Delta u_{dq}\\ \Delta i_{dq}\end{bmatrix} \\ \left[\Delta\dot{u}_{dqref}\right]=C_i\left[\Delta\mu_{dq}\right]+D_{i1}\left[\Delta i_{dqref}\right]+D_{i2}\begin{bmatrix}\Delta i_{ldq}\\ \Delta u_{dq}\\ \Delta i_{dq}\end{bmatrix} \end{cases} \tag{6.5}$$

Coefficients in Equation (6.5) are

$$C_u=\begin{bmatrix} k_{i1} & 0 \\ 0 & k_{i1} \end{bmatrix},\quad D_{u1}=\begin{bmatrix} k_{p1} & 0 \\ 0 & k_{p1} \end{bmatrix},\quad D_{u2}=\begin{bmatrix} 1 & 0 & -k_{p1} & -\omega C_f & 0 & 0 \\ 0 & 1 & \omega C_f & -k_{p1} & 0 & 0 \end{bmatrix}$$

$$C_i=\begin{bmatrix} k_{i2} & 0 \\ 0 & k_{i2} \end{bmatrix},\quad D_{i1}=\begin{bmatrix} k_{p2} & 0 \\ 0 & k_{p2} \end{bmatrix},\quad D_{i2}=\begin{bmatrix} 0 & -\omega L_f & 1 & 0 & -k_{p2} & 0 \\ \omega L_f & 0 & 0 & 1 & 0 & -k_{p2} \end{bmatrix}$$

6.2.2.2 Small-signal Modelling for RLC filter

In addition to inverters, DGs are connected to the main grid via RLC filters and transmission lines. According to Fig. 6.6, following equations can be derived:

$$\begin{cases} L_f \dfrac{di_{ld}}{dt} = u_{id} - u_d - R_f i_{ld} + \omega L_f i_{lq} \\ L_f \dfrac{di_{lq}}{dt} = u_{iq} - u_q - R_f i_{lq} - \omega L_f i_{ld} \\ C_f \dfrac{du_d}{dt} = i_{ld} - i_d + \omega C_f u_q \\ C_f \dfrac{du_q}{dt} = i_{lq} - i_q - \omega C_f u_d \\ L \dfrac{di_d}{dt} = u_d - u_{Cd} - R i_d + \omega L i_q \\ L \dfrac{di_q}{dt} = u_q - u_{Cq} - R i_q - \omega L i_d \end{cases} \tag{6.6}$$

The small-signal state equation of RLC filter and transmission lines is

$$\begin{bmatrix} \Delta \dot{i}_{ldq} \\ \Delta \dot{u}_{dq} \\ \Delta \dot{i}_{dq} \end{bmatrix} = A_{LW} \begin{bmatrix} \Delta i_{ldq} \\ \Delta u_{dq} \\ \Delta i_{dq} \end{bmatrix} + B_{LW} \left[\Delta u_{idq} \right] + C_{LW} \left[\Delta u_{Cdq} \right] + D_{LW} \left[\Delta \omega \right] \tag{6.7}$$

where $A_{LW}=\begin{bmatrix} -\frac{R_f}{L_f} & \omega_0 & -\frac{1}{L_f} & 0 & 0 & 0 \\ -\omega_0 & -\frac{R_f}{L_f} & 0 & -\frac{1}{L_f} & 0 & 0 \\ \frac{1}{C_f} & 0 & 0 & \omega_0 & -\frac{1}{C_f} & 0 \\ 0 & \frac{1}{C_f} & -\omega_0 & 0 & 0 & -\frac{1}{C_f} \\ 0 & 0 & \frac{1}{L} & 0 & -\frac{R}{L} & \omega_0 \\ 0 & 0 & 0 & \frac{1}{L} & -\omega_0 & -\frac{R}{L} \end{bmatrix}$, $B_{LW}=\begin{bmatrix} \frac{1}{L_f} & 0 \\ 0 & \frac{1}{L_f} \\ 0 & 0 \\ 0 & 0 \\ 0 & 0 \\ 0 & 0 \end{bmatrix}$

$C_{LW}=\begin{bmatrix} 0 & 0 \\ 0 & 0 \\ 0 & 0 \\ 0 & 0 \\ -\frac{1}{L} & 0 \\ 0 & -\frac{1}{L} \end{bmatrix}$, $D_{LW}=\begin{bmatrix} I_{lq} & -I_{ld} & U_q & -U_d & I_q & -I_d \end{bmatrix}^{T}$

Table 6.2 Control parameters of inverters

V-f control				P-Q control	
k_{p1}	k_{i1}	k_{p2}	k_{i2}	k_p	k_i
1	0.04	1	0.04	20	0.001

6.2.2.3 Eigenvalues and stability analysis

Based on the state equations of dual-loop controller and RLC filter aforementioned, five pairs eigenvalues of the state matrix can be obtained according to the data in Table 6.2 and Table 6.3. When k_p varies from 0.01 to 100, and the other control parameters are constant, the most representative root locus of this system is shown in Fig. 6.7. It can be seen that real part of the eigenvalue decreases until k_p is equal to 1, then real

part of the eigenvalue increases. Hence, the damping of this system reaches to the maximum value when k_p is 1. At this point, system stability is the best.

Table 6.3 System parameters in static state operation

Component	U_d (V)	U_q (V)	I_d (A)	I_q (A)	I_{ld} (A)	I_{lq} (A)	C_f (mF)	L_f (mH)	ω (A)
Data	328	0	125	15	125	20	1.5	0.6	377

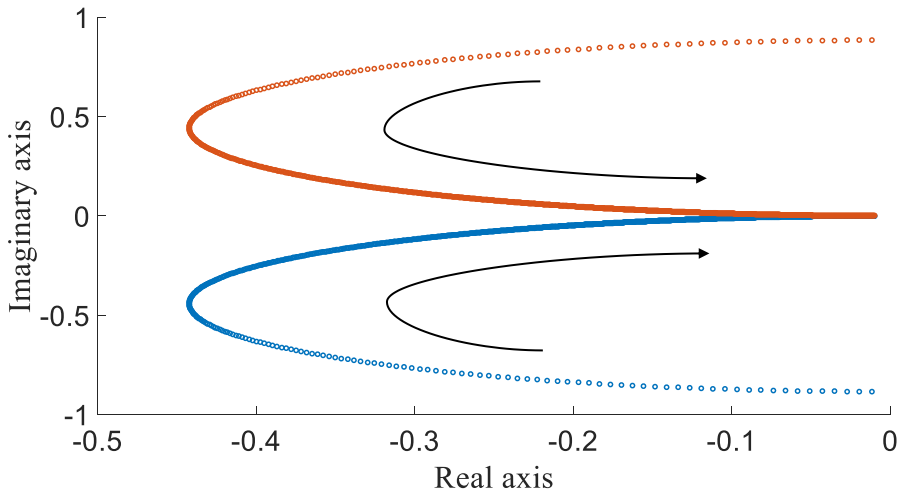

Fig. 6.7 The root locus of the inverter under different proportional gain (k_p) values.

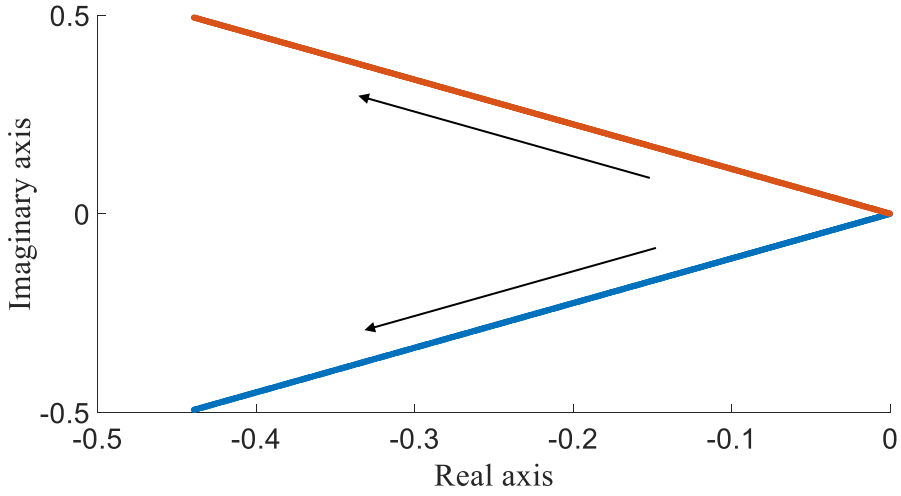

Fig. 6.8 The root locus of the inverter under different integral time constant (k_i) values.

When k_i changes from 0.0001 to 1, and the other control parameters are invariable, Fig. 6.8 shows the root locus for one pair of eigenvalues. It can be found that the real part of the eigenvalue reduces with the increasing of k_i, so the system is stable.

By analysing the root locus of each eigenvalue, the most suitable k_p and k_i are selected. Similarly, the stability and small signal model of the inverter under *P-Q* control strategy is performed and parameters are listed in Table 6.2.

6.3 Hybrid Protection Scheme

In Fig. 6.1, two kinds of loads are considered in the microgrid system: non-sensitive load in feeder 1 and sensitive loads in feeder 2 and 3. Because power flow through the feeders without DGs is unidirectional, so inverse-time overcurrent protection is applied to feeder 1 which contains non-sensitive loads [119]. However, for feeder 2 and feeder 3, inverse-time overcurrent protection cannot be used because the power flow on these two feeders are bi-directional. Therefore, biased differential protection is used, which relies on measuring electrical variables on two ends. The principles of these two kinds of protection methods are discussed below.

6.3.1 Inverse-time Overcurrent Protection

Inverse-time overcurrent protection is based on measuring fault current through relays. If fault current is bigger than setting values, relays will operate to trip related circuit breakers [120]. Tripping time has an inversely proportional relationship with fault current. For bigger fault current, relays operate more quickly [121]. The property of inverse-time overcurrent protection is illustrated in Fig. 6.9 (a), and time-current equations are

$$t_{trip}(I) = T_D \cdot \left(\frac{A}{M^P - 1} + B \right) + K \tag{6.8}$$

$$t_{reset}(I) = T_D \cdot \left(\frac{t_r}{1 - M^2} \right) \tag{6.9}$$

where t_{trip} is the operating time of tripping; t_{reset} represents the operating time of resetting; t_r is the reset time when current is zero; T_D represents time dial options; M represents the ratio of actual current to rated current; A, B, K, p are time constant values according to operation characteristics.

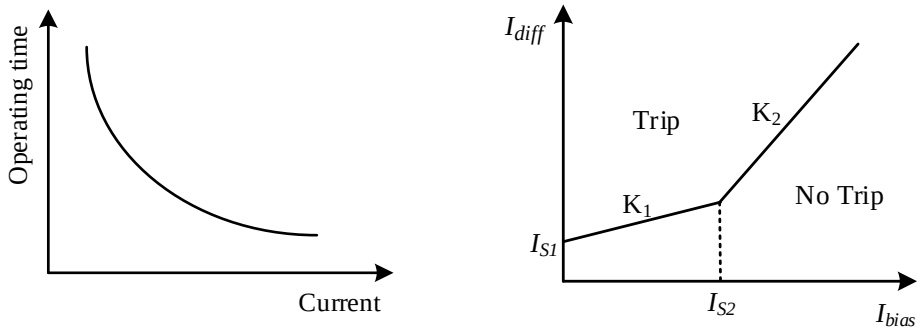

(a) (b)

Fig. 6.9 Characteristics of different protection methods. (a) Inverse-time overcurrent protection; (b) Biased differential protection.

6.3.2. Biased Differential Protection

Basic principles of biased differential protection are to compare directional current of two terminals on lines. There are two cases which refer to the fault in a feeder or out of a feeder, as illustrated in Fig. 6.10. Assuming that the current flows from a bus to the circuit line is positive, and the current goes from a circuit line to buses is negative. Accordingly, if a fault happens between bus 1 and bus 2, the total directional current will be the sum of I_1 (positive) and I_2 (positive) as illustrated in Fig. 6.10 (a). So relays send tripping signals to corresponding circuit breakers for the purpose of protecting electrical equipment. If a fault is not in the area between bus 1 and bus 2 as shown in Fig. 6.10 (b), the direction of fault current is opposite (I_1 is positive and I_2 is negative), so the total current in the faulted point is equal to zero. Differential protection does not operate for this case.

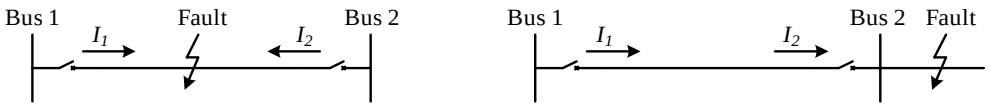

(a) (b)

Fig. 6.10 Two cases of biased differential protection. (a) Case one: fault between two feeders; (b) Case two: fault out of the zone between two feeders.

Based on the principle of differential protection, biased differential protection is used for DGs in feeder 2 and 3. Fig. 6.9 (b) shows the characteristics of this strategy. Firstly, differential current and biased current are calculated based on measured data from current transformers (CTs). Once the point (I_{bias}, I_{diff}) is in the trip area, relays will operate to isolate faults. The trip and no trip areas are divided by different slopes (K_1 and K_2). The expressions for differential and bias current are

$$I_{diff} = \left|I_1 + I_2\right| \tag{6.10}$$

$$I_{bias} = \frac{\left|I_1\right| + \left|I_2\right|}{2} \tag{6.11}$$

where I_1 and I_2 are the secondary side current of CTs.

The characteristics of biased differential protection can be expressed as

$$\text{If } \left|I_{bias}\right| < I_{s2}, \ \left|I_{diff}\right| > K_1 \cdot \left|I_{bias}\right| + I_{S1} \tag{6.12}$$

$$\text{If } \left|I_{bias}\right| \geq I_{s2}, \ \left|I_{diff}\right| > K_2 \cdot \left|I_{bias}\right| - \left(K_1 - K_2\right) \cdot I_{S2} + I_{S1} \tag{6.13}$$

where K_1 and K_2 are restraint coefficients. I_{S1} is the minimum pickup current of relays. I_{S2} is the minimum brake current.

6.3.3 Parameter Setting for Relays

By using Fast Fourier transform (FFT) in MATLAB, simulation results obtained from Power Systems Computer Aided Design (PSCAD) in time domain can be transformed to that in frequency domain. Therefore, the features of fault current are obtained easily, and then parameters of overcurrent and differential relays can be set based on calculation results.

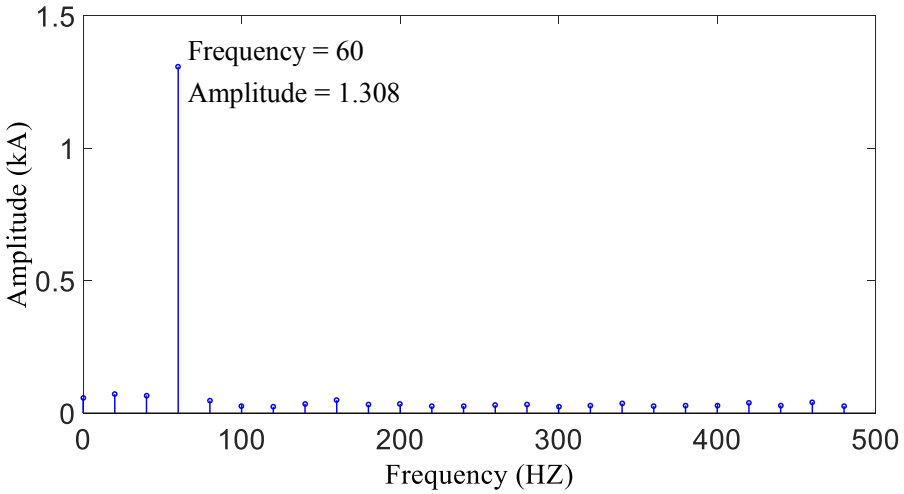

(a)

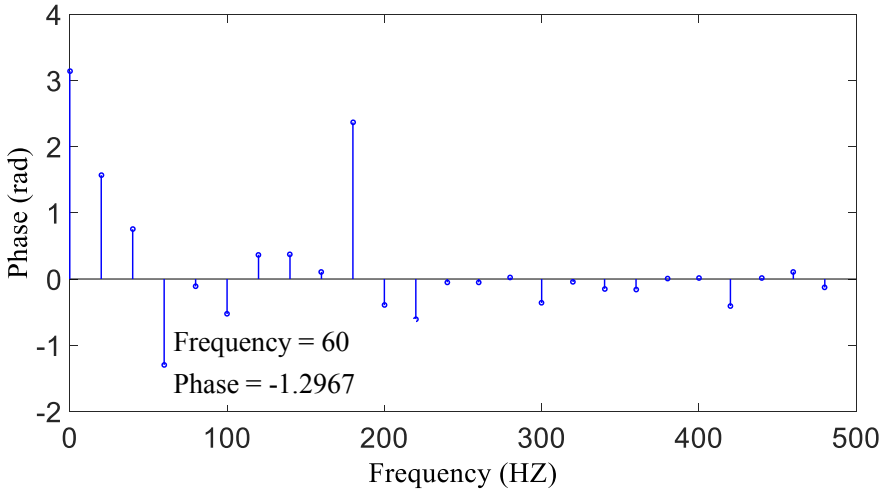

(b)

Fig. 6.11 Amplitude and phase values of DG1 side fault current in the frequency domain under fault 2. (a) The amplitude value; (b) The phase value.

Taking the single phase to ground fault in grid-connected mode (fault 2) as an example, amplitude and phase values of DG1 side fault current which is converted by FFT algorithm is presented in Fig. 6.11. Based on Equation (6.10) and Equation (6.11), differential and biased current can be calculated

$$\left|I_{diff}\right| = \left|I_{CT2} + I_{CT3}\right| = \left|1.3080 - j1.2967 + 3.2882 - j1.0189\right| = 5.1466kA \quad (6.14)$$

$$\begin{aligned}\left|I_{bias}\right| &= \frac{1}{2} \times \left(\left|I_{CT2}\right| + \left|I_{CT3}\right|\right) \\ &= \frac{1}{2} \times \left(\left|1.3080 - j1.2967\right| + \left|3.2882 - j1.0189\right|\right) = 2.6421kA \end{aligned} \quad (6.15)$$

Table 6.4 Fault current in frequency domain

Fault conditions	Grid-connected mode				Islanding mode			
	Single phase to ground fault		Three phase fault		Single phase to ground fault		Three phase fault	
	I_{DG}	I_{grid}	I_{DG}	I_{grid}	I_{DG}	I_{grid}	I_{DG}	I_{grid}
Amplitude (kA)	1.3080	3.2882	0.4824	31.3746	0.2235	1.6280	0.1484	1.0469
Phase (rad)	-1.2967	-1.0189	0.03754	-0.06779	0.6963	0.5941	0.7212	1.3501

Table 6.5 The values of differential current and bias current

Fault conditions	Grid-connected mode		Islanding mode	
	Single phase to ground fault	Three phase fault	Single phase to ground fault	Three phase fault
I_{diff} (kA)	5.1466	31.8570	2.2568	2.3914
I_{bias} (kA)	2.6421	15.9293	1.2322	1.2224

The other fault current values in the frequency domain under different operating modes and fault types are presented in Table 6.4. Table 6.5 shows all calculation results

of differential and bias current. Then these calculation results can be labelled on the characteristic curve of biased differential protection as shown in Fig. 6.12, and these faulted points should in the trip area for the purpose of opening corresponding circuit breakers to isolate all kinds of faults.

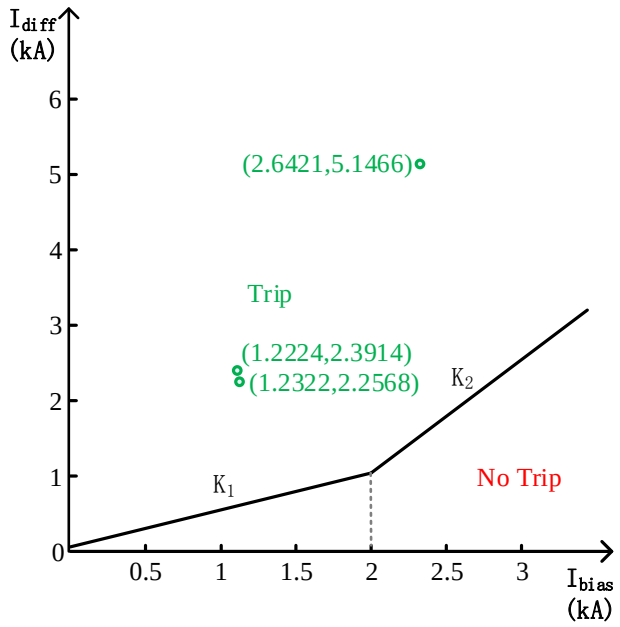

Fig. 6.12 Characteristic curve of biased differential protection for the simulation model.

According to [122], the percentage bias setting of biased differential protection is 0.3-0.8 in the general case, and it is recommended to keep the percentage bias setting bigger than 0.5. However, the percentage bias setting should rely on real operating data of devices, and malfunction should also be taken into account in real power systems. Therefore, percentage bias settings depend more on real operating conditions of systems, and it is easy to be reset by applying microcomputer protection. As there is no principle for the parameter settings of biased differential protection in microgrid systems, so in this chapter, percentage bias settings for K_1 and K_2 are set to 0.5 and 1.5 respectively in order to ensure the reliable operating of circuit breakers for different fault types. Finally, operation equations of biased differential protection are determined as

$$\text{When } |I_{bias}| < 2kA, \ |I_{diff}| > 0.5 \cdot |I_{bias}| + 0.05 \tag{6.16}$$

$$\text{When } |I_{bias}| \geq 2kA, \ |I_{diff}| > 1.5 \cdot |I_{bias}| - 1.95 \tag{6.17}$$

For inverse-time overcurrent protection, FFT can also be used for transforming fault current from time domain to frequency domain. Therefore, the pickup current of overcurrent relays is easy to obtain, and the other fixed parameter settings for overcurrent relay are shown in Table 6.6.

Table 6.6 Parameters of inverse-time overcurrent protection and biased differential protection

Component	Inverse-time overcurrent protection							Biased differential protection			
	A	*B*	*K*	*P*	t_r	*q*	T_D	IS_1	K_1	IS_2	K_2
Data	0.0104	0.0226	0	0.02	1.08	2	0.1	0.05	0.5	2	1.5

6.4 Simulation Analysis

In this section, different kinds of faults are tested in the microgrid model to evaluate the validity of the proposed protection scheme. One is single phase to ground fault, which is the most common fault in electrical power systems. The other one is three phase fault, which represents the most serious fault in microgrids. For each kind of fault, three fault scenarios are defined. Fault 1 and fault 2 are applied to feeder 1 (without DG) and feeder 2 (with DG1) independently in grid-connected mode, while fault 3 occurs on feeder 3 (with DG2) in islanding mode as shown in Fig. 6.1. Table 6.6 lists main parameters of inverse-time overcurrent protection and biased differential protection.

The working process of the proposed protection scheme is illustrated in Fig. 6.4. When the microgrid operates in grid-connected mode, all three feeders are connected to the main grid. If a fault happens on feeder 1, it should be detected by inverse-time

overcurrent protection, then the circuit breaker on feeder 1 (BRK1) should open to isolate this fault after receiving tripping signals from the relay. Biased differential protection is used to protect feeder 2, so BRK2 and BRK3 will operate if a fault happens on feeder 2. Firstly, the differential current and biased current are calculated based on fault current from CT2 and CT3. Secondly, relays send tripping signals to BRK2 and BRK3 if the point (I_{bias}, I_{diff}) is in the trip area. After that, the fault is able to be isolated from the system by opening BRK2 and BRK3. Because the duration time of fault is 0.5 s, so all circuit breakers which open in fault conditions reclose again after 0.5 s, then the system can recover to normal operating condition. The protection process of feeder 3 in islanding mode is similar to that of feeder 2 in grid-connected mode. The only difference is that BRK4 and BRK5 are responsible for protecting feeder 3.

The simulation model of the microgrid and related protection scheme are established in PSCAD and presented in Fig. 6.13. Four cases are discussed and main simulation results for different fault types and operating modes are illustrated.

6.4.1 Single Phase to Ground Fault in Grid-connected Mode

To check the validity of the protection scheme when the microgrid operates in grid-connected mode, phase C to ground fault is applied to feeder 1 and feeder 2 respectively. Because there is no sensitive load, and the power flow on feeder 1 is unidirectional, so inverse-time overcurrent protection is applied on feeder 1. Fig. 6.14 shows phase C current of feeder 1. It can be seen that phase C current becomes high suddenly when the fault happens at 1.5 s, and this fault only lasts for few seconds before it is cleared by BRK1 on feeder 1. The state change of BRK1 can be seen from Fig. 6.15. It changes from 0 to 1 when fault 1 happens, and BRK1 recloses again at 2 s after the fault is isolated from the system, so the system operates healthily after 2 s. Therefore, inverse-time overcurrent protection scheme is able to detect the fault in feeder 1, and related circuit breakers can operate to isolate this fault.

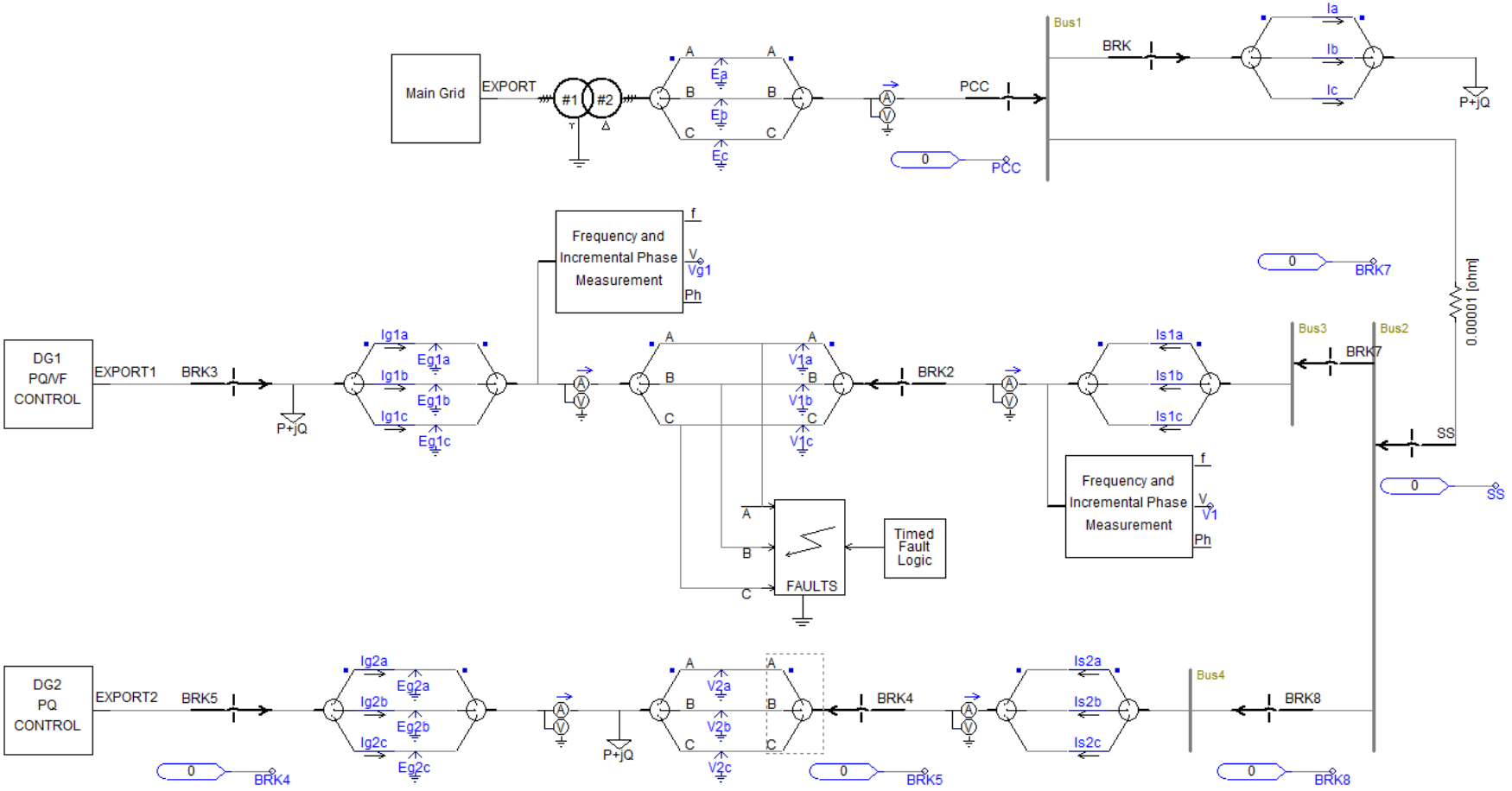
Main Grid
EXPORT
#1
#2
Ea
Eb
Ec
PCC
Bus1
BRK
Ia
Ib
Ic
P+jQ
0
PCC
Frequency and Incremental Phase Measurement
f
V
Vg1
Ph
0
BRK7
0.00001 [ohm]
DG1 PQ/VF CONTROL
EXPORT1
BRK3
P+jQ
Ig1a
Ig1b
Ig1c
Eg1a
Eg1b
Eg1c
V1a
V1b
V1c
BRK2
Is1a
Is1b
Is1c
Bus3
Bus2
BRK7
SS
0
SS
Frequency and Incremental Phase Measurement
f
V
V1
Ph
Timed Fault Logic
FAULTS
DG2 PQ CONTROL
EXPORT2
BRK5
Ig2a
Ig2b
Ig2c
Eg2a
Eg2b
Eg2c
P+jQ
V2a
V2b
V2c
BRK4
Is2a
Is2b
Is2c
Bus4
BRK8
0
BRK4
0
BRK5
0
BRK8

(a)

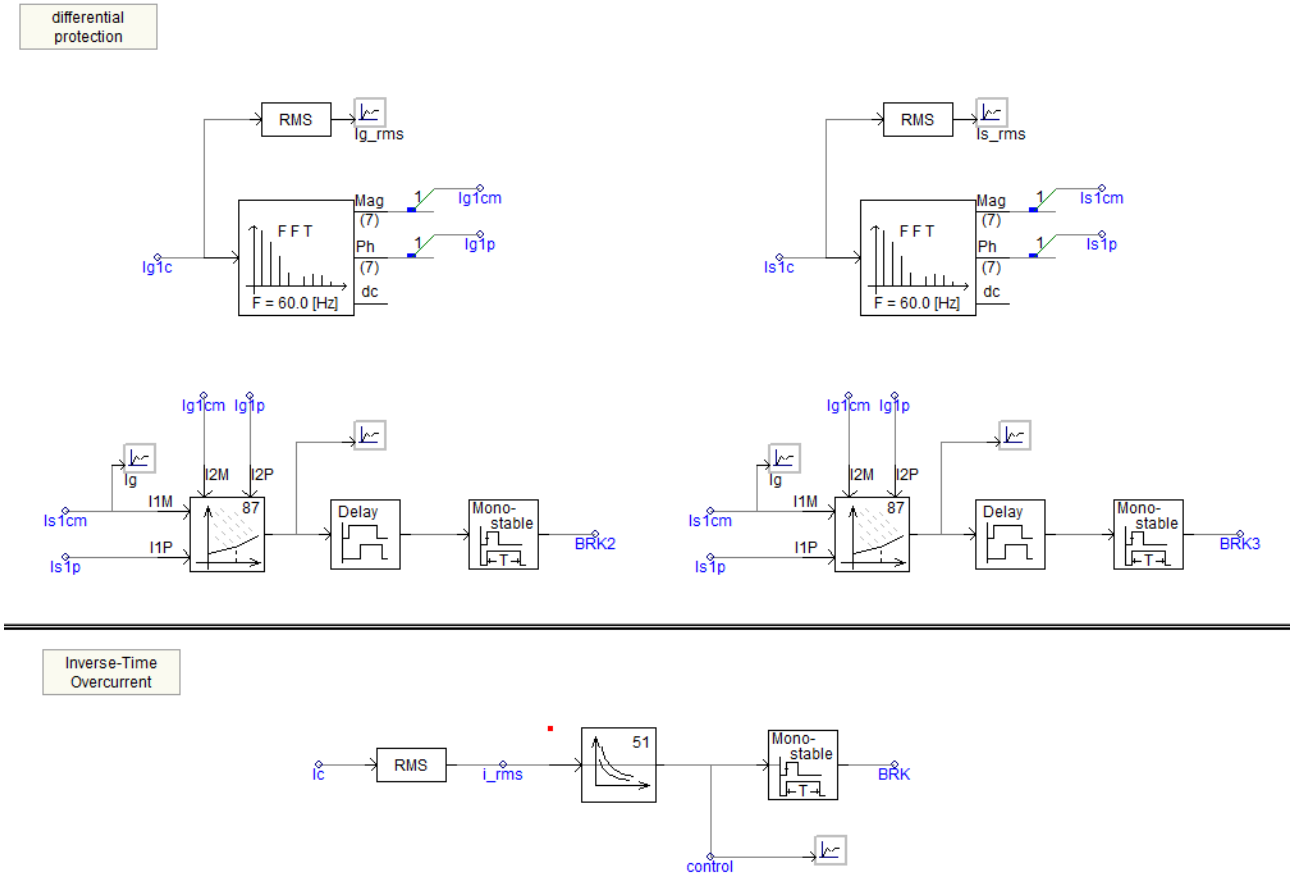

(b)

Fig. 6.13 Simulation model in PSCAD. (a) Microgrid model; (b) Protection model.

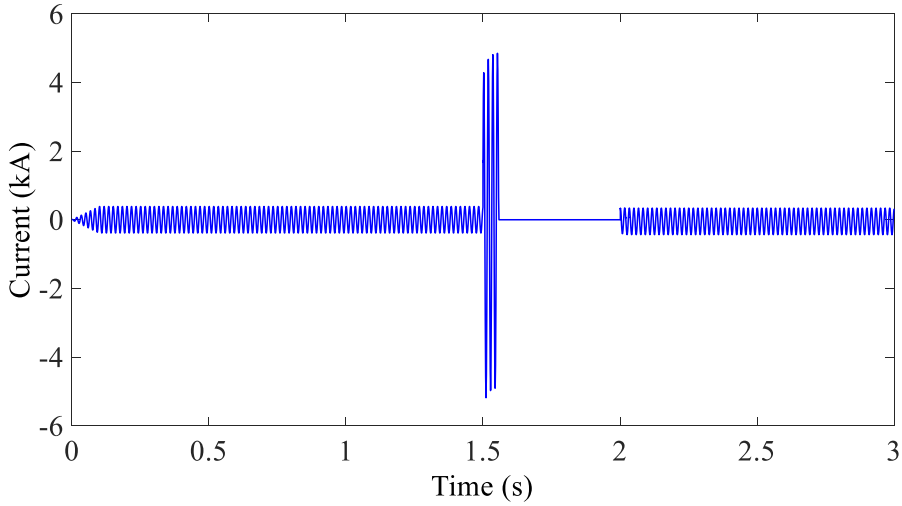

Fig. 6.14 Simulated current of phase C in feeder 1 under phase C to ground fault (fault 1).

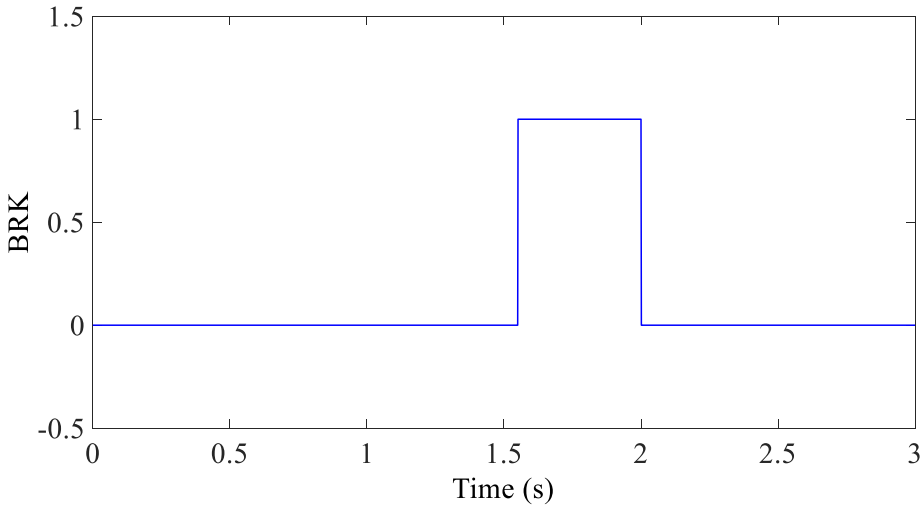

Fig. 6.15 State change of the circuit breaker in feeder 1 under phase C to ground fault (fault 1).

Biased differential protection is used to protect sensitive loads on feeder 2 against fault 2. This protection scheme is based on calculating differential current and biased current, and these values are obtained from CT2 and CT3 which measure the current in DG side and the grid side. Simulation curves of phase C current in DG1 side and the grid side are presented in Fig. 6.16. It shows that both the current of phase C in DG1 side and the grid side increases rapidly at 2 s when single phase C to ground fault

happens. Fault current from the grid side is much larger than that from DG1 side. To ensure the power supply of the other parts in this system, biased differential protection detects this fault, and sends tripping signals to circuit breakers (BRK2 and BRK3) which are located on both sides of the fault point. Because fault 2 lasts for 0.5 s, so BRK2 and BRK3 reclose at 2.5 s, then current goes back to the normal value.

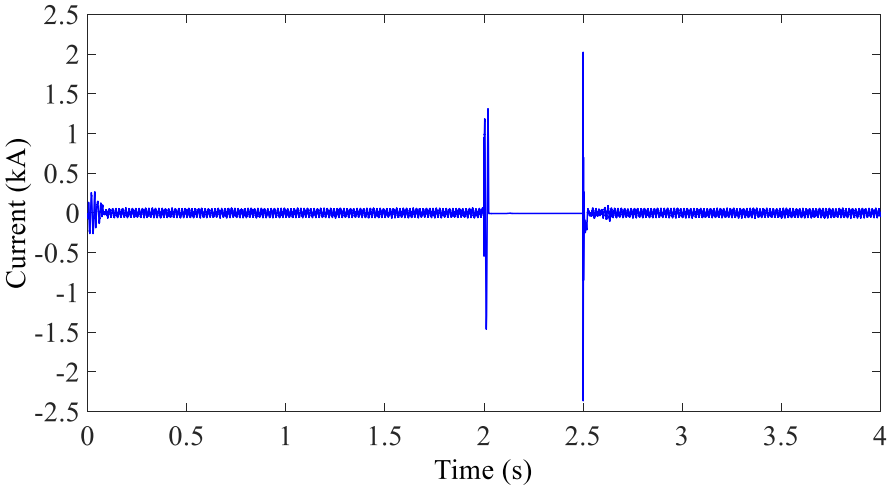

(a)

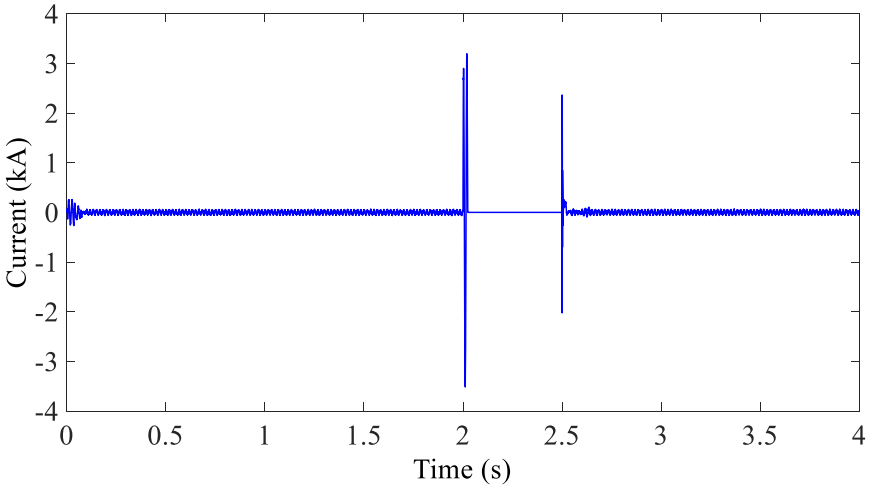

(b)

Fig. 6.16 Simulated current of phase C in feeder 2 under phase C to ground fault (fault 2). (a) The current in DG1 side; (b) The current in the grid side.

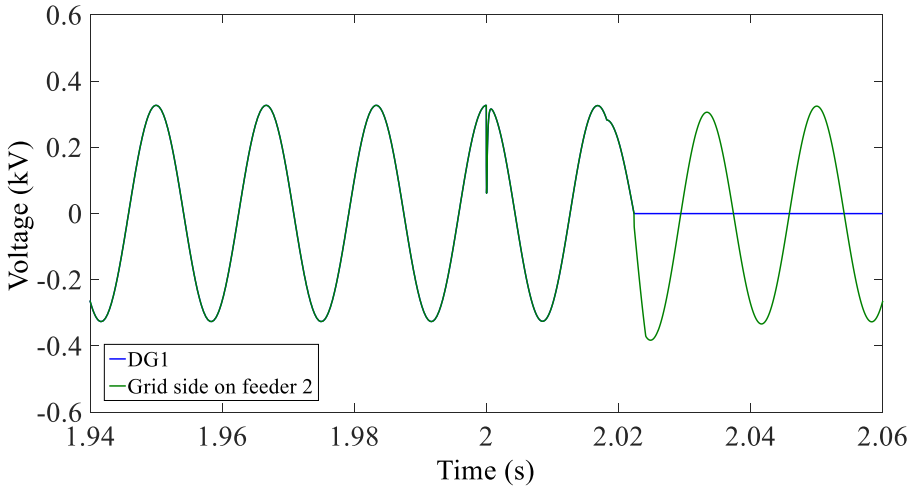

(a)

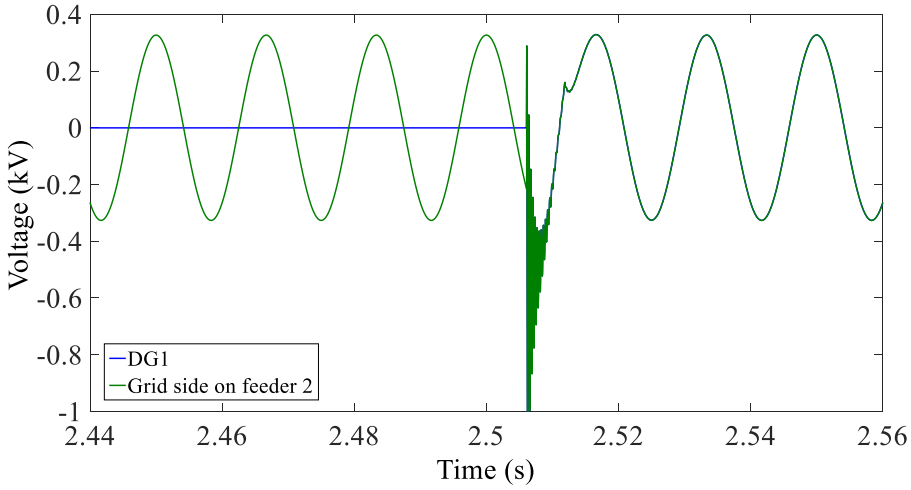

(b)

Fig. 6.17 Simulated voltage of phase C in feeder 2 under three phase fault (fault 2). (a) Voltage variation during fault 2; (b) Voltage variation after isolating fault 2.

6.4.2 Three phase fault in Grid-connected mode

Simulation results of three phase fault on feeder 1 are similar to that of phase C to ground fault except for larger fault current. Inverse-time overcurrent protection is able to detect and isolate three phase fault on feeder 1 without sensitive loads. When three phase fault (fault 2) happens on feeder 2, the voltage of DG1 side (the blue line) and the grid side (the green line) are shown in Fig. 6.17. Both the voltage of DG1 side and the grid side oscillates when fault 2 occurs at 2 s, then fault 2 is detected by biased

differential protection, and related circuit breakers open to clear the fault, so the voltage of DG1 side becomes zero, while voltage of the grid side is stable after oscillation. At about 2.5 s, BRK2 and BRK 3 close again, and the voltage of DG1 side is equal to the voltage of the grid side after synchronization process. Because DG1 is controlled by *P*-*Q* method, so active power and reactive power of DG1 remain constant (0.04 MW and 0.01 MVar) as shown in Fig. 6.18. Therefore, it is concluded that the control strategy and protection scheme are effective in grid-connected mode.

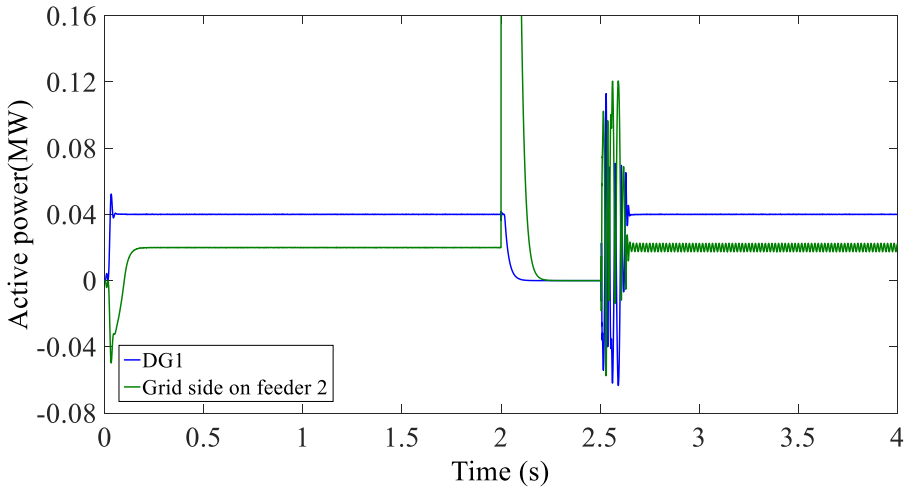

(a)

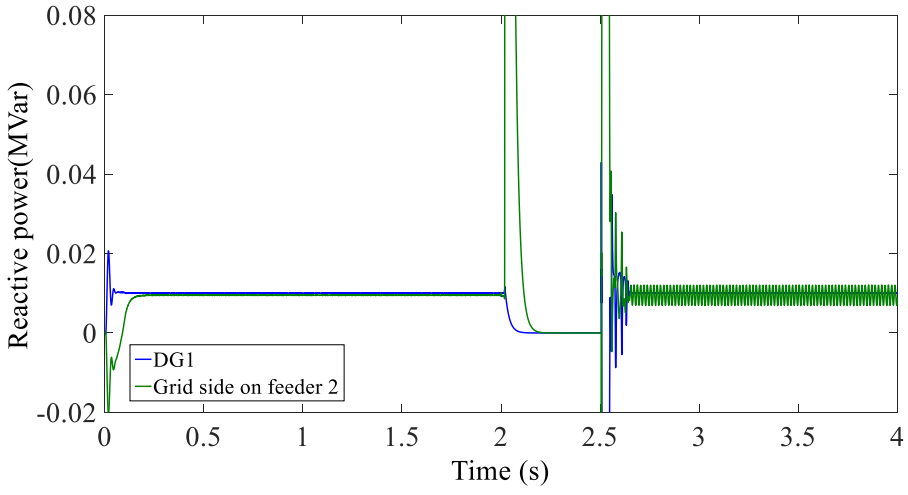

(b)

Fig. 6.18 Simulated active power and reactive power in DG1 side and the grid side under three phase fault (fault 2). (a) Active power; (b) Reactive power.

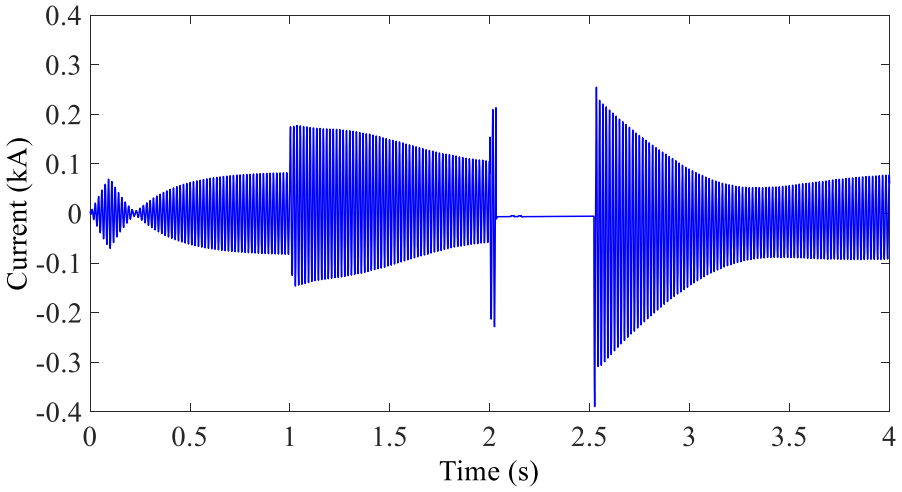

(a)

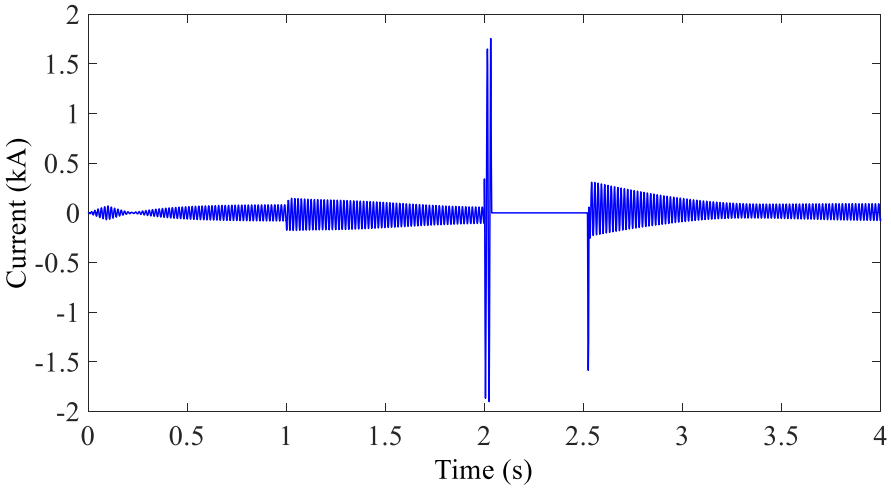

(b)

Fig. 6.19 Phase C current in feeder 3 under phase C to ground fault (fault 3). (a) Current in the grid side; (b) Current in DG2 side.

6.4.3 Single Phase to Ground Fault in Islanding Mode

For the purpose of ensuring the power supply of some sensitive loads, the operating mode of the microgrid will change to islanding mode if a fault happens in the main grid. On this occasion, PCC and SS open, and load 1 is separated from the network. In order to regulate the voltage and frequency of the microgrid, the control strategy of DG1 changes from *P*-*Q* control to *V*-*f* control, while DG2 is still regulated by *P*-*Q* control method. Because load 2 and load 3 are sensitive loads, and the power flow on

these two feeders is bidirectional, so feeder 2 and feeder 3 are protected by biased differential protection.

Fig. 6.19 shows the current of phase C in the whole simulation process when phase C to ground fault (fault 3) occurs on feeder 3. The microgrid operates in grid-connected mode before the microgrid is disconnected from the main grid at 1 s, and phase C current becomes stable after oscillation. Then fault 3 happens at 2 s, and the current on two sides of the fault point goes up immediately. Based on calculating differential and biased current from DG2 side and the grid side, it can be found that this fault current is in the trip area, so relays send tripping signals to related circuit breakers. The states of BRK4 and BRK5 change from 0 to 1 at 2 s, and the current of phase C both in DG2 side and the grid side reduces to 0 at the same time, so the single phase to ground fault can be separated from the network successfully by applying biased differential protection. The islanding microgrid can return to the normal condition slowly after 2.5 s.

6.4.4 Three Phase Fault in Islanding Mode

Compared to phase C current when single phase to ground fault happens on feeder 3, phase C current is much bigger when three phase fault occurs on feeder 3. Biased differential protection is able to detect this fault, and tripping signals are sent to circuit breakers on DG2 side (BRK5) and the grid side (BRK4), so fault 3 is able to be isolated when the microgrid operates in islanding mode whether it is single phase to ground or three phase fault.

Since the microgrid operates in islanding mode, so it loses the support of voltage and frequency from the main grid. In this case, *V-f* control takes the place of main grid to regulate voltage and frequency in the microgrid. Because the stable operating of microgrids is very important, so load variation cases are added in this part in order to verify the effectiveness of the control strategy. Fig. 6.20 to Fig. 6.22 show detailed simulation results when the system operates in different situations.

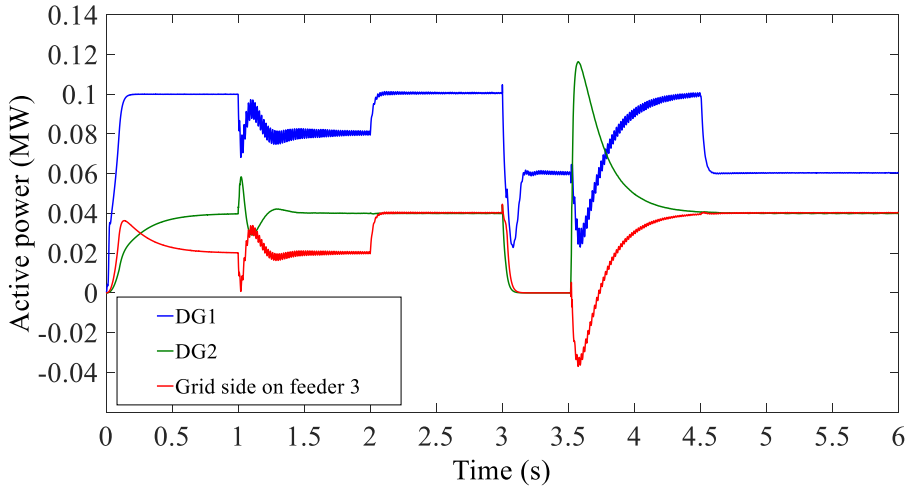

(a)

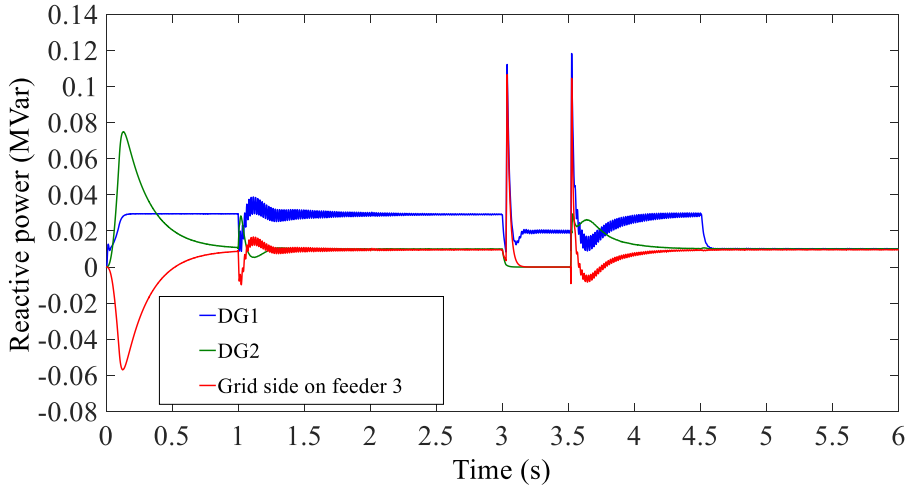

(b)

Fig. 6.20 Active power and reactive power in DG2 side and the grid side under three phase fault (fault 3). (a) The active power; (b) The reactive power.

Active and reactive power variation under different situations can be founded in Fig. 6.20. Before 1 s, the microgrid operates in grid-connected mode with a voltage ramp up time of 0.1 s, and total load demands of load 2 and load 3 are 0.12 MW + j0.039 MVar. The microgrid is separated from the main grid at 1 s, then it operates in islanding mode. After that, the active power of load 2 increases to 0.08 MW at 2 s, and load 3 remains constant. Because DG2 is controlled by *P-Q* method, and it outputs unchangeable power, so the output power of DG1 goes up to meet the increased load

demands. Meanwhile, the voltage and frequency of the microgrid system can keep stable under the *V-f* control applied in DG1 as shown in Fig. 6.21 and Fig. 6.22. Three phase fault occurs on feeder 3 at 3 s, so voltage drops a lot, and the output power from DG2 becomes zero. Then the fault is cleared by biased differential protection, and related circuit breakers on feeder 3 close again after 0.5 s. The root mean square (RMS) value of voltage can recover to 0.4 kV after oscillation. At 4.5 s, load 3 reduces from 0.06 MW + j0.0195 MVar to 0.02 MW + j0.0005 MVar, and the output power of DG1 decreases at the same time.

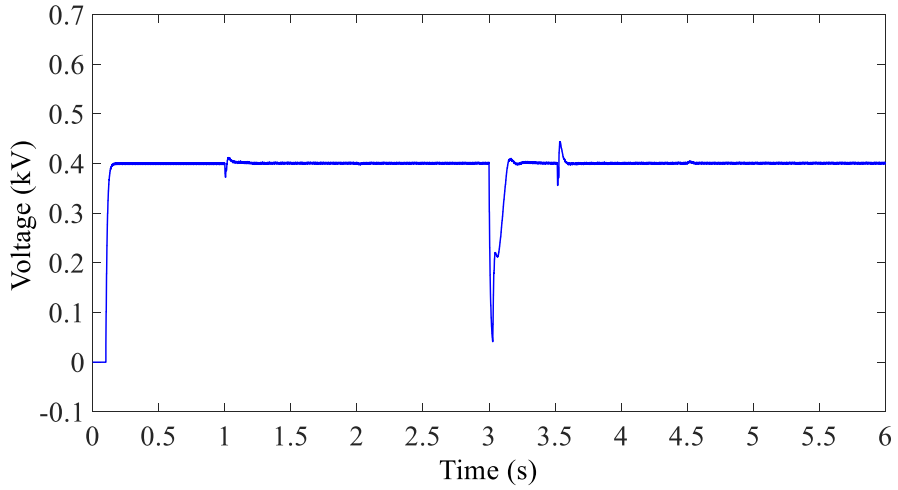

Fig. 6.21 Voltage of microgrid in islanding mode.

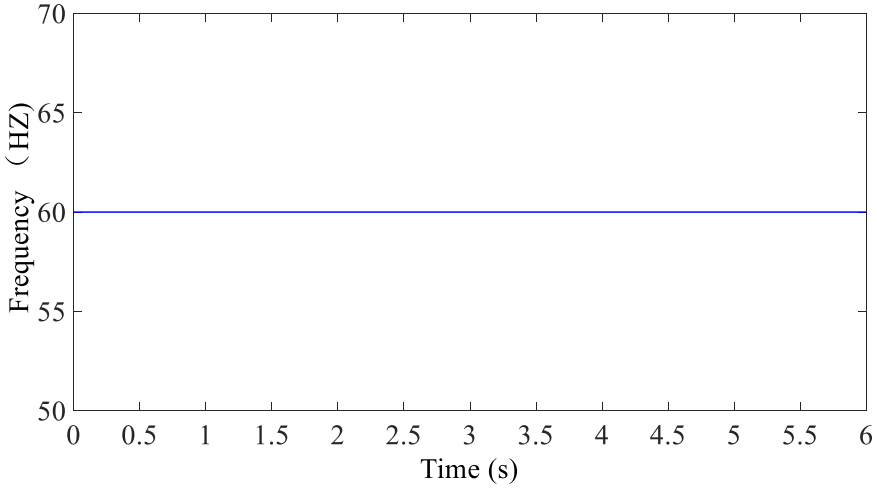

Fig. 6.22 Frequency of microgrid in islanding mode.

As shown in Fig. 6.21 and Fig. 6.22, in the whole simulation process, the voltage and frequency of the microgrid can recover to the normal value even under the most serious three phase fault. The fluctuation of voltage and frequency is tiny under load variation conditions. DG2 is controlled by P-Q method, so the output power from DG2 is constant when the microgrid operates in normal cases. Therefore, it can be concluded that the proposed control strategy and protection scheme is able to ensure the stability of the microgrid system.

6.5 Extending the Proposed Schemes to VMs

By analysing the simulation results of different operating modes and fault types in Section 6.4, it can be found that the proposed scheme is effective to microgrids. In this section, the feasibility of applying these technologies to VMs is discussed.

From the control point of view, since the future control mode of electrical networks will finally transfer from centralised control to decentralised control, the operating ability of VMs in islanding mode is very important, which is similar to a microgrid when it operates in islanding mode. As the scale of a VM is much smaller than the entire power system, so ensuring the stability of voltage and frequency for a small VM system in islanding mode is a challengeable problem. The popular V-f control strategy can provide a choice to ensure that the voltage and frequency are within their limit range in this case. If V-f control is applied to VMs, for each VM, at least one dispatchable DG should have the electronic device with V-f control. For the other DGs in a VM, in order to meet the power supply requirements of loads, a constant output of active power and reactive power is needed, so P-Q control is suitable. Considering the stochastic nature of non-dispatchable DGs, energy storage devices are essential to be applied to compensate for the output of DGs. In some emergency conditions, when two or several VMs need to be connected together, power exchange happens among these VMs. The settings of electronic devices in these VMs should be adjusted automatically according to new operating requirements, such as updated load demands. Moreover, for different VMs, setting values of voltage and frequency should be the

same to ensure the synchronization of operating states in the case of combined operation of VMs.

From the protection point of view, as discussed in Section 6.1, fault current variation and the appearance of bi-directional power flow are two issues. Similar to microgrids, for a VM operating in islanding mode, the direction and value of fault current should be able to be detected by biased differential protection scheme based on appropriate setting values, and inverse-time overcurrent protection can be used to the feeders without DGs due to unidirectional power flow. For each VM, the settings of related relays can be determined based on the analysis of fault current for different fault types. It makes the situation become more complicated when a VM need to run in combined mode by making connection with other VMs because new fault current may be very different compared to the previous one, which may cause some relays not to work properly. Therefore, some principles should be made to adjust relay settings according to different operating modes simultaneously. Although constructing VMs make contribute to a more reliable and flexible network, various operating modes also bring many challenges, therefore, a more comprehensive scheme including backup protection should be made to improve the reliability of the protection.

6.6 Summary

This chapter is to explore the control and protection issues of VMs from the operation point of view. Since there are few studies focusing on this aspect, due to the similarities between VMs and microgrids, a hybrid control and protection scheme for microgrids is proposed and analysed in this chapter.

In the proposed control strategy, DGs are regulated by *P*-*Q* control and *V*-*f* control in different operating modes. Inverse-time overcurrent protection and biased differential protection are used to protect different kinds of feeders. The feeders with non-sensitive load is protected by inverse-time overcurrent protection, while the feeders with DGs are protected by biased differential protection. From the simulation results, it can be seen that this protection scheme is able to protect these two kinds of

feeders both in grid-connected and islanding modes, and the stability of the microgrid can be guaranteed under the proposed control strategy whether the fault type is single phase to ground fault or three phase fault.

The feasibility of applying this scheme to VMs is also discussed. For a VM operates in islanding mode, the proposed control techniques, such as P-Q control, V-f control, inverse-time overcurrent protection and biased differential protection, are suitable for VMs. However, many issues are still needed to be considered, such as automatic setting of related devices according to different operating conditions. For example, when VMs operate in combined mode, it is more complicated for both control and protection. Therefore, a more comprehensive study should be carried out in the future to improve the performance of SDNs.

Chapter 7
Conclusions and Future Work

7.1 Conclusions

It is widely agreed that the integration of DGs to distribution networks is helpful to solve the issues in traditional power systems. So it is necessary to design a planning to construct SDNs with integration of DGs. Unlike passive planning methods which are used by most of studies based on conventional control and operating mechanisms of CDNs, in this thesis, a three-layer active planning for upgrading CDNs to SDNs is proposed by considering both current structure of CDNs and future decentralised vision of SDNs. VMs are basic units to realise decentralised control, and they are self-sufficient and autonomous systems. Active energy management ability of SDNs is considered as an important function in the three-layer active planning. The three-layer active planning consists of physical system layer, cyber system layer and socioeconomic system layer. Cyber system layer is the intermediate between physical system layer and socioeconomic system layer, and it is responsible for collecting and analysing the data from physical system layer and sending control commands to socioeconomic system layer for transaction decision making.

The most important part of the three-layer active planning is physical system layer, which affects the topology and function of other two layers. Hence, a two-phase strategy is put forward to develop physical system layer. Phase 1 is to determine boundaries of VMs by partitioning CDNs. Based on the partitioning results in phase 1, phase 2 is to optimise the DG allocation in VMs.

7.1.1 A Hierarchical Partitioning Method for CDNs

Operating states of power systems depend on three factors, i.e. DG allocation, load distribution and network structure. For most of CDNs, DG allocation is not performed yet, and it should be an evolutionary process to integrate DGs to distribution networks.

Load distribution may be changed since load demands are increasing. Compared to DG allocation and load distribution, network structure is already formed, and it is unlikely to be changed much. Therefore, to determine VM boundaries in phase 1, a partitioning method based on structural information is proposed, which is different from most of existing studies based on operating states analysis with the assumption of DG allocation results. Considering specific characteristics of electrical networks, distance and capacity are two important items to describe structural characteristics of electrical networks. Based on equivalent impedance (distance) and power transmission capacity (capacity), ECS is defined as a composite weight index to measure electrical connection in distribution networks. Since VMs in distribution networks are similar to communities in complex networks, a modularity-based community detection method, Newman Fast algorithm, is applied to partition CDNs by upgrading modularity to electrical modularity which is used to judge the quality of partitioning results in CDNs. According to the simulation analysis of three distribution networks in Section 4.5, major findings are summarized as follows:

- ECS can reflect structural characteristics of distribution networks very well, and electrical modularity is effective to be used to determine optimal partitioning results, since transmission lines with big impedance are detected as VM boundaries, which indicates weak electrical connection (small ECS values).
- Comparing to other partitioning results based on operating states analysis, the partitioning results using proposed hierarchical partitioning method have bigger values of electrical modularity, so the partitioning results using hierarchical partitioning method are more adaptive considering structural characteristics of distribution networks.
- By applying the proposed hierarchical partitioning method, the strength of community structure for different networks can be seen. If the curve of modularity for different number of VMs is slighter, the network has a stronger community structure. See Section 4.5.3 for more details.

- Dynamic boundaries of SDNs can be determined based on hierarchical partitioning method, which can provide some optional schemes for VMs when VMs are required to operate with connection to other VMs. So operating modes of SDNs are more various and flexible.

7.1.2 A Bi-level Optimisation Method for DG Allocation

Considering different objective functions, many methods are proposed to optimise DG allocation. However, most of these methods are assessed based on a unique monopoly control unit by centralised decision-making and hierarchical control. They may not be fully appropriate with consideration of trend in fully decentralised control for future SDNs. Based on the partitioning results in phase 1, a bi-level optimisation method consisting of an outer optimisation and an inner optimisation is introduced to find the optimal DG allocation of VMs in phase 2. The main goal of this bi-level optimisation is to maximise the capabilities of active energy management in system operation. In the outer planning optimization, it is to determine the optimal DG allocation (DG type, location, number and capacity) with the aim to realise autonomy of VMs by minimising the power flow on boundaries and total power losses. In the inner optimisation, active energy management is performed by adjusting output power of DGs to minimize generation costs. GA is applied as a main algorithm in the outer optimisation while POPF is used in the inner optimisation. The effectiveness of this optimisation method is verified by analysing the results for three cases, i.e. original networks without DG allocation (case 1), minimising power losses without VMs (case 2), maximizing the ability of active energy management with VMs (case 3). Major findings are summarized as follows:

- The proposed bi-level optimisation method can be convergent to find optimal results for DG allocation.
- The total power losses of case 3 decrease by 82% approximately compared with case 1, which enhance the power transmission efficiency of the network.

- Comparing to the results in case 2, the power supply of insensitive loads in all VMs can be guaranteed by considering the minimum capacity constraints of controllable DGs in case 3. In addition, the power flow on all VM boundaries in case 3 is smaller than that in case 2. Hence, the autonomous ability of VMs is improved.

7.1.3 Control and Protection Schemes from Microgrids to VMs

The two-phase strategy focuses on planning issues of SDNs, including determination of VM boundaries and DG allocation. In addition to these issues, due to the integration of DGs, several operating issues arise, such as bi-directional power flow and fault current variation, and they affect the normal operation of CDNs. Since there are almost no studies which directly focus on the protection and control issues of VMs, a hybrid control and protection scheme for microgrids is introduced considering similarities between VMs and microgrids. P-Q and V-f control strategies are applied to inverters of DGs in grid-connected mode and islanding mode. Inverse-time overcurrent protection is employed on feeders without DG allocation while biased differential protection are assigned to feeders with DGs. The proposed scheme is tested on a microgrid model, simulations results of two fault types (the most common single phase to ground fault and the most serious three phase fault) in different operating modes (grid-connected mode and islanding mode) are obtained. Based on the simulation results in Section 6.4, major findings are concluded as follows:

- P-Q control can ensure DGs to output constant active power and reactive power corresponding to setting values in both grid-connected mode and islanding mode. It is effective to adjust the output power of DGs in the case of load variation.
- In islanding mode, V-f control on DGs can adjust voltage and frequency to setting values before and after occurrence of different fault types and in load variation cases to ensure the stability of the microgrid.

- Different fault types can be detected and isolated by related protection methods effectively and accurately, and the microgrid can recover to normal operation after fault clearance.
- The proposed control and protection method can be applied to VMs, but more exploration is required since the operation of VMs is more complicated due to flexible structure.

7.2 Future Work

In this thesis, all work is carried out based on the proposed active planning framework for upgrading CDNs to SDNs. Based on the current results in this thesis, future work can be carried out in the following aspects:

- In this thesis, dispatchable and non-dispatchable DGs are considered as main devices for DG allocation. In the future, many other devices, such as energy storage devices and electric vehicles, will heavily integrate into power systems. Taking energy storage devices as an example, they can compensate for the intermittent output caused by non-dispatchable DGs, but their charging and discharging behaviour affect the stable operation of power systems. Therefore, it is more meaningful to consider other kinds of devices in optimisation, but it will obviously make the planning for SDNs become more complex.
- According to the definition of microgrids, a microgrid has a clearly defined boundary, and it acts as a single controllable entity. Commonly, a microgrid is connected to the main grid through the PPC. As a VM has some similarities with a microgrid, in this thesis, possible issues and solutions for VMs are discussed, and they are based on methodologies in microgrids. However, a network with VMs is more complex than a microgrid system. Taking the number of connecting points as an example, for a microgrid system, there is only one connection point, i.e. the PCC, to the other parts of the network. However, for a SDN consisting of VMs, there are many boundaries, so it has multiple connecting points with the other part of the network. What is more, a

single VM system may exchange power with many other VMs and the main grid at the same time. Therefore, more work should be done to realise and improve the functions of VM systems.

- In this thesis, methodologies for constructing the physical system layer of SDNs is proposed. According to the proposed active planning framework in Chapter 2, future research can focus on the development and construction of cyber system layer and socioeconomic system layer to fully realise the function of SDNs.

Appendix: A List of Publication

A list of research publications during my Ph.D. studies are listed below:

- **Journal Papers:**

  1. X. Xu, F. Xue, S. Lu, H. Zhu, L. Jiang and B. Han, "Structural and Hierarchical Partitioning of Virtual Microgrids in Power Distribution Network," in *IEEE Systems Journal*, vol. 13, no. 1, pp. 823-832, 2019.

  2. X. Xu, H. Wen, L. Jiang, and Y. Hu, "Hybrid Control and Protection Scheme for Inverter Dominated Microgrids," *J. Power Electron.*, vol. 17, no. 3, pp. 744–755, 2017.

  3. B. Han, S. Lu, F. Xue, L. Jiang and X. Xu, "Three-stage electric vehicle scheduling considering stakeholders economic inconsistency and battery degradation," in *IET Cyber-Physical Systems: Theory & Applications*, vol. 2, no. 3, pp. 102-110, 2017.

  4. C. Wu, F. Xue, X. Xu, S. Lu, L. Jiang, and G. Li. "Partitioning method of virtual microgrid based on electrical coupling strength." (Accepted by *Automation of electric Power Systems*)

- **Conference Papers**:

  1. X. Xu, H. Li and H. Wen, "Performance evaluation of busbar protection schemes under different fault scenarios," *2015 9th International Conference on Power Electronics and ECCE Asia (ICPE-ECCE Asia)*, Seoul, 2015, pp. 1597-1602.

  2. X. Xu, H. Wen and K. Zheng, "The layered control strategy for the converter dominated DC Microgrid," *2016 IEEE PES Asia-Pacific Power and Energy Engineering Conference (APPEEC)*, Xi'an, 2016, pp. 2017-2022.

  3. C. Wu, X. Wang, F. Xue, X. Xu, S. Lu, L. Jiang and Y. Zhai, "Evaluation of Buses in Power Grids by Extended Entropic Degree," *2018 37th Chinese Control Conference (CCC)*, Wuhan, 2018, pp. 1092-1097.

References

[1] H. Farhangi, “The path of the smart grid,” *IEEE Power Energy Mag.*, vol. 8, no. 1, pp. 18–28, 2010.

[2] S. Yun, *et al.*, “The development and empirical evaluation of the Korean smart distribution management system,” *Energies*, vol. 7, no. 3, pp. 1332–1362, 2014.

[3] T. Adefarati and R. C. Bansal, “Integration of renewable distributed generators into the distribution system: A review,” *IET Renew. Power Gener.*, vol. 10, no. 7, pp. 873–884, 2016.

[4] S. A. A. Kazmi, *et al.*, “Smart distribution networks: A review of modern distribution concepts from a planning perspective”, *Energies*, vol. 10, no. 4. 2017.

[5] M. Ourahou, *et al.*, “Review on smart grid control and reliability in presence of renewable energies : Challenges and prospects,” *Math. Comput. Simul.*, pp. 1–13, 2018.

[6] C. D'Adamo, S. Jupe and C. Abbey, “Global survey on planning and operation of active distribution networks - update of CIGRE C6.11 working group activities,” in 20th International Conference and Exhibition on Electricity Distribution - Part 1, 2009, pp. 1–4.

[7] N. Komninos, E. Philippou and A. Pitsillides, “Survey in smart grid and smart home security : Issues, challenges and countermeasures,” *IEEE Commun. Surv. Tutorials*, vol. 16, no. 4, pp. 1933–1954, 2014.

[8] C. F. Calvillo, A. Sánchez-Miralles and J. Villar, “Energy management and planning in smart cities,” *Renew. Sustain. Energy Rev.*, vol. 55, pp. 273–287, 2016.

[9] P. Asmus, “Microgrids, virtual power plants and our distributed energy future,” *Electr. J.*, vol. 23, no. 10, pp. 72–82, 2010.

[10] M. Smith and D. Ton, “The U.S. department of energy’s microgrid initiative,” *IEEE power energy Mag.*, vol. 11, no. 4, pp. 22–27, 2013.

[11] “Technology roadmap smart grids,” International Energy Agency, 2011. [Online] Available: https://www.iea.org/publications/freepublications/publication/smartgrids_roadmap.pdf

[12] H. Farzin, M. Fotuhi-Firuzabad and M. Moeini-Aghtaie , “Enhancing power system resilience through hierarchical outage management in multi-microgrids,” *IEEE Trans. Smart Grid*, vol. 7, no. 6, pp. 2869–2879, 2016.

[13] S. Chowdhury, S.P. Chowdhury and P. Crossley , “Microgrids and active distribution networks, ” London, U.K. Inst. Eng. Technol., 2009.

[14] N. Nikmehr and S. N. Ravadanegh , “Optimal power dispatch of multi-microgrids at future smart distribution grids,” *IEEE Trans. Smart Grid*, vol. 6, no. 4, pp. 1648–1657, 2015.

[15] N. C. Koutsoukis, P. S. Georgilakis, and N. D. Hatziargyriou, “Multistage coordinated planning of active distribution networks,” *IEEE Trans. Power Syst.*, vol. 33, no. 1, pp. 32–44, 2018.

[16] G. Celli, *et al.*, “A comparison of distribution network planning solutions: Traditional reinforcement versus integration of distributed energy storage,” *2013 IEEE Grenoble Conf.*, pp. 1–6, 2013.

[17] R. Li, W. Wang, and M. Xia, “Cooperative planning of active distribution system with renewable energy sources and energy storage systems,” *IEEE Access*, vol. 6, pp. 5916–5926, 2017.

[18] V. F. Martins and C. L. T. Borges, “Active distribution network integrated planning incorporating distributed generation and load response uncertainties,” *IEEE Trans. Power Syst.*, vol. 26, no. 4, pp. 2164–2172, 2011.

[19] X. Shen, *et al.*, “Multi-stage planning of active distribution networks considering the co-optimization of operation strategies,” *IEEE Trans. Smart Grid*, vol. 9, no. 2, pp. 1425–1433, 2018.

[20] R. D’Hulst *et al.*, “Voltage and frequency control for future power systems: The ELECTRA IRP proposal,” *Proc. - 2015 Int. Symp. Smart Electr. Distrib. Syst. Technol. EDST 2015*, pp. 245–250, 2015.

[21] I. Oleinikova and A.Obushevs, “Market design for electricity ensuring operational flexibility,” in 2015 IEEE 5th International Conference on Power Engineering, Energy and Electrical Drives (POWERENG), Riga, 2015, pp. 239–243.

[22] L. Mehigan, *et al.*, “A review of the role of distributed generation (DG) in future electricity systems,” *Energy*, vol. 163, pp. 822–836, 2018.

[23] L. Martini, “Trends of smart grids development as fostered by European research coordination,” *Int. Conf. Power Eng. Energy Electr. Drives*, pp. 23–30, 2015.

[24] "IEEE guide for design, operation, and integration of distributed resource island systems with electric power systems," *IEEE Std 1547.4*, pp. 1–54, 2011.

[25] Z. Wang, *et al.*, "Networked microgrids for self-healing power systems," *IEEE Trans. Smart Grid*, vol. 7, no. 1, pp. 310–319, 2016.

[26] H. Haddadian and R. Noroozian, "Multi-microgrids approach for design and operation of future distribution networks based on novel technical indices," *Appl. Energy*, vol. 185, pp. 650–663, 2017.

[27] S. A. Arefifar, Y. A. R. I. Mohamed, and T. H. M. El-Fouly, "Comprehensive operational planning framework for self-healing control actions in smart distribution grids," *IEEE Trans. Power Syst.*, vol. 28, no. 4, pp. 4192–4200, 2013.

[28] X. Xu, *et al.*, "Hybrid control and protection scheme for inverter dominated microgrids," *J. Power Electron.*, vol. 17, no. 3, pp. 744–755, 2017.

[29] Z. Wang and J. Wang, "Self-healing resilient distribution systems based on sectionlization into microgrids," *IEEE Trans. Power Syst.*, vol. 30, no. 6, pp. 3139–3149, 2015.

[30] S. A. Arefifar, Y. A. R. I. Mohamed, and T. H. M. El-Fouly, "Optimum microgrid design for enhancing reliability and supply-security," *IEEE Trans. Smart Grid*, vol. 4, no. 3, pp. 1567–1575, 2013.

[31] S. A. Arefifar, Y. A. I. Mohamed, and T. El-fouly, "Optimized multiple microgrid-based clustering of active distribution systems considering communication and control requirements," *IEEE Trans. Ind. Electron.*, vol. 62, no. 2, pp. 711–723, 2015.

[32] Y. Tan, S. Goddard and L. C. P´erez, "A prototype architecture for cyber-physical systems," ACM SIGBED Rev., vol. 5, no. 1, pp. 1–2, 2008.

[33] X. Yu and Y. Xue, "Smart grids : A cyber–physical systems perspective," *Proc. IEEE*, vol. 104, no. 5, pp. 1058–1070, 2016.

[34] C. Wang, *et al.*, "Impacts of cyber system on microgrid operational reliability," *IEEE Trans. Smart Grid*, vol. 10, no. 1, pp. 105–115, 2019.

[35] W. Liu, *et al.*, "Reliability modeling and evaluation of active cyber physical distribution system," *IEEE Trans. Power Syst.*, vol. 33, no. 6, pp. 7096–7108, 2018.

[36] F. Xue and G. Li, “Discussion on networking energy integration for energy internet,” *Autom. Electr. Power Syst.*, vol. 40, no. 1, pp. 9–16, 2016.

[37] M. G. Vayá and G. Andersson, “Optimal bidding strategy of a plug-in electric vehicle aggregator in day-ahead electricity markets under uncertainty,” IEEE Trans. Power Syst., vol. 30, no. 5, pp. 2375–2385, 2015.

[38] R. J. Sánchez-García, *et al.*, “Hierarchical spectral clustering of power grids,” *IEEE Trans. Power Syst.*, vol. 29, no. 5, pp. 2229–2237, 2014.

[39] J. Guo, G. Hug and O. K. Tonguz , “Intelligent partitioning in distributed optimization of electric power systems,” *IEEE Trans. Smart Grid*, vol. 7, no. 3, pp. 1249–1258, 2016.

[40] K. Balasubramaniam, *et al.*, “Balanced, non-contiguous partitioning of power systems considering operational constraints,” *Electr. Power Syst. Res.*, vol. 140, pp. 456–463, 2016.

[41] E. Cotilla-Sanchez, *et al.*, “Multi-attribute partitioning of power networks based on electrical distance,” *IEEE Trans. Power Syst.*, vol. 28, no. 4, pp. 4979–4987, 2013.

[42] B. Zhao, *et al.*, “Network partition based zonal voltage control for distribution networks with distributed PV systems,” *IEEE Trans. Smart Grid*, vol. PP, no. 99, pp. 1–1, 2017.

[43] Z. Chen, Z. Xie, and Q. Zhang, “Community detection based on local topological information and its application in power grid,” *Neurocomputing*, vol. 170, pp. 384–392, 2015.

[44] G. R. V. latora, V. Nicosia, “Complex networks,” Cambridge, UK: Cambridge University Press, 2017.

[45] M. E. J. Newman, “Analysis of weighted networks,” *Phys. Rev.*, vol. 70, no. 5, 2004.

[46] D. D. Fatta, *et al.*, “Small world theory and the World Wide Web: Linking small world properties and website centrality,” *Int. J. Mark. Bus. Syst.*, vol. 2, no. 2, pp. 126–140, 2016.

[47] E. Bompard, R. Napoli, F. Xue, “Analysis of structural vulnerabilities in power transmission grids,” *Int. J. Crit. Infrastruct. Prot.*, vol. 2, no. 1–2, pp. 5–12, 2009.

[48] E. Bompard, D. Wu, and F. Xue, “Structural vulnerability of power systems: A topological approach,” *Electr. Power Syst. Res.*, vol. 81, no. 7, pp. 1334–1340, 2011.

[49] E. Bompard, R. Napoli and F. Xue, “Extended topological approach for the assessment of structural vulnerability in transmission networks,” *IET Gener. Transm. Distrib.*, vol. 4, no. 6, pp. 716–724, 2010.

[50] K. Erciyes, “Complex networks an algorithmic perspective, ” Boca Raton, U.S: CRC Press, 2015.

[51] J. Macqueen, “Some methods for classification and analysis of multivariate observations,” *Proc. Fifth Berkeley Symp. Math. Stat. Probab.*, pp. 281–297, 1967.

[52] S. Fortunato, “Community detection in graphs,” *Phys. Rep.*, vol. 486, pp. 75–174, 2010.

[53] L. Yen, *et al.*, “Graph nodes clustering based on the commute-time kernel,” in *PAKDD*, 2007, pp. 1037–1045.

[54] C. R. Palmer and C. Faloutsos, “Electricity based external similarity of categorical attributes,” *Proc. PAKDD 2003*, pp. 486–500, 2003.

[55] A. K. Chandra, *et al.*, “The electrical resistance of a graph captures its commute and cover times,” in *STOC ’89: Proceedings of the twenty-first annual ACM symposium on Theory of computing*, 1989, pp. 574–586.

[56] M. E. J. Newman, “Fast algorithm for detecting community structure in networks,” *Phys. Rev.*, 2003.

[57] S. Boettcher and A. G. Percus, “Extremal optimization for graph partitioning,” *Phys. Rev. E*, vol. 64, no. 2, pp. 1107–1112, 2001.

[58] M. Chen, K. Kuzmin and B. K. Szymanski, “Community detection via maximization of modularity and its variants,” *IEEE Trans. Comput. Soc. Syst.*, vol. 1, no. 1, pp. 46–65, 2014.

[59] M. A. Javed, *et al.*, “Community detection in networks : A multidisciplinary review,” *J. Netw. Comput. Appl.*, vol. 108, pp. 87–111, 2018.

[60] S. A. Soliman A. H. Mantawy, “Modern optimization techniques with applications in electric power systems, ” New York, USA, 2012.

[61] P. S. Georgilakis and N. D. Hatziargyriou, “Optimal distributed generation placement in power distribution networks : Models, methods, and future research,” *IEEE Trans. Power Syst.*, vol. 28, no. 3, pp. 3420–3428, 2013.

[62] N. S. Rau and Y. Wan, “Optimum location of resources in distributed planning,” *IEEE Trans. Power Syst.*, vol. 9, no. 4, pp. 2014–2020, 1994.

[63] Z. Abdmouleh, *et al.*, "Review of optimization techniques applied for the integration of distributed generation from renewable energy sources," *Renew. Energy*, vol. 113, pp. 266–280, 2017.

[64] P. N. Vovos, *et al.*, "Optimal power flow as a tool for fault level-constrained network capacity analysis," *IEEE Trans. Power Syst.*, vol. 20, no. 2, pp. 734–741, 2005.

[65] R. A. Jabr and B. C. Pal, "Ordinal optimisation approach for locating and sizing of distributed generation," *IET Gener. Transm. Distrib.*, vol. 3, no. 8, pp. 713–723, 2009.

[66] A. W. Geem, J. H. Kim and G.V. Loganathan, "A new heuristic optimization algorithm: harmony search," *Simulation*, vol. 76, no. 2, pp. 60–68, 2001.

[67] J. Kennedy and R. Eberhart, "Particle swarm optimization," in *Proceedings of ICNN'95 - International Conference on Neural Networks*, 1995, pp. 1942–1948.

[68] X. Yang, "Harmony search as a metaheuristic algorithm," in *Music-Inspired Harmony Search Algorithm: Theory and Applications*, vol. 191, Springer Berlin, 2009, pp. 1–14.

[69] D. Karaboga, "An idea based on honey bee swarm for numerical optimization," in *Technical Report-TR06*, 2005.

[70] E. K. Buike and G. Kendall, "Search methodologies : Introductory tutorials in optimization and decision support techniques," Boston: Springer US, 2014.

[71] M. Srinivas and L. M. Patnaik, "Genetic algorithms: A survey," *Computer*, vol. 27, no. 6, pp. 17–26, 1994.

[72] S. A. Arefifar, Y. A. R. I. Mohamed, and T. H. M. El-Fouly, "Supply-adequacy-based optimal construction of microgrids in smart distribution systems," *IEEE Trans. Smart Grid*, vol. 3, no. 3, pp. 1491–1502, 2012.

[73] K. Buayai, W. Ongsakul and N. Mithulananthan , "Multi-objective micro-grid planning by NSGA-II in primary distribution system," *Eur. Trans. Electr. POWER*, vol. 22, pp. 170–187, 2012.

[74] M. V. Kirthiga, S. A. Daniel, and S. Gurunathan, "A methodology for transforming an existing distribution network into a sustainable autonomous micro-grid," *IEEE Trans. Sustain. Energy*, vol. 4, no. 1, pp. 31–41, 2013.

[75] M. E. Nassar and M. M. A. Salama, "Adaptive self-adequate microgrids using dynamic boundaries," *IEEE Trans. Smart Grid*, vol. 7, no. 1, pp. 105–113, 2016.

[76] M. E. J. Newman, "Networks : An introduction," Oxford, UK: Oxford University Press, 2010.

[77] S S. Arianos, *et al.*, "Power grids vulnerability: A complex network approach," *Chaos An Interdiscip. J. Nonlinear Sci.*, vol. 19, no. 1, 2009.

[78] D. F. Pires, C. H. Antunes, and A. G. Martins, "NSGA-II with local search for a multi-objective reactive power compensation problem," *Electr. Power Energy Syst.*, vol. 43, pp. 313–324, 2012.

[79] G. Bounova and O. de Weck, "Overview of metrics and their correlation patterns for multiple-metric topology analysis on heterogeneous graph ensembles," *Phys. Rev. E*, vol. 85, no. 1, 2012.

[80] W. El-Khattam, *et al.*, "Optimal investment planning for distributed generation in a competitive electricity market," *IEEE Trans. Power Syst.*, vol. 19, no. 3, pp. 1674–1684, 2004.

[81] M. Raoofat, "Simultaneous allocation of DGs and remote controllable switches in distribution networks considering multilevel load model," *Electr. Power Energy Syst.*, vol. 33, no. 8, pp. 1429–1436, 2011.

[82] E. Naderi, H. Seifi, and M. S. Sepasian, "A dynamic approach for distribution system planning considering distributed generation," *IEEE Trans. Power Deliv.*, vol. 27, no. 3, pp. 1313–1322, 2012.

[83] J. M. López-Lezama, J. Contreras, and A. Padilha-Feltrin, "Location and contract pricing of distributed generation using a genetic algorithm," *Electr. Power Energy Syst.*, vol. 36, no. 1, pp. 117–126, 2012.

[84] Y. M. Atwa and E. F. El-Saadany, "Probabilistic approach for optimal allocation of wind-based distributed generation in distribution systems," *IET Renew. Power Gener.*, vol. 5, no. 1, pp. 79–88, 2011.

[85] Y. M. Atwa, *et al.*, "Optimal renewable resources mix for distribution system energy loss minimization," *IEEE Trans. Power Syst.*, vol. 25, no. 1, pp. 360–370, 2010.

[86] S. A. Arefifar, M. Ordonez, and Y. A. I. Mohamed, "V-I controllability-based optimal allocation of resources in smart distribution systems," *IEEE Trans. Smart Grid*, vol. 7, no. 3, pp. 1378–1388, 2016.

[87] V. Kalkhambkar, R. Kumar, and R. Bhakar, "Joint optimal allocation methodology for renewable distributed generation and energy storage for economic benefits," *IET Renew. Power Gener.*, vol. 10, no. 9, pp. 1422–1429, 2016.

[88] M. Akbari, J. Aghaei, and M. Barani, "Convex probabilistic allocation of wind generation in smart distribution networks," *IET Renew. Power Gener.*, vol. 11, no. 9, pp. 1211–1218, 2017.

[89] H. Ren, *et al.*, "Feedforward feedback pitch control for wind turbine based on feedback linearization with sliding mode and fuzzy," *Math. Probl. Eng.*, vol. 2018, no. 8, pp. 1–13, 2018.

[90] M. E. Nassar, et al., "A Novel Load Flow Algorithm for Islanded AC/DC Hybrid Microgrids, " *IEEE Transactions on Smart Grid*, vol. 10, no. 2, pp. 1553-1566, 2019.

[91] C. Grigg, *et al.*, "The IEEE reliability test system -1996 a report prepared by the reliability test system task force of the application of probability methods subcommittee," *IEEE Trans. Power Syst.*, vol. 14, no. 3, pp. 1010–1020, 1999.

[92] B. Borkowska, "Probabilistic load flow," *IEEE Trans. Power Appar. Syst.*, vol. PAS-93, no. 3, pp. 1–6, 1974.

[93] J. Tang, *et al.*, "Dimension-adaptive sparse grid interpolation for uncertainty quantification in modern power systems: Probabilistic power flow," *IEEE Trans. Power Syst.*, vol. 31, no. 2, pp. 907–919, 2016.

[94] M. Fan, *et al.*, "Probabilistic power flow studies for transmission systems with photovoltaic generation using cumulants," *IEEE Trans. Power Syst.*, vol. 27, no. 4, pp. 2251–2261, 2012.

[95] M. Hajian, W. D. Rosehart, and H. Zareipour, "Probabilistic power flow by Monte Carlo simulation with Latin supercube sampling," *IEEE Trans. Power Syst.*, vol. 28, no. 2, pp. 1550–1559, 2013.

[96] M. Fan, *et al.*, "Probabilistic power flow analysis with generation dispatch including photovoltaic resources," *IEEE Trans. Power Syst.*, vol. 28, no. 2, pp. 1797–1805, 2013.

[97] D. Villanueva, J. L. Pazos, and A. Feijóo, "Probabilistic load flow including wind power generation," *IEEE Trans. Power Syst.*, vol. 26, no. 3, pp. 1659–1667, 2011.

[98] M. E. Baran and F. F. Wu, "Optimal capacitor placement on radial distribution systems," *IEEE Trans. Power Deliv.*, vol. 4, no. 1, pp. 725–734, 1989.

[99] T. K. Nagsarkar and M. S. Sukhija, “Power system analysis, ” New Delhi, India, Oxford University Press, 2014.

[100] I. Rhyne, J. Klein, and B. Neff, “Estimated cost of new renewable and fossil generation in California,” 2015.

[101] J. A. P. Lopes, C. L. Moreira, and A. G. Madureira, “Defining control strategies for microgrids islanded operation,” *IEEE Trans. Power Syst.*, vol. 21, no. 2, pp. 916–924, 2006.

[102] S. Adhikari and F. Li, “Coordinated V-f and P-Q control of solar photovoltaic generators with MPPT and battery storage in microgrids,” *IEEE Trans. Smart Grid*, vol. 5, no. 3, pp. 1270–1281, 2014.

[103] A. Micallef, *et al.*, “Single-Phaspe microgrid with deamless transition capabilities between modes of operation,” *IEEE Trans. Smart Grid*, vol. 6, no. 6, pp. 2736–2745, 2015.

[104] M. Khederzadeh, “Preservation of overcurrent relays coordination in microgrids by application of static series compensators,” *11th IET Int. Conf. Dev. Power Syst. Prot. (DPSP 2012)*, pp. 1–5, 2012.

[105] N. Jayawarna and M. Barnes, “Central storage Uunit response requirement in ‘ Good Citizen ’ microgrid,” *2009 13th Eur. Conf. Power Electron. Appl.*, pp. 1–10, 2009.

[106] S. M. Brahma and A. A. Girgis, “Microprocessor-based reclosing to coordinate fuse and recloser in a system with high penetration of distributed generation,” *2002 IEEE Power Eng. Soc. Winter Meet.*, pp. 453–458, 2002.

[107] W. El-Khattam and T. S. Sidhu, “Restoration of directional overcurrent relay coordination in distributed generation systems utilizing fault current limiter,” *IEEE Trans. Power Deliv.*, vol. 23, no. 2, pp. 576–585, 2008.

[108] W. K. A. Najy, H. H. Zeineldin, and W. L. Woon, “Optimal protection coordination for microgrids with grid-connected and islanded capability,” *IEEE Trans. Ind. Electron.*, vol. 60, no. 4, pp. 1668–1677, 2013.

[109] J. Hwang, *et al.*, “Validity analysis on the positioning of superconducting fault current limiter in neighboring AC and DC microgrid,” *IEEE Trans. Appl. Supercond.*, vol. 23, no. 3, pp. 5600204–5600204, 2013.

[110] A. Hooshyar and R. Iravani, "Microgrid protection," *Proc. IEEE*, vol. 105, no. 7, pp. 1332–1353, 2017.

[111] S. Mirsaeidi, *et al.*, "A protection strategy for micro-grids based on positive-sequence impedance," *IET Renew. Power Gener.*, vol. 9, no. 6, pp. 600–609, 2015.

[112] E. Casagrande, *et al.*, "A differential sequence component protection scheme for microgrids with inverter-based distributed generators," *IEEE Trans. Smart Grid*, vol. 5, no. 1, pp. 29–37, 2014.

[113] M. Baran and I. El-Markabi, "Adaptive over current protection for distribution feeders with distributed generators," *IEEE PES Power Syst. Conf. Expo.*, vol. 2, pp. 715–719, 2004.

[114] D. M. Bui, *et al.*, "Investigate dynamic and transient characteristics of microgrid operation and develop a fast-scalable-adaptable algorithm for fault protection system," *Electr. Power Syst. Res.*, vol. 120, pp. 214–233, 2015.

[115] R. M. Kamel, M. A. Alsaffar and M. K. Habib, "Novel and simple scheme for Micro-Grid protection by connecting its loads neutral points: A review on micro-grid protection techniques," *Renew. Sustain. Energy Rev.*, vol. 58, pp. 931–942, 2016.

[116] S. Mirsaeidi, *et al.*, "Modeling and simulation of a communication-assisted digital protection scheme for micro-grids," *Renew. Sustain. Energy Rev.*, vol. 57, pp. 867–878, 2016.

[117] F. Coffele, C. Booth and A. Dyśko , "An adaptive overcurrent protection scheme for distribution networks," *IEEE Trans. Power Deliv.*, vol. 30, no. 2, pp. 561–568, 2015.

[118] M. Dewadasa, A. Ghosh and G. Ledwich, "Protection of microgrids using differential relays," *Univ. Power Eng. Conf.*, pp. 1–6, 2011.

[119] E. Sortomme, *et al.*, "Fault analysis and protection of a microgrid," *40th North Am. Power Symp. NAPS2008*, pp. 1–6, 2008.

[120] J. C. Tan, *et al.*, "Software model for inverse time overcurrent relays incorporating IEC and IEEE standard curves," *Can. Conf. Electr. Comput. Eng.*, pp. 37–41, 2002.

[121] C. F. Henville, "Combined use of definite and inverse time overcurrent elements assists in transmission line ground relay coordination," *IEEE Trans. Power Deliv.*, vol. 8, no. 3, pp. 925–932, 1993.

[122] X. Li, *et al.*, “Selection of settings of differential protection based on fault component,” *Power Syst. Techonology*, vol. 25, no. 4, pp. 47–50, 2001.